

European Workshop POLYMER SCIENCE AT NANOSCALE

Proceedings

“Petru Poni” Institute of Macromolecular Chemistry
41A, Aleea Grigore Ghica Voda, 700487 Iasi, Romania
October 22-23, 2013

Organized under the auspices of the bilateral Romanian-Ukrainian interacademic project entitled “Development of multifunctional organic and organic-inorganic polymeric materials on the base of components with different chemical nature”, 2012-2016.



European Workshop POLYMER SCIENCE AT NANOSCALE
22-23 October 2013
Iasi, Romania

Workshop Topic

Nanomaterials, a route for advanced applications: preparation, structural and physico-chemical characterization

International Scientific Committee:

- Acad. Bogdan SIMIONESCU (Romania)
- Acad. Eugene LEBEDEV (Ukraine)
- Dr. Valeria HARABAGIU (Romania)
- Prof. Yuri SAVELYEV (Ukraine)
- Prof. Yevgen MAMUNYA (Ukraine)
- Dr. Gisele BOITEUX (France)

Organizing committee:

- Dr. Madalina ZANOAGA (Romania)
- Dr. Fulga TANASA (Romania)
- Dr. Marioara NECHIFOR (Romania)
- Dr. Maksym IURZHENKO (Ukraine)
- Dr. Viorica GAINA (Romania)
- Mrs. Mioara SAVA (Romania)

Sponsors

We gratefully acknowledge the financial support of our sponsors:



European Union



REGPOT



“Petru Poni” Institute of
Macromolecular
Chemistry



FP7-REGPOT-2010-1 Nr. 264115

ELECTROACTIVE HYBRID POLYMER NANOMATERIALS CONTAINING IONIC LIQUIDS

**M. V. Iurzhenko^{1,2}, Ye. P. Mamunya^{1,2}, G. Boiteux³, A. Serghei³,
O. S. Sverdlikovs'ka⁴, O. V. Chervakov⁴, V. I. Stompel¹, E. V. Lebedev¹**

¹*Institute of Macromolecular Chemistry of the NAS of Ukraine, 48 Kharkivske shose, 02160 Kyiv, Ukraine*

4ewip@ukr.net

²*Center of Collective Use of scientific Equipment for Thermophysical Investigations and Analysis of the NAS of Ukraine in the Institute of Macromolecular Chemistry of the NAS of Ukraine, 48 Kharkivske shose, 02160 Kyiv, Ukraine*

³*Université de Lyon, Université Lyon 1, Ingénierie des Matériaux Polymères, UMR CNRS 5223, IMP@LYON1, France*

⁴*Ukrainian State University of Chemical Technology, Gagarina prospect 8, 4900, Dnipropetrovsk, Ukraine*

LECTURES

Nowadays electroactive polymer materials and, firstly, materials with ionic conductivity attract a great interest as solid flexible electrolytes for power supply devices, and electronics for everyday utilization. Taking this into consideration, the development, investigation and implementation of electrolyte systems of different nature, notably organic liquid electrolytes, ionic liquids, polymer electrolytes and inorganic solid electrolytes, attract a great interest. In brief electrolyte systems can be conditionally divided as follows:

- polymer + organic liquid (polymer gel);
- polymer + ionic liquid;
- polymer + inorganic solid electrolyte + ionic liquids;
- polymer electrolyte + ionic liquid;
- polymer electrolyte + ionic liquid + liquid organic electrolyte;
- ionic liquids + liquid organic electrolyte;
- polymer electrolyte + inorganic solid electrolyte.

The blends consisting of two and more electrolytes are used and studied for obtaining materials with combined merits of selected electrolytes [1].

“Polymer + ionic liquid” as far as “polymer + inorganic solid electrolyte + ionic liquids” may deserve much attention as potential materials for electrochemical devices. Earlier in [2] it was found that ionic conductivity of the systems, which consisted of conductive halogenide (chloride or bromide) poly(1-butyl-4-vinylpyridine) and ionic liquid depends on content and ambient conditions (temperature). The tetrafluoroborate and triphthalate 1-ethyl-3-methylimidazole ionic liquids react with vinylidene fluoride and hexafluoropropylene co-polymer

L1

and form the conductive polymer electrolyte [3]. A nonvolatility and high thermal stability of ionic liquids and polymer electrolyte on their base enable using high temperature ranges for increasing their ionic conductivity up to decades.

Electroactive hybrid polymer nanocomposites (EaHPNs) have been synthesized in the reactive mixture of organic component, which had free reactive NCO-groups and the inorganic component with reactive OH-groups. Oligoetherurethane (UO) was macrodiisocyanate with $M_w = 4500$ and 3,6% of NCO-groups synthesized on 2,4 and 2,6-toluenediisocyanate (TDI 80/20) and oligoxypropyleneglycol with molecular weight 2100, and used as organic component. The inorganic component was metal silicate (MS), which exists in the form of oligomer. The ratio of organic/inorganic components was equal to 70/30.

Two types of ionic liquids (IL), namely quaternary ammonium salts (C-4) and diquaternary ammonium salts (C-20- α) based on morpholine, were used (Fig. 1). The chemical contents of IL are described in Table 1.

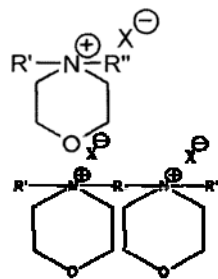


Fig. 1. Structural formulas of IL C-4 and C-20- α .

Table 1. Chemical contents of IL.

	R'	R''	
IL C-4	$—CH_2—CH_2—OH$	$—CH_2—CH_2—OH$	1
IL C-20- α	$—CH_2—CH—CH_2$ OH	$—CH_2—CH_2—OH$	1

Fig. 2 shows the kinetic curves of electrophysical parameters during sorption (empty dots) and desorption (full dots) processes of the IL C-4 in EaHPNs. One can see that the weight of adsorbed IL C-4 during 75 days equals to 7 % RW and permittivity gradually increases with the RW, whereas the values of AC and DC conductivity rise rapidly at the beginning and reach the saturation in 20 days. During the exposition in air the desorption process runs quicker than the sorption process due to internal macromolecular forces. The residual of IL C-4 may be connected with clusters formation, which are localized in defects of hybrid network or nearby nanoinclusions of hydrophilic inorganic phase. It is significant that the decrease of AC and DC conductivity is negligible (less than decade) vs. the considerable decrease of the sample weight and permittivity. That is the proof that the conductivity depends not so much on amount of IL C-4 as on configuration of the conductive phase formed during sorption and desorption processes.

Fig. 3 represents the kinetic curves of electrophysical parameters during sorption (empty dots) and desorption (full dots) processes of the IL C-20- α in EaHPNs.

[5]

L1

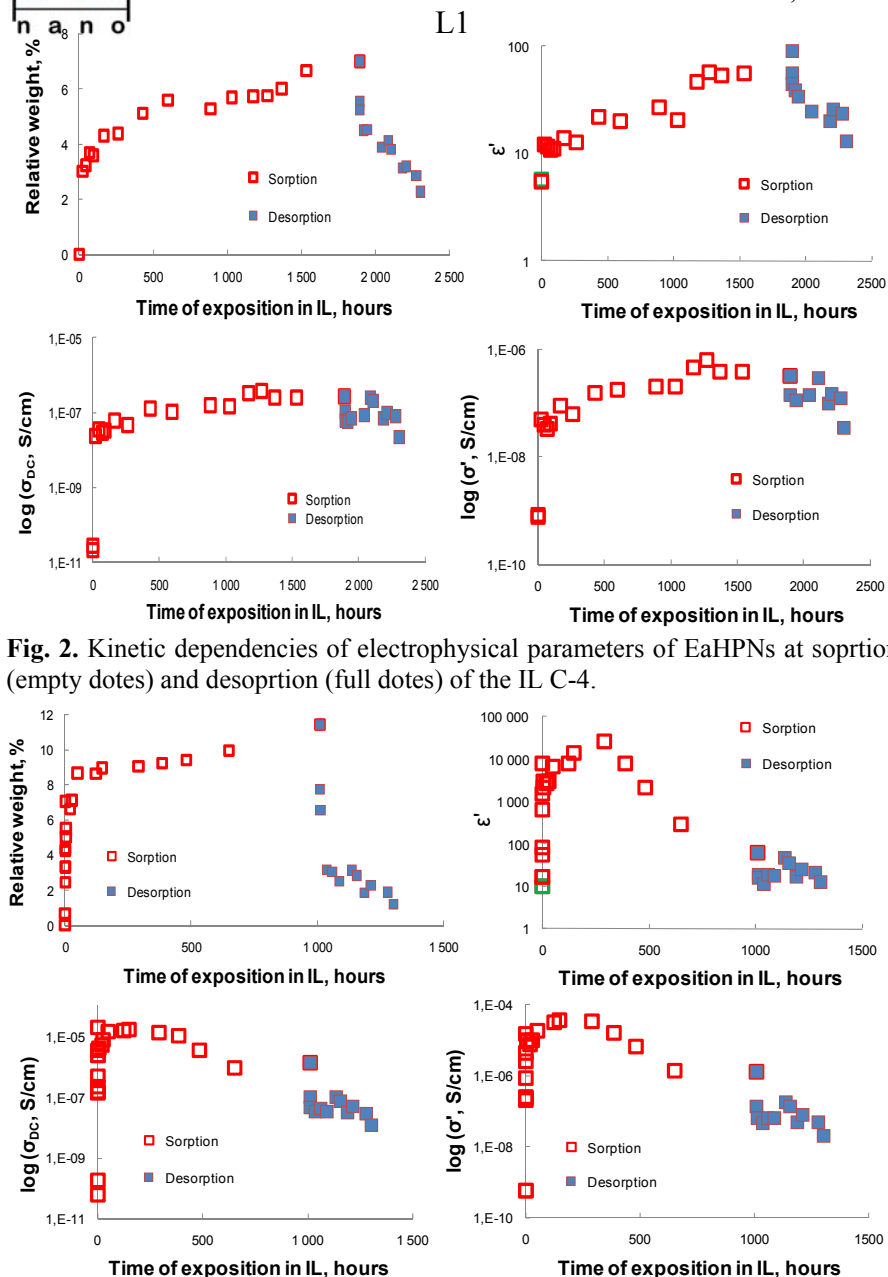


Fig. 2. Kinetic dependencies of electrophysical parameters of EaHPNs at sorption (empty dots) and desorption (full dots) of the IL C-4.

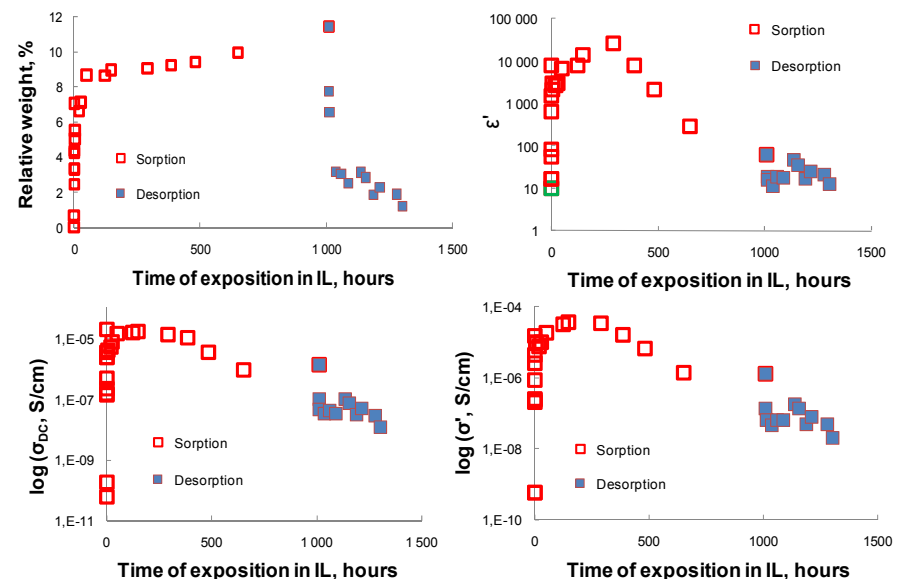


Fig. 3. Kinetic dependencies of electrophysical parameters of EaHPNs at sorption (empty dots) and desorption (full dots) of the IL C-20- α .

[6]

It is obvious that the saturation dependences of the permittivity and conductivity have maximums and show the decrease of their values after 10 days, whereas the sample was remained in ionic liquid and its relative weight slightly increased. That can be explained by the interaction of the IL with nanoinclusions of hydrophilic mineral phase and its destruction with the parallel process of substitution by the IL. It is shown by WAXS (Fig. 4) and optical microscopy (Fig. 5) that the doping of EaHPNs by the molecules of IL leads to destruction of the mineral phase with the simultaneous formation of new crystalline structures of ionic crystals due to MS/IL reactions. Because of that the number of charge carriers rapidly decreased and one can see the decrease of permittivity and conductivity values. Also one can see that the rate of structure changes is different for ionic liquids. The duplet reflex of the structured mineral phase changes insignificantly for IL C-4, whereas for IL C-20- α mineral phase is considerably destroyed with appearance of crystalline phase reflex of the ionic crystals. Such behavior can be easily explained by doubled number of anions and cations in the IL C-20- α that react with mineral phase of EaHPNs.

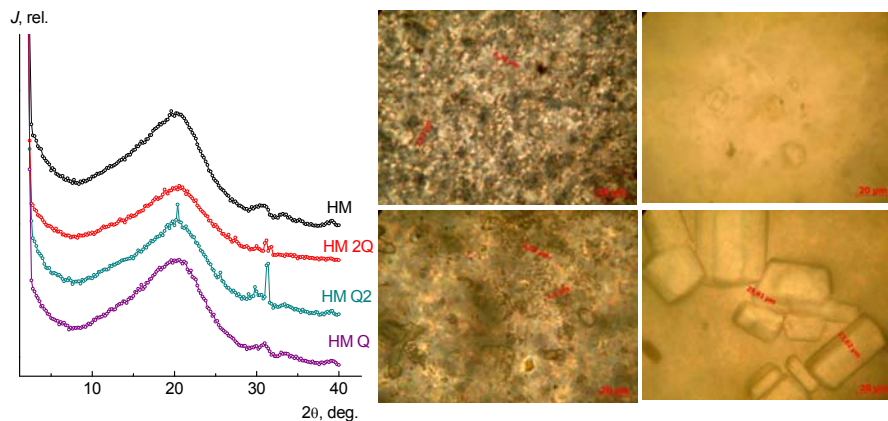


Fig. 4. WAXS spectra of the EaHPNs.

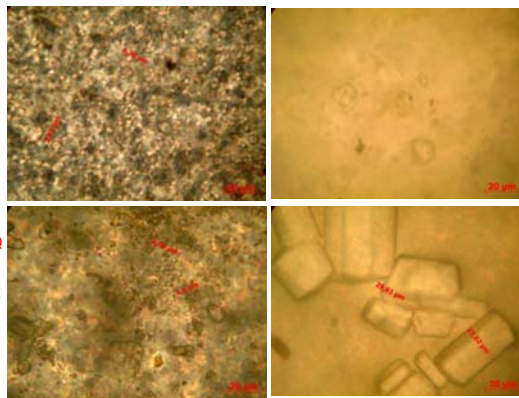


Fig. 5. Microphotos of the EaHPNs.

1. S.R. Younesi, K. Ciosek, K. Edstrom, 214-th ECS Meeting (2008), 465.
2. M. Watanabe, S.I. Yamada, N. Ogata, Electrochim. Acta 40 (1995) 2285.
3. J. Fuller, A.C. Breda, R.T. J. Carlin, Electrochem. Soc. 144 (1997) 67.

FUNCTIONAL POLYMERS AND MICRO- /NANOPARTICLES – ROUTES TOWARDS CONTROLLED DESIGN OF NEW MATERIALS

G. David¹, B. C. Simionescu^{1,2}

¹“Gh. Asachi” Technical University of Iasi, Faculty of Chemical Engineering and Environmental Protection, Department of Natural and Synthetic Polymers, Bd. Prof. Dimitrie Mangeron, 71A, Iasi 700050, Romania

dgeta54@yahoo.com

² “Petru Poni” Institute of Macromolecular Chemistry, Grigore Ghica Voda Alley 41A, Iasi 700487, Romania

bcsimion@icmpp.ro

Nowadays, the challenges lie fundamentally with the design of complex, multifunctional materials, envisaging new performances, never achieved before, with traditional chemistry. A combination between knowledge on functional polymers synthesis/characterization and knowledge on surface/interface phenomena became both a requirement and a tool for synthesis and preparation routes towards new advanced materials. Thus, the achievement of the control in the synthesis by new preparative methods, as well as the use of new strategies to gain control over the intermolecular bonds permit now the tailoring of polymer structure, architecture and properties from nano- to macroscopic level.

The present work reviews data on the synthesis of some simple functional polymers (poly(2-alkyl-2-oxazolines) or poly(ϵ -caprolactone) derivatives: telomers, macromonomers) and their use in the preparation of new polymer materials (Fig. 1):

- block and graft copolymers acting as compatibilizers or non-ionic surfactants;
- micro-/nanoparticles with possible use as a sorbent, catalyst support, drug carrier or as a tool for the *building* of multifunctional materials (hydrogels with high rate response to external stimuli; injectable formulations; non-viral vector for gene delivery) [1,2];
- hydro-/amphigels with possible applications in biomedical domain (immobilization/storage of biomolecules; scaffold in tissue engineering; components in wounds dressings etc.) [3-6];
- polymeric nanocomposites with improved mechanical properties [7].

Possibilities to obtain advanced materials from common functional polymers by appropriate selection of preparation protocols and parameters are also presented (Fig. 2).

L2

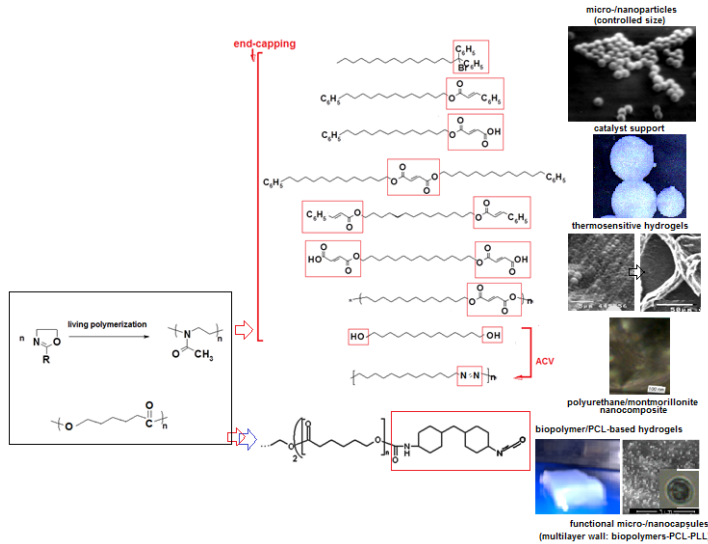


Fig. 1. Use of poly(2-alkyl-2-oxazolines) (PROZO) or poly(ϵ -caprolactone) (PCL) derivatives as building blocks / bricks with controlled functionality towards multifunctional materials.

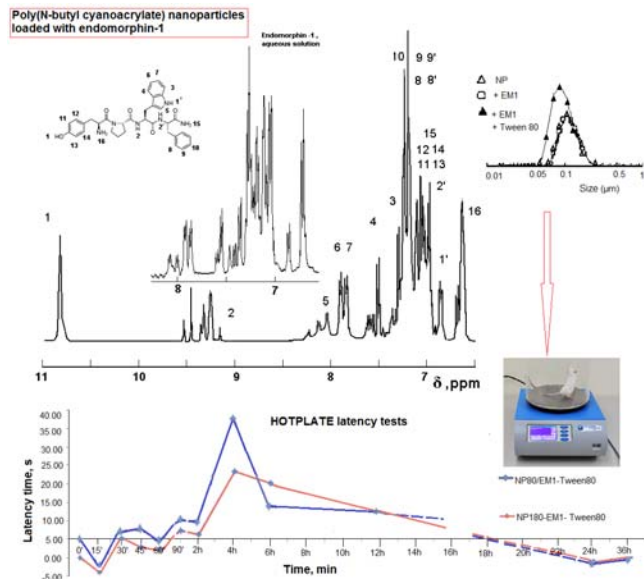


Fig. 2. Preparation and testing of poly(N-butyl cyanoacrylate) nanoparticles loaded with endomorphin-1.

L2

The opportunities and challenges offered by the use of functional polymers as building blocks for advanced materials are pointed and discussed. Future developments are suggested, in accordance with the topical trends and efforts to find a way allowing the research to face the industry requirements and the challenges of tomorrow's marketplace.

Acknowledgement: This work was financially supported by PN-II-ID-PCCE-2011-2-0028, contract grant number: 4/30.05.2012.

1. David G., Simionescu B. C., Simionescu Cr. Functional Micro- and nanoparticles- a possible tool for nanostructured materials // Rev Roum Chim. 52 (2007) 105 –112.
2. David G., Simionescu B. C., Albertsson A.-C. Rapid Deswelling Response of Poly(N-isopropylacrylamide)/Poly(2-alkyl-2-oxazoline)/Poly(2-hydroxyethyl methacrylate) Hydrogels //Biomacromolecules 9 (2008) 1678–1683.
3. David G., Pinteala M., Simionescu B. C. Biomedical Applications of poly[(N-acylimino)ethylene]s Gels, interpenetrating polymer networks // Dig J Nanomater Biostruct. 1 (2006) 129 – 138.
4. David G., Simionescu B. C., Maier S., Balhui C. Micro-/nanostructured polymeric materials: poly(ϵ -caprolactone) crosslinked collagen sponges// Dig J Nanomater Biostruct. 6 (2011) 1575-1585.
5. David G., Cristea M., Balhui C., Timpu D., Doroftei F., Simionescu B. C. Effect of Crosslinking Methods on Structure and Properties of Poly(ϵ -caprolactone) Stabilized Hydrogels Containing Biopolymers // Biomacromolecules 13 (2012) 2263–2272.
6. Simionescu B. C., Neamtu A., Balhui C., Danciu M., Ivanov D., David G. Macroporous structures based on biodegradable polymers-candidates for biomedical application //Biomed Mater Res A. 101(2013) 2689-2698.
7. David G., Simionescu B. C., Ibanescu S., Vearba F. Effect of montmorillonite content in nanocomposites of segmented polyurethanes with poly(2-alkyl-2-oxazoline) sequences // High Perform Polym. 23 (2011) 74-84.

**FROM BULK TO ATTOGRAMS OF MATTER:
APPLICATIONS OF BROADBAND DIELECTRIC
SPECTROSCOPY IN POLYMER NANOSCIENCE**

A. Houachtia, G. Boiteux, J. F. Gerard, A. Serghei*

Université Lyon 1, CNRS UMR 5223, IMP, Ingénierie des Matériaux
Polymères, 69622 Villeurbanne, France
anatoli.serghei@univ-lyon1.fr

The present contribution aims to review the applications of Broadband Dielectric Spectroscopy in polymer nanoscience. The broad frequency and temperature range of this technique allows one investigations on a variety of different physical phenomena taking place on different time- and length-scales: density fluctuations (and thus phase transitions), polymer dynamics (molecular fluctuations, glass transition, chain dynamics, capillary flow), charge transport phenomena in the bulk and at interfaces. Its high accuracy in measuring low signals enables one measurements on extremely small amounts of matter, down to the level of attograms ($1 \text{ attogram} = 10^{-18} \text{ gram}$). The present contribution will exemplify the strength of Broadband Dielectric Spectroscopy in measuring polymer systems having one, two or three dimensions on the nanometric length scales (ultra-thin layers, monolayers and sublayers, polymer nanorods, nanowires and nanotubes, single polymer chains, attograms of matter). It will be demonstrated how nanotechnology can be used to develop new types of sample cells which allow one electrical measurements on extremely small amounts of material (Fig. 1).

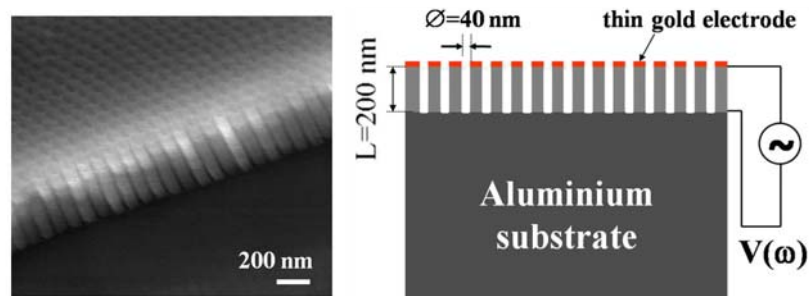


Fig. 1: Highly ordered arrays of identical, independent, additive nano-containers employed to hold and measure attograms partitions of matter.

1. A. Serghei, W. Zhao, D. Miranda, T.P. Russell, *Nanoletters* 13, 577 (2013).
2. A. Serghei, D. Chen, D.H. Lee, and T.P. Russell, *Soft Matter* 6, 1111 (2010).
3. A. Serghei, J. Lutkenhaus, D. Miranda, K. McEnnis, F. Kremer, and T.P. Russell, *Small* 6, 1822 (2010).

**POLYMER-CONTROLLED CaCO_3 CRYSTALLIZATION IN
COMPLEX STRUCTURES**

M. Mihai

“Petru Poni” Institute of Macromolecular Chemistry, Grigore Ghica Voda Alley
41A, Iasi 700487, Romania
marcelas@icmpp.ro

Intensive work has been focused last years on the synthesis of hybrid inorganic/organic materials with specific size, shape, orientation, organization, and complex form, aiming thus to design new materials and devices used in various fields such as catalysis, medicine, electronics, ceramics, pigments, etc. Thus, the architectural control of nano- and microcrystals with well-defined shapes is a significant goal of modern materials chemistry.

Calcium carbonate is an important mineral in nature, having three anhydrous crystalline polymorphs: calcite, aragonite, and vaterite. The stability of these CaCO_3 crystalline polymorphs decreases in the following order: vaterite < aragonite < calcite [1]. Most of the research with respect to CaCO_3 has been focused in understanding formation of inorganic microparticles in saturated solutions, understanding precipitation kinetics, mechanisms of crystallization and polymorphic transformations between calcite, aragonite and vaterite forms [2]. The basis for the possible applications is its micro-porous nature and the ability to be dissolved in mild conditions of acidic pH and in presence of complexing agents. It has wide applications, as filler in pigment, paper, rubber, plastic industries [3]. Recently, it has also been tested for pharmaceutical and biomedical applications owing to its biocompatible and biodegradable nature [4].

Organic (macro)molecules have the ability to control nucleation/growth of certain polymorph(s) of inorganic materials and to organize their growth into desired patterns by controlling hierarchically their structure, shape, size, and orientation [5,6]. Various organic compounds, especially the acidic macromolecules, are shown to be responsible for nucleation and/or stabilization of the particular CaCO_3 polymorphs [7,8]. Difficulties in understanding their roles arise from the complexity of the study of such mechanisms in the solid-liquid system and the large ability of the CO_3^{2-} anions to form different supramolecular structures. Thus, it is still far away to fully understand the formation processes of CaCO_3 composites with varied shapes, polymorph, composition, and stability, etc. in either the natural or mimic system, especially those mediated by biomacromolecules or synthetic polymers.

In this context, our studies aims to control *in vitro* the polymorphs ratio and

the orientation of CaCO_3 crystals, as these factors have a strong influence on the composite material properties such as solubility (biodegradability) and mechanical properties. The main parameter which may influence the structure of the polymer/ CaCO_3 composites is the structure of the synthetic/natural polyanions used as templates. Different polymers were used in our studies: synthetic polymers (PAMPSAA – 55 mol.% 2-acrylamido-2-methylpropanesulfonic acid and 45 mol.% acrylic acid [9-11], PHOS-*b*-PMAA – poly(*p*-hydroxystyrene – *b* – methacrylic acid) [12], P(NVP-MA-Ox) – polymer–drug conjugate based on poly(N-vinylpyrrolidone-co-maleic anhydride) and 2-amino-5-(4-methoxy-phenyl)-1,3,4-oxadiazole [13, 14] and natural polymers (CSA – chondroitin sulfate A [11,15], Xnt – xanthan, Alg – alginate). A common feature of the used polymers is the presence of carboxylic groups along the polymeric chain. Figure 1 shows some SEM images of polymer/ CaCO_3 composite structures obtained using different polymers as organic soluble templates.

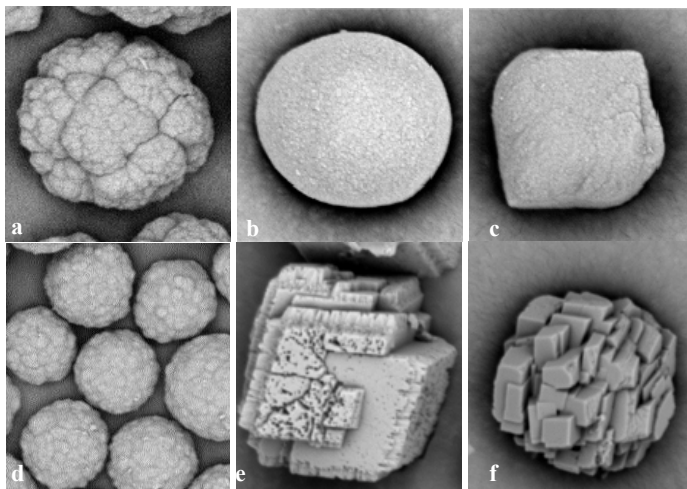


Fig. 1. SEM images of (a) bare CaCO_3 particles and some polymer/ CaCO_3 composites with: (b) PAMPSAA, (c) P(NVP-MA-Ox), (d) PHOS-*b*-PMAA, (e) xanthan, (f) alginate.

The differences observed in the polymer/ CaCO_3 composite structures (Fig. 1) could be ascribed to the chains flexibility, as statistic copolymers (PAMPSAA), block-copolymers (PHOS-*b*-PMAA) and polysaccharides (Xnt, Alg) were used.

The calcium carbonate/polymer microparticles showed in Fig. 1 were obtained from supersaturated aqueous solutions, in the presence of soluble polymers. The crystallization of calcium carbonate could also occur in a gas diffusion process [16,17]. The decomposition of ammonium (bi)carbonate in a

closed environment produce CO_2 and ammonia gas. The crystallization is achieved *via* the diffusion of CO_2 gas into a solution filled with calcium chloride (and polymer). Figure 2 shows some structures obtained on glass or polypropylene supports, and using CSA as soluble polymeric crystal modifier.

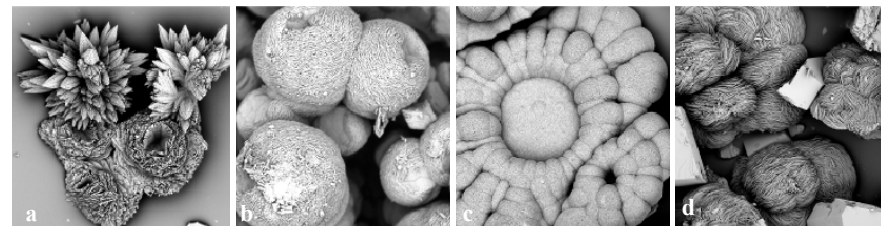


Fig. 2. SEM images of (a,b) bare CaCO_3 and (c,d) CSA/ CaCO_3 composite on glass (a,c) and polypropylene (b,d) substrate.

There are numerous factors (inorganic/organic ratio, polymer structure and concentration, generated of CO_2 , solutions pH, crystallization time, diffusion rate, and so on) which influence the CaCO_3 /polymer polymorphs characteristics (particles size, polymorphs type and ratio, crystallite size, charge density) and which can be used to tune the composite particles for specific applications. The comprehension of the way in which polymorph selection, as well as crystal shape and orientation are controlled in biomineralization would offer new opportunities for the design of novel biomimetic organic-inorganic composites for different applications.

1. Andreassen J.-P. Formation mechanism and morphology in precipitation of vaterite—nano-aggregation or crystal growth? // *J. Cryst. Growth* 274 (2005) 256–264.
2. Gebauer D., Völkel A., Cölfen H. Stable Prenucleation Calcium Carbonate Clusters // *Science* 322 (2008) 1819-1822.
3. Gorna K., Hund M., Vucak M., Gröhn F., Wegner G. Amorphous calcium carbonate in form of spherical nanosized particles and its application as fillers for polymers // *Mat. Sci. Eng.* 477 (2008) 217-225.
4. Wei W., Ma G.-H., Hu G., Yu D., Mcleish T., Su Z.-G., Shen Z.-Y. Preparation of Hierarchical Hollow CaCO_3 Particles and the Application as Anticancer Drug Carrier // *J. Am. Chem. Soc.* 130 (2008) 15808-15810.
5. Lakes R.S. Materials with structural hierarchy // *Nature* 361 (1993) 511-515.
6. Hernández-Hernández A., Gómez-Morales J., Rodríguez-Navarro A. B., Gautron J., Nys Y., García-Ruiz J.M. Identification of Some Active Proteins in the Process of Hen Eggshell Formation // *Cryst. Growth Des.* 8 (2008) 4330-4339.

7. Colfen H., Mann S. Higher-Order Organization by Mesoscale Self-Assembly and Transformation of Hybrid Nanostructures // *Angew. Chem. Int. Ed.* 42 (2003) 2350-2365.

8. Butler, M. F., Frith, W. J., Rawlins, C., Weaver, A. C. & Heppenstall-Butler M. Hollow Calcium Carbonate Microsphere Formation in the Presence of Biopolymers and Additives // *Cryst. Growth Des.* 9 (2009) 534-545.

9. Mihai M., Bucătariu F., Aflori M., Schwarz S. Synthesis and characterization of new CaCO₃ / poly(2-acrylamido-2-methylpropanesulfonic acid-co-acrylic acid) polymorphs, as templates for core/shell particles // *J. Cryst. Growth* 351 (2012) 23-31

10. Mihai M., Bucătariu F., Doroftei F. Synthesis and Characterization of New Hollow Calcium Carbonate/Polyanion Microspheres // *Rev. Chim.* 64(3) (2013) 338-342.

11. Mihai M., Schwarz S., Simon F. Nonstoichiometric Polyelectrolyte Complexes Versus Polyanions as Templates on CaCO₃ - Based Composite Synthesis // *Cryst. Growth Des.* 13 (2013) 3144-3153.

12. Mihai M., Mountrichas G., Pispas S., Stoica I., Aflori M., Auf der Landwehr M., Neda I., Schwarz S. Calcium carbonate microparticle templates using a PHOS-b -PMAA double hydrophilic copolymer // *J. Appl. Cryst.* 46 (2013) 1455-1466.

13. Damaceanu M.-D., Mihai M., Popescu I., Bruma M., Schwarz S. Synthesis and characterization of a new oxadiazole-functionalized maleic anhydride-N-vinyl-pyrrolidone copolymer and its application in CaCO₃ based microparticles // *React. Funct. Polym.* 72 (2012) 635-641.

14. Mihai M., Damaceanu M.-D., Aflori M., Schwarz S. Calcium carbonate microparticles growth templated by an oxadiazole-functionalized maleic anhydride-co-N-vinyl-pyrrolidone copolymer, with enhanced pH stability and variable loading capabilities // *Cryst. Growth Des.* 12 (2012) 4479-4486.

15. Mihai M., Socoliuc V., Doroftei F., Ursu E.-L., Aflori M., Vekas L., Simionescu B.C. Calcium Carbonate-Magnetite-Chondroitin Sulfate Composite Microparticles with Enhanced pH Stability and Superparamagnetic Properties // *Cryst. Growth Des.* 13 (2013) 3535-3545.

16. Faatz M., Grohn F., Wegner G. Mineralization of calcium carbonate by controlled release of carbonate in aqueous solution // *Mat. Sci. Eng. C* 25 (2005) 153-159.

17. Oaki Y., Adachi R., Imai H. Self-organization of hollow-cone carbonate crystals through molecular control with an acid organic polymer // *Polymer j.* 44 (2012) 612-619.

POLYELECTROLYTE MULTILAYERS WITH TUNED PROPERTIES AND THEIR INTERACTION WITH ENZYMES AND DYES

F. Bucătariu, C.-A. Ghiorghita, E. S. Dragan

"Petru Poni" Institute of Macromolecular Chemistry, Grigore Ghica Voda Alley 41A, Iasi 700487, Romania

fbucataru@icmpp.ro

Two types of polyelectrolyte multilayers (PEM), based on linear poly(ethyleneimine) [PEI(L)], branched PEI [PEI(B)], poly(vinylamine) (PVAm), chitosan (CS), poly(acrylic acid) (PAA) have been prepared using (i) a cross-linking method with 3,3',4,4'-benzophenonetetracarboxylic-dianhydride (BTCDA) or glutaraldehyde (GA)-mediated electrostatics and hydrogen bonds layer-by-layer assembly (Fig. 1), and (ii) polycation/polyanion layer-by-layer deposition followed by thermal cross-linking.

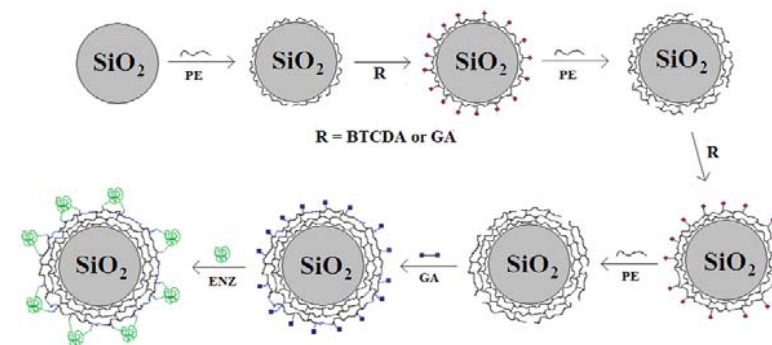


Fig. 1. Construction of PEM film onto silica microparticles and immobilization of enzymes on it.

Polyelectrolytes were adsorbed from salt-free aqueous solution, either onto silica microparticles, with particle diameter of 40 - 60 μm (Daisogel type) and 9 - 11 μm (Davisil type), or silicon wafers. In the layer-by-layer strategy the deposition conditions (pH, polymer concentration, ionic strength, charge density, temperature), and the nature of building blocks (polyelectrolytes, inorganic nanoparticles, biomacromolecules, dyes) have an important role on the driving

forces which lead to the formation of PEM [1-5]. An important goal in the application of PEM is to obtain a mechanical stable architecture under external stimuli and a good loading capacity for different molecular species. The chemical cross-linking with BTCDA and GA of the PEM films deposited onto solid surfaces resulted in a surface covered with carboxylic and amino groups. The PEM based on the single polycations deposited onto Daisogel and Davisil microparticles was studied by zeta-potential measurements (streaming potential, electrophoresis) and X-ray photoelectron spectroscopy (Fig. 2). After the construction of PEM, three enzymes (trypsin, pepsine and lysozyme) were immobilized onto Daisogel//PEM composite microparticles. The enzyme amount immobilized on the surface significantly depended on the isoelectric point of the enzyme.

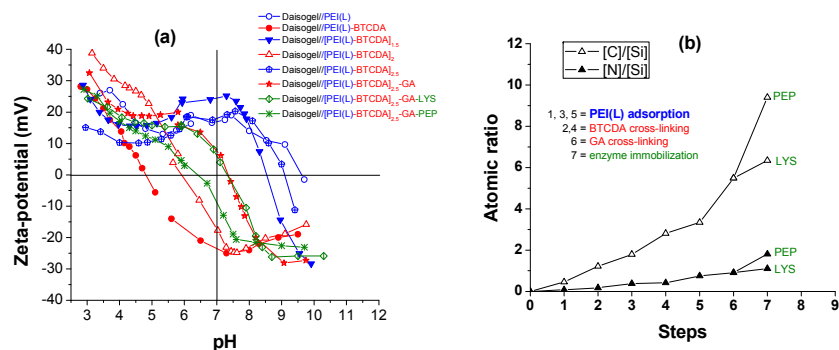


Fig. 2. Zeta-potential values (a) and atomic ratios (b) of Daisogel microparticles modified with PEI(L) and enzymes.

The atomic force microscopy (AFM) showed that the average height, h_a , and average roughness, R_a , of surface slightly increased after each modification step of the PEM.

To create pores inside the PEM architecture the PEM based on CS and PAA were subjected to different post-treatment strategies: (i) 5 min in water (pH = 2.4), and 60 min thermal treatment at 120 °C, and (ii) glutaraldehyde cross-linking of PEM. The influence of the contact time and the dye concentration on the dye adsorbed amount onto Daisogel// $(CS/PAA)_4$, before and after the post-treatment T_1 , can be seen in Fig. 3. Two isotherm models, Langmuir and Freundlich, were used to fit the experimental data of the MB sorption onto untreated and post-treated Daisogel// $(CS/PAA)_4$ composite microparticles.

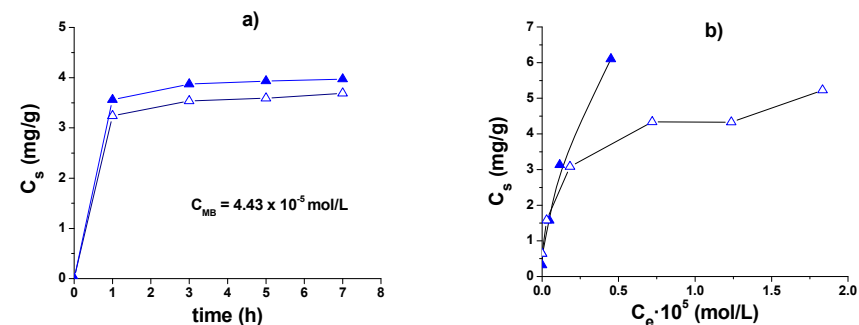


Fig. 3. Dependence of MB sorbed amount, C_s , onto Daisogel// $(CS/PAA)_4$ before (▲) and after (△) treatment T_1 on time (a) and equilibrium concentration, C_e (b).

The loading/release ability of $(CS/PAA)_n$ multilayers, before and after post-treatments, was investigated as a function of the number of double layers deposited using methylene blue, as a model cationic dye (Fig. 4a and b).

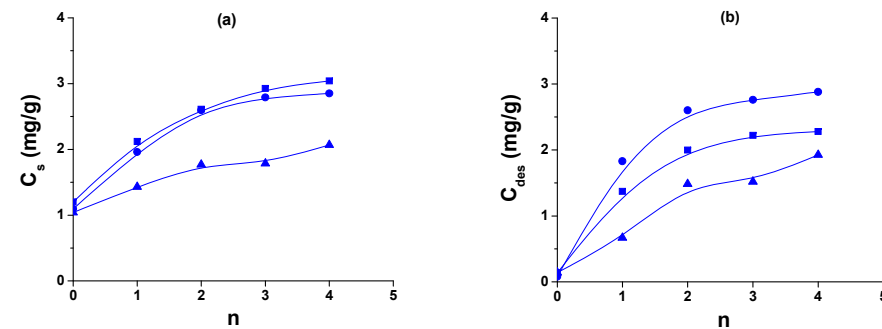


Fig. 4. The MB sorbed (a) and desorbed (b) amount after the 1st (■), the 2nd (●), and the 3rd (▲) sorption cycle onto Daisogel// $(CS/PAA)_n$ obtained after treatment T_1 , as a function of the PEM number, n .

After three cycles of sorption/desorption the sorption capacity of the Daisogel// $(CS/PAA)_n$ composite resulted after the thermal treatment (T_1), remained about the same, demonstrating the stability of PEM film onto Daisogel under the MB sorption/desorption conditions.

1. Berg M.C., Zhai L., Cohen R.E., Rubner M.F., Controlled drug release

from porous polyelectrolyte multilayers, *Biomacromolecules* 7 (2006) 357-364.

2. Bucatariu F., Fundueanu G., Hitruc G., Dragan E.S., Single polyelectrolyte multilayers deposited onto silica microparticles and silicon wafers, *Colloid Surf. A* 380 (2011) 111-118.

3. Irigoyen J., Han L., Llarena I., Mao Z., Gao C., Moya S.E., Responsive polyelectrolyte multilayers assembled at high ionic strength with an unusual collapse at low ionic strength, *Macromol. Rapid Commun.* 33 (2012) 1964-1969.

4. Ding C., Xu S., Wang J., Li Y., Chen P., Feng S., Controlled loading and release of methylene blue in layer-by-layer assembled polyelectrolyte films, *Mater. Sci. Eng. C* 32 (2012) 670-673.

5. Bucatariu F., Ghiorghita C.-A., Simon F., Bellmann C., Dragan E.S., Poly(ethyleneimine) cross-linked multilayers deposited onto solid surfaces and enzyme immobilization as a function of the film properties, *Appl. Surf. Sci.* 280 (2013) 812-819.

CYANATE ESTER RESIN/LAYERED SILICATE NANOCOMPOSITES: FROM SYNTHESIS TO CHARACTERIZATION

**K. G. Gusakova, O. M. Fainleib, O. P. Grigoryeva, N. S. Lavrenyuk,
M. V. Iurzhenko**

*Institute of Macromolecular Chemistry of the National Academy of Sciences of
Ukraine, Kharkivske shose 48, Kyiv 02160, Ukraine*
polymernano@ukr.net

Producing of polymer-based composites with nanofillers of different chemical nature is one of the leading up-to-date technologies providing significant enhancement in functional properties of the final materials, thermal stability, fire resistance, mechanical strength and toughness etc. [1]. The latter becomes more important when cross-linked polymers possessing significant fragility and brittleness are used as matrices [2]. Certainly, the reinforcement of high crosslink density high-performance cyanate ester resins (CER) [3] having the undeniable unique combination of high thermal stability, high glass transition temperature, high adhesion to different substrates, low dielectric loss and low water uptake, with nanofillers of different chemical nature (carbon nanotubes, graphene, layered silicates, etc.) is currently of a great interest [4, 5]. One of the most effective nanofillers are layered silicates, for example, montmorillonite [6]. Several studies have confirmed [4, 6, 7] the improvement in mechanical and thermal properties when exfoliated or at least intercalated structure of the final CER/clay nanocomposites was reached. To generate CER nanocomposite with well dispersed MMT the covalent bonding between nanofiller and polymer matrix is desirable. Therefore the present communication is focused on synthesis and characterization of CER-based nanocomposites filled with different reactive amino-functionalized MMTs. The basic strategy used was synthesis of CER *in situ* with nanoparticles of amino-functionalized MMT. The effect of different type and amount of the amino-groups on the MMT surface used and content of the MMT in the system on the CER matrix formation process as well as on the structure-property relationships for the final material is also discussed [8].

1. Olad A. *Polymer/Clay Nanocomposites in "Advances in Diverse Industrial Applications of Nanocomposites"*, ed. B. Reddy, InTech, Rijeka, 2011.

2. Demir K.D., Kukut M., Tasdelen M.A., Yagci Y. *New methods for the preparation of metal and clay thermoset nanocomposites in "Thermoset Nanocomposites"*, ed. V. Mittal, John Wiley & Sons, 2013.

3. *Chemistry and Technology of Cyanate Ester Resins*, ed. I. Hamerton, Glasgow, Chapman & Hall, 1994.

4. *Thermostable Polycyanurates: Synthesis, Modification, Structure and Properties*, ed. A.M. Fainleib, Nova Science Publishers Inc., 2011.

5. A. Fainleib, L. Bardash, G. Boiteux, O. Grigoryeva. Thermosetting Cyanate Ester Resins filled with CNTs in “*Advances in progressive thermoplastic and thermosetting polymers, perspectives and applications*”, eds. Ye. Mamunya, M. Iurzhenko, Technopress, Iasi, 2012.

6. Gangulia S., Deana D., Jordan K., Price G., Vaia R. Chemorheology of cyanate ester-organically layered silicate nanocomposites // *Polymer* 44 (2003) 6901-6911.

7. US Patent 20130131248 (2013). Tanase T., Kagawa H., Amou S. Organic-inorganic composite materials containing triazine rings and electrical devices using the same.

8. K. Gusakova, A. Fainleib, O. Grigoryeva, B. Youssef, J.-M. Saiter. Reactive dispersing and catalytic effect of amino-functionalized MMT in cyanate ester resins, *ROuen Symposium on Advanced Materials, 5-7 June, 2013, Abstract book*, P. 49.

NANOPOROUS HIGH-PERFORMANCE CYANATE ESTER RESINS: RECENT DEVELOPMENTS AND PERSPECTIVES

K. G. Gusakova¹, **A. M. Fainleib**¹, **O. P. Grigoryeva**¹, **O. N. Starostenko**¹,
J.-M. Saiter², **B. Youssef**², **A. Serghei**³, **E. Espuche**³, **F. Gouanve**³,
G. Boiteux³, **D. Grande**⁴

¹ *Institute of Macromolecular Chemistry of the National Academy of Sciences of Ukraine, 02160 Kyiv, Ukraine*
polymernano@ukr.net

² *AMME-LECAP International Laboratory, Institute for Material Research, Université de Rouen, Faculté des Sciences, BP12, 76801 Saint Etienne du Rouvray, France*

³ *Ingénierie des Matériaux Polymères, Université de Lyon, Université Lyon 1, IMP@LYON1, UMR CNRS 5223, 69622 Villeurbanne, France*

⁴ *Institut de Chimie et des Matériaux Paris-Est, UMR 7182 CNRS – Université Paris-Est Créteil, 94320 Thiais, France*

The present report summarizes the latest results obtained on novel thermostable nanoporous films based on cyanate ester resins (CER) for membrane and low permittivity materials. Under the framework of joint Ukrainian-French collaboration thermally stable nanoporous membranes with a high added value based on CER by simple and highly reproducible methods were developed and comprehensively characterized. The structure-property relationships were analyzed as a function of:

- 1) synthesis approach used;
- 2) using porogen or not;
- 3) chemical nature and reactivity of the porogen applied;
- 4) initial porogen content loaded;
- 5) method of porogen removal employed (pore formation method chosen).

The whole spectrum for characterization of structure and porosity organization as well as of basic chemical-physical properties of the nanoporous materials produced was involved including FTIR spectroscopy, NMR, SEM, TGA, DSC, DSC-based thermoporometry, DMTA, DRS, gel fraction content determination, density measurements, permeability measurements, etc. The comprehensive analysis of the experimental results has shown that nanoporous film materials developed combine high thermal and chemical stability with low

dielectric constant (decreasing from 3.3-3.4 for non-porous samples to 3.0 for nanoporous ones) and high gas permeability (especially for He) and high selectivity for He in separation of He/O₂ and He/CO₂ mixtures. Therefore, the CER-based nanoporous films produced may be regarded as promising membranes for commercial applications, namely in separation processes in aggressive media at evaluated temperatures, and in microelectronics.

Acknowledgement. The authors gratefully acknowledge the National Academy of Sciences of Ukraine and the Centre National de la Recherche Scientifique (France) for financial support through PICS project No. 5700 (Ukraine-France cooperation 2011-2013).

ORAL COMMUNICATIONS

OBTAINING OF TITANIA AND TITANIA/Ag OR Au NANOPARTICLES IN HYBRID PHOTOPOLYMERIZED MATRIX

A. L. Chibac, V. Melinte, T. Buruiana, E. C. Buruiana

“Petru Poni” Institute of Macromolecular Chemistry, Grigore Ghica Voda Alley
41A, Iasi 700487, Romania
andreea.chibac@icmpp.ro

The UV curing of (meth)acrylate derivatives represents a subject of great interest for modern (nano)technologies due to the various advantages of this photoprocess: high curing rate at room temperature, ecofriendly features, and low cost [1,2]. On the other hand, extensive researches are devoted to the development of hybrid organic–inorganic nanocomposites that combine the advantages of organic polymers (flexibility, good impact resistance, high processability) with those manifested by the inorganic materials (high mechanical strength, rigidity, good chemical resistance, enhanced thermal stability and particularly, optical properties) [3]. An interesting method for obtaining such hybrid materials is the combination of the photopolymerization process with the sol–gel reaction and the preparation *in situ* of noble metal nanoparticles into a polymer matrix.

In the present study we describe the preparation of sol–gel hybrid composites containing TiO₂ nanoparticles through photopolymerization of urethane oligodimethacrylate, 3-(acryloyloxy)-2-hydroxypropyl methacrylate, titanium butoxide and silyl derivative, 3-(trimethoxysilyl)propyl methacrylate. The last two compounds can undergo hydrolysis/condensation reactions in air, at room temperature, for a predetermined period of time. The photobehavior of different formulations was studied by FTIR spectroscopy and photoDSC technique in presence of photoinitiator (Irgacure 819). The final hybrid films were optically transparent, the transparency being evidence that the organic–inorganic phase separation is in the scale under 400 nm. The presence of TiO₂ nanoparticles in the polymer matrix is also confirmed by UV-Vis spectrum, the samples having a strong absorption at a wavelength around 400 nm. Furthermore, in some formulations, silver or gold precursor (AgNO₃/AuBr₃) was incorporated before photopolymerization, in order to achieve sol–gel materials doped with silver/gold nanoparticles. The formation of silver/gold nanoparticles through the reduction process of silver/gold ions in the presence of the Irgacure 819 was investigated by UV-Vis spectroscopy. In this regard, the absorption peak originating from the surface plasmon resonance of silver nanoparticles appeared in the range of 410–440 nm, while for the gold nanoparticles this parameter is around 520–540 nm. The

existence of silver/gold nanoparticle is confirmed by the color of the resultant composites films (brown or purple), TEM and X-ray analysis.

Acknowledgements

This work was financially supported by CNCIS-UEFISCDI, project number PN-II-ID-PCE-2011-3-0164 (40/5.10.2011).

1. Yagci Y., Jockusch S., Turro N. J. Photoinitiated polymerization: advances, challenges, and opportunities // *Macromolecules* 43 (2010) 6245–6260.
2. Chibac A., Melinte V., Buruiana T., Balan L., Buruiana E. C. One-pot synthesis of photocrosslinked sol–gel hybrid composites containing // *Chem Eng J.* 200-202 (2012) 577–588.
3. Yagci Y. New photoinitiating systems designed for polymer/inorganic hybrid nanocoatings // *J. Coat. Technol. Res.* 9 (2012) 125–134.

**MACROPOROUS ICE-TEMPLATED METHACRYLIC ACID
BASED HYDROGELS WITH CONTROLLED
RESPONSIVITY**

A.I. Cocarta¹, M. Gierszewska-Druzynska², E.S. Dragan^{1*}

¹ "Petru Poni" Institute of Macromolecular Chemistry, Grigore Ghica Voda Alley
41A, Iasi 700487, Romania

ana_irinac@yahoo.com, sdragan@icmpp.ro

² "Nicolaus Copernicus" University, Gagarina 7, 87-100 Torun, Poland

Hydrogels are three-dimensional high molecular weight networks composed of a polymer backbone, water and a cross-linking agent. [1] They swell considerably in an aqueous medium [2] and demonstrate extraordinary capacity (>20%) for imbibing water into the network structure. Due to their resemblance to living tissues they are widely applied in medicine, in controlled drug delivery, tissue engineering, cell separation etc. [1, 3] They are also useful in wastewaters remediation. [4]

Conventional hydrogels are characterized by a low equilibrium swelling and a low mechanical strength. These disadvantages could be improved by obtaining macroporous hydrogels. Formation of macroporous hydrogels could be performed by: cross-linking polymerization in the presence of a pore-forming agent, lyophilization of the hydrogel swollen in water, and cryogelation. [5-7] Cryogelation is a technique of synthesis of organic or inorganic materials in aqueous media at temperatures lower than the freezing point of the pure solvent. Cryogel preparation can be divided into three main stages: (I) preparation of a solution of monomers or polymers with a cross-linker, (II) freezing of the system, and (III) thawing (Fig. 1).

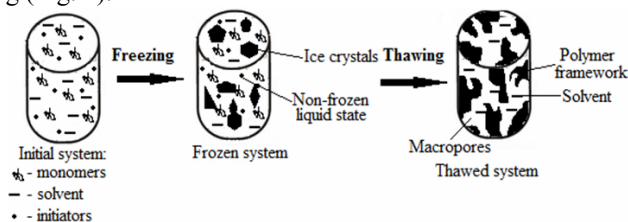


Fig. 1. Cryogel preparation.

Advantages of cryogelation in the preparation of hydrogels consist of the absence of any organic porogen, the ice crystals playing the role of inert template, the microstructure of the gel being the negative replica of the ice crystals. Thus

cryogelation is a low cost and very friendly technique for the fabrication of supermacroporous gels [8].

The aim of this study was to synthesize some cryogels at -18 °C, having cross-linked poly(methacrylic acid-co-acrylamide), P(MAA-co-AAm), as a matrix. N,N'-methylenebisacrylamide (BAAm) was used as a crosslinker. Polymer matrix was obtained by free radical cross-linking polymerization of monomers in aqueous medium using the redox initiator system consisting of ammonium persulfate (APS) and N,N,N',N'- tetramethylethylenediamine (TEMED). The parameters varied in the synthesis of cryogels were: the molar ratio between MMA and AAm, the cross-linking ratio, and the initial concentration of monomers. The sample code consists of CG followed by three numbers separated by dots, which represent: the first number is the molar ratio between MAA and AAm, the second number is the cross-linking ratio (moles of AAm to one mole of BAAm), and the third number is the initial monomer concentration. For example, CG55.20.10 means 5 moles MAA to 5 moles of AAm, cross-linking ration 1/20, and monomer concentration of 10%.

The gels have been characterized first by the swelling kinetics in water. In Fig. 2 some results of cryogels swelling are shown.

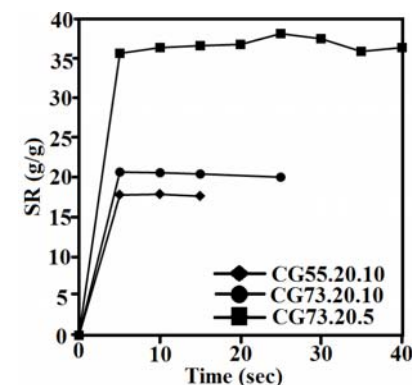


Fig. 2. Swelling behavior of the analyzed cryogels.

In general, it was found that at the initial concentration of monomers of 10 wt.%, the equilibrium swelling ratio, SR_{eq} , increased from about 18 g/g gel up to about 21 g/g gel, when the molar ratio between MAA and AAm increased from 5:5 up to 7:3. The decrease of the initial monomer concentration from 10 to 5 wt.%, for the molar ratio between MAA and AAm of 7:3, led to the increase of SR_{eq} from 21 g/g gel up to 35 g/g gel. The essential feature of cryogels was their superfast swelling, the time necessary to reach the equilibrium swollen state being 3-5 sec, irrespective of the molar ratio between monomers.

Also, the state of water in the synthesized cryogels was evaluated. The

Co2

nature of water in hydrogels is very important in understanding their equilibrium and dynamic swelling behavior as well as in analyzing a solute transport and other diffusive properties of such systems. Water sorbed by polymers can be classified into three main categories; free water, freezable bound water, and non-freezable bound water. There are different techniques used to analyze the state of water in polymeric systems, the most used being: differential scanning calorimetry (DSC), NMR spectrometry, and FTIR spectroscopy. DSC is in many ways the most convenient and informative method.

The state of water in cryogels was analyzed by DSC. A Pyris Diamond DSC (Perkin Elmer USA) differential scanning calorimeter equipped with an intracooler accessory was used to monitor both bound as well as free water in cryogels. The amount of water able to crystallize (freezable water), W_f , was determined by direct integration of the melting endotherm, using double distilled water as a reference and assuming both melting enthalpies for freezing free water (W_{ff}) and freezing bound water (W_{fb}) to be the same as that of bulk water ($\Delta H_0=334 \text{ J}\cdot\text{g}^{-1}$). The amount of freezable water was calculated from the following equation:

$$W_f = W_{ff} + W_{fb} = \frac{\Delta H_m}{\Delta H_0}$$

where ΔH_m is the melting enthalpy for freezable water in crygel obtained from the DSC thermogram and ΔH_0 is the melting enthalpy of pure water. The total amount of non-freezing bound water, W_{nf} , was obtained from the difference between the amount of sorbed water, W_c , and the total amount of freezable water W_f .

Fig. 3 shows the DSC curves obtained for the cryogel CG55.20.10.

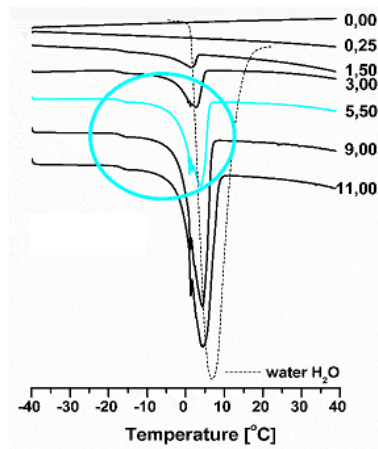


Fig. 3. The DSC curves obtained for the cryogel sample.

Co2

For all the systems analyzed, no peaks were observed below a certain water content. The absence of endothermic peaks above a certain water content threshold indicates that this water is of the nonfreezable bound type. Generally, for all studied hydrogels of higher water content, the endothermic peaks are broad and structured. Cryogels exhibit poorly resolved multi-peaks with distinct submaxima composed of several endothermic peaks. Because of the overlapping of the two peaks, their quantitative analysis was not possible. The amounts of this kind of water (able to freeze) in cryogels can be only qualitatively compared.

Based on the DSC curves, a plot of the enthalpy of melting of freezing water per gram of polymer versus the water content, W_c was obtained. The slope of the linear plot represents the “average apparent” value of the melting enthalpy associated with the freezable water (ΔH_m), and the intercept with the horizontal axis corresponds to the maximum amount of non-freezable water ($W_{nf,max}$) in the hydrogel, defined as the maximum amount of water present in the polymer, which is not associated with any endothermic peak.

After analyzing all the samples we obtained a plot of non freezing water content versus the molar ratio between MAA and AAm. It was found that the amount of this type of water in cryogel samples increases with increasing MAA/AAm molar ratio. Also, initial monomer concentration and monomer/crosslinker ratio affects water state in analyzed cryogels.

1. Bajpai A.K., Shukla S.K., Bhanu S., Kankane S. Responsive polymers in controlled drug delivery // Prog. Polym. Sci. 33 (2008) 1088-1118.
2. Peppas N.A., Huang Y., Torres-Lugo M., Ward J.H., Zhange J. Physio-chemical foundation and structure design of hydrogel in medicine and biology // Annu. Rev. Biomed. Eng. 2 (2000) 9-29.
3. Yang J., Chen J., Pan D., WanY., Wang Z. pH-sensitive interpenetrating network hydrogels based on chitosan derivatives and alginate for oral drug delivery // Carbohydr. Polym. 92 (2013) 719-725.
4. Dragan E.S., Perju M.M., Dinu M.V. Preparation and characterization of IPN composite hydrogels based on polyacrylamide and chitosan and their interaction with ionic dyes // Carbohydr. Polym. 88 (2012) 270-281.
5. Lozinsky V.L., Plieva F.M., Galaev I.M., Mattiasson B. The potential of polymeric cryogels in bioseparation // Bioseparation 10 (2001) 163-188.
6. Hajizadeh S., Kirsebom H., Galaev I.Y., Mattiasson B. Evaluation of selective composite cryogel for bromate removal from drinking water // J. Sep. Sci. 33 (2010) 1752-1759.
7. Dinu M.V., Prádny M., Drăgan E.S., Michálek J. Ice-templated hydrogels based on chitosan with tailored porous morphology // Carbohydr. Polym. 94 (2013) 170- 178.

8. Dragan E.S., Lazar M.M., Dinu M.V., Doroftei F. Macroporous composite IPN hydrogels based on poly(acrylamide) and chitosan with tuned swelling and sorption of cationic dyes // Chem. Eng. J. 204–206 (2012) 198–209.

HYBRID NANOARCHITECTONICS BASED ON POLYMERS – LAYERED DOUBLE HYDROXIDES

L. E. Bibire^{1,2}, M. Bercea¹, S. Morariu¹, G. Carja²

¹"Gh. Asachi" Technical University, Faculty of Chemical Engineering and Environmental Protection, Department of Chemical Engineering, 71 Bd. Mangeron, 700050 Iasi, Romania

²"Petru Poni" Institute of Macromolecular Chemistry, 41-A Grigore Ghica Voda Alley, 700487 Iasi, Romania

livia.bibire@gmail.com

Hybrids based on mixtures of layered double hydroxides (LDH) - poly(vinyl alcohol) (PVA) - chitosan (CH) were prepared by using the structural reconstruction of the calcined MgAlLDH layered clay. Hybrid nanoarchitectonics based on homogeneous solutions of polymers and clays are important for the development of new composite materials - in the conditions that they could not only join together the properties of the polymers and the specific characteristics of the layered clay but also could develop new specific features.

This work presents the physical-chemical characteristics, pointing out on the nanoarchitectonics, of LDH/PVA/CH hybrids. The formation of interpolymer complexes through hydrogen bonds was evidenced for well-defined polymer compositions. The new hybrid structures were then designed for CH/PVA complexes in the presence of MgAlLDH and their behavior was investigated through rheological measurements as a function of pH. The micromorphological features of LDH/PVA/CH hybrids were investigated using scanning electron microscopy (FESEM).

Acknowledgement. This work was supported by a grant of the Romanian National Authority for Scientific Research, CNCS-UEFISCDI, project number PN-II-ID-PCE-2011-3-0199 (contract number 300/2011).

MULTILAYER FILMS BASED ON MALEIC ACID TERPOLYMERS AND WEAK POLYCATIONS WITH pH-DEPENDENT LOADING AND RELEASE BEHAVIOUR OF SMALL MOLECULES

I. Popescu, D. Timpu

*“Petru Poni” Institute of Macromolecular Chemistry, Grigore Ghica Voda Alley
41A, Iasi 700487, Romania
ipopescu@icmpp.ro*

Nanostructured architectures can be obtained by alternant deposition of complementary polyelectrolytes on different supports [1] and were proposed for various biomedical applications: in controlled drug release, as coatings of implantable materials, in tissue engineering, in the construction of biosensors [2]. When weak polyelectrolytes are used in the multilayers fabrication, the properties of the obtained films can be tailored by the variation of the solution pH during the assembly process [3] or in the post-treatment process [4,5].

In our work we used anionic polyelectrolytes with strong and weak acid groups in the layer-by-layer (LbL) deposition. The weak groups assure the pH-responsiveness of the films and the introduction of strong acid groups lead to the increased film stability. Thus, poly[(maleic acid-*alt*-styrene)-*co*-2-acrylamido-2-methyl-1-propansulfonic acid] was deposited in alternation with poly(allylamine hydrochloride) or chitosan hydrochloride in order to obtain stable films whose loading/release capacity was pH-dependent.

Two maleic acid terpolymers with different ratio between the sulfonic and the carboxylic acid group were synthesized and characterized by potentiometric titration, FTIR, and ¹H NMR spectroscopy. New LbL films were then obtained from the aqueous solution of these copolymers at pH = 2.5 and 5.5. The layer growth was monitored by UV spectroscopy and the films morphology investigated by AFM showed that the films thickness increase with the decrease of the assembling pH from 5.5 to 2.5 and with the increase of the carboxylic acid amount from the terpolymer. The polycation nature also influences the films structure, the thicker films being obtained when chitosan was used instead of synthetic poly(allylamine hydrochloride).

In order to examine the utility of the multilayer films as potential carriers for small molecules, the cationic dye Rhodamine 6G was used as model. Glass slides coated with 19 layers were immersed in R6G solutions at different pHs. Generally, the amount of the dye that entered the films increased with the solution pH due to the dissociation of the carboxylic groups from the polyanion. The

fabrication pH and the ratio between weak and strong acid moieties from the maleic terpolymer also influenced the dye loading. Anyway, the dye molecules adsorbed into the polymeric films formed aggregates, as shown by the UV spectra.

The modification of the films topography after the exposure to basic aqueous solution (without dye) was investigated by AFM. A certain rearrangement of the layers was observed, but the films roughness and its variation with the scan-size were not influenced much by the pH change, showing that the films were not removed by the exposure at basic pH.

Dye release studies showed that at acidic pH (where both of the carboxylic groups from maleic acid units become predominantly uncharged) the dye was quickly released, but at neutral pH only 55% of the dye was released after 16 hours.

In conclusion, stable films with controlled architecture can be obtained with poly[(maleic acid-*alt*-styrene)-*co*-2-acrylamido-2-methyl-1-propansulfonic acid] and weak polycations by the variation of the terpolymer composition, assembling pH or polycation structure. The films assembled at acidic pH can load large amounts of small dye/drug molecules from basic solution and release them by decreasing the pH of the medium. This property can be used in drug controlled release applications.

Acknowledgement: This work was supported by a grant of the Romanian Ministry of Education, CNCS – UEFISCDI, project number PN-II-RU-PD-2012-3 -0059.

1. Decher G., Hong J.D., Schmitt J. Buildup of ultrathin multilayer films by a self-assembly process: III. Consecutively alternating adsorption of anionic and cationic polyelectrolytes on charged surfaces // *Thin Solid Films* 210–211(1992) 831-835.
2. Boudou T., Crouzier T., Ren K., Blin G., Picart C. Multiple functionalities of polyelectrolyte multilayer films: new biomedical applications // *Adv. Mater.* 21 (2009) 1-27.
3. Shiratori S.S., Rubner M.F. pH-dependent thickness behavior of sequentially adsorbed layers of weak polyelectrolytes // *Macromolecules* 33 (2000) 4213-4219
4. Mendelsohn J.D., Barrett C.J., Chan V.V., Pal A.J., Mayes A.M., Rubner M.F. Fabrication of microporous thin films from polyelectrolyte multilayers // *Langmuir* 16 (2000) 5017-5023.
5. Glinel K., Déjugnat C., Prevot M., Schöler B., Schönhoff M., Klitzing R.V. Responsive polyelectrolyte multilayers // *Colloids Surf. A: Physicochem. Eng. Asp.* 303 (2007) 3–13

PLASMA POLYMER FILMS FOR QCM BIOACTIVE SURFACES

M. Asandulesa¹, G. B. Rusu^{2,3}, M. Barboiu³, M. I. Totolin¹, V. Harabagiu¹

¹ “Petru Poni” Institute of Macromolecular Chemistry, Grigore Ghica Voda Alley
41A, Iasi 700487, Romania

asandulesa.mihai@icmpp.ro

² Faculty of Physics, Alexandru Ioan Cuza University of Iasi, 11 Carol I Boulevard,
Iasi 700506, Romania

³ Institut Européen des Membranes, Adaptive Supramolecular Nanosystems Group,
ENSCMUMII-CNRS UMR-5635, Place Eugène Bataillon, CC 047, F-34095,
Montpellier, France

Chemical reactions induced by cold plasmas are recognized in synthesis of macromolecular networks by fragmentation of organic compounds into active species and their recombination on the surfaces in contact with plasma. The final compounds are conventionally called plasma polymer films. Such materials are adherent to different substrates, durable, mechanically resistant and thermally stable. They can be deposited as thin layers with controllable thickness and a wide range of starting precursors can be used in the synthesis process [1].

Plasma polymerization represents a technological solution to coat various substrates with functional polymer layers. We employed this technique to modify the surface properties of standard QCM electrodes. Our aim relies to compare the biosensing properties of these QCM electrodes with existing commercial ATTANA polystyrene electrodes [2]. The plasma polystyrene QCM electrodes present a higher adsorption of Concanavalin A (ConA) and Bovine Serum Albumin (BSA) proteins when compared with the commercial coated polystyrene ones.

1. M. Asandulesa, I. Topala, V. Pohoata, Y.-M. Legrand, M. Dobromir, M. Totolin, N. Dumitrascu Chemically polymerization mechanism of aromatic compounds under atmospheric pressure plasma conditions, *Plasma Process. Polym.* 10 (2013) 469-480.

2. G.-B. Rusu, M. Asandulesa, I. Topala, V. Pohoata, N. Dumitrascu, M. Barboiu Atmospheric pressure plasma polymers for tuned QCM detection of protein adhesion, *Biosensors and Bioelectronics*, <http://dx.doi.org/10.1016/j.bios.2013.09.035>.

AN AFM STUDY OF AZO-POLYIMIDE PERIODIC 3D NANOGROOVES INDUCED BY LASER IRRADIATION

I. Stoica¹, L. Epure², I. Sava¹, V. Damian³, N. Hurduc²

¹ “Petru Poni” Institute of Macromolecular Chemistry, Aleea Grigore Ghica Voda
41A, 700487, Iasi, Romania

stoica_iuliana@icmpp.ro

² Department of Natural and Synthetic Polymers, “Gheorghe Asachi” Technical
University of Iasi, Bd. Mangeron 71, Iasi, Romania

³ National Institute for Laser, Plasma and Radiation Physics, Str. Atomistilor 409,
077125 Bucharest-Magurele, Romania

Polymeric materials are important candidates for applications at the interface between biological systems and electronics. Therefore, polymers can be chemical or physical tailored to interact with biological surroundings, while at the same time being able to interface with electronics. The alignment of the molecules, which can be induced by micrometric or nanometric grooved substrates varying in height, width and spacing, has many significant applications in molecular electronics, biotechnology, optoelectronic devices and liquid crystal display manufacturing.

There are several methods used to generate micro- and nanopatterned polymer surfaces, a single step processing technique able to create surface relief modulation preserving material properties being UV laser irradiation. The polymeric materials suitable for such a technique are those who have a photochromic behavior, namely azopolymers [1, 2]. Among them, azo-polyimides, due to their diversity of the chemical structure and the acceptance of a wide variety of chemical additives, allow tailoring their physical characteristics to meet the requirements of many different applications. Additionally, the presence of the azobenzene side groups in the polyimide chemical structure induce the surface relief grating by laser irradiation [3, 4].

Based on the photochromic behavior induced in the polymeric materials by the UV light [3, 5-6], we have studied the possibility to obtain tridimensional surface structuration by laser irradiation. Some films of polyimide with azobenzene groups in the side chain prepared using the method of two-step polycondensation reaction were irradiated using a Nd:YAG laser, with two different incident fluence of 8.4 mJ/cm² and 35 mJ/cm² and different number of pulses, starting from 1 to 100. Atomic force microscopy (AFM) was employed to correlate the laser-induced

tridimensional nanogrooved surface relief with the irradiation conditions.

Using the same numbers of irradiation pulses and increasing the incident fluence, the nanogrooves depth determinate from the height images cross-section profiles increased even tens of times. For a large number of pulses of irradiation (till 100) and incident fluence of 8.4 mJ/cm², the film was uniformly patterned, but when using 35 mJ/cm², the precision of the modulated relief was reduced only after 15 pulses of irradiation. This behavior could be explained by means of two different mechanisms, one that suppose the film photo-fluidization due to the cis-trans isomerization processes of the azo-groups and the second one responsible for the directional mass displacement [7].

The dominant surface direction and parameters like isotropy, periodicity, and period were evaluated from the polar representation for texture analysis, revealing the appearance of ordered and directionated nanostructures for most of the experimental conditions.

The graphical studies of the functional volume parameters have evidenced the improvement of the relief structuration during surface nanostructuring and the ability of the modulated surfaces to carry out their function in a tribological contact, for different applications.

The correlation of these statistical texture parameters with the irradiation characteristics is important in controlling the alignment of either the liquid crystals or the cells/tissues on patterned azo-polyimide surfaces for optoelectronic devices and implantable biomaterials, respectively.

1. Petrova T.S., Mancheva I., Nacheva E., Tomova N., Dragostinova V., Todorov T., Nikolova L. New azobenzene polymers for lightcontrolled optical elements // J Mater Sci: Mater Electron 14 (2003) 823–824.

2. Zucolotto V., Barbosa Neto N.M., Rodrigues J.J. Jr, Constantino C.L., Zilio S.C., Mendonsa C.R., Aroca R.F., Olivera O.N. Jr. Photoinduced phenomena in layer-by-layer films of poly(allylamine hydrochloride) and Brilliant Yellow azodye // J Nanosci Nanotechnol 4 (2004) 855–860.

3. Sava I., Resmerita A.M., Lisa G., Damian V., Hurduc N. Synthesis and photochromic behavior of new polyimides containing azobenzene side groups // Polymer 49 (2008)1475–1482.

4. Schab-Balcerzak E., Sobolewska A., Miniewicz A., Jurusik J. Chromophore concentration effect on holographic grating formation efficiency in novel azobenzene-functionalized polymers // Polym Eng Sci 48 (2008) 1755–1767.

5. Sava I., Sacarescu L., Stoica I., Apostol I., Damian V., Hurduc N. Compared photochromic properties of some polymers containing azobenzene side groups // Polym Int 58 (2009)163–170.

6. Sava I, Hurduc N, Sacarescu L, Apostol I, Damian V. Study of the nanostructuring capacity of some azopolymers with rigid or flexible chains // High Perform Polym 25 (2013) 13–24.

7. Stoica I., Epure L., Sava I., Damian V., Hurduc N. An atomic force microscopy statistical analysis of laser-induced azo-polyimide periodic tridimensional nanogrooves // Microsc. Res. Tech. 76 (2013) 914–923.

**CHROMITE NANOPARTICLES
SELF-ASSEMBLING INTO SMECTIC MESOPHASES**

M. Iacob^{1,2}, M. Cazacu², C. Racles¹, M. Ignat¹, V. Cozan¹, L. Sacarescu¹, D. Timpu¹, M. Kajňaková³, M. Botko³, A. Feher³, C. Turta^{1,2}

¹ "Petru Poni" Institute of Macromolecular Chemistry, Grigore Ghica Voda Alley 41A, Iasi 700487, Romania

mcazacu@icmpp.ro

² Institute of Chemistry of ASM, Academiei str. 3, Chisinau 2028, Republic of Moldova.

iacob.mihai@icmpp.ro

³ Center of Low Temperature Physics, Faculty of Science, P. J. Šafárik University, Park Angelinum 9, 04154 Košice, Slovakia

Iron oxides-based nanomaterials attracted the attention of researchers due to their possible use in applications such as: drug delivery, magnetic storage media, contrast agents in NMR imaging, biosensor application, catalyst, magnetic inks [1]. Organic-coated iron-chromium oxide (chromite) nanoparticles have been prepared by using the thermal-induced ligands exchange procedure. The main characteristics and behaviors of the obtained nanoparticles were investigated by combined techniques. Thus, the size of the formed nanoparticles was estimated by transmission electron microscopy, wide angle X-rays diffraction (WAXD), and small angle X-ray scattering, the found average values being around 11 nm. The bimetallic nature of the nanoparticles was emphasized by EDX and confirmed by WAXD. The behaviors due to the co-existence of the organic coatings and metallic core were studied by thermogravimetric analysis, differential scanning calorimetry and polarized optical microscopy. The coated bimetallic nanoparticles proved to be thermostable up to 252°C and thermotropic showing a highly organized crystalline smectic mesophase (3D plastic mesophase). The results of the magnetic measurements suggest superparamagnetic behavior of the iron-chromium oxide nanoparticles and a weak ferromagnetic behavior.

Acknowledgements

This research was financially supported by SOP, Contract 129/2010-POLISILMET and project PN-II-ID-PCE-212-4-0261

1. *Sophie Laurent et al.*, Magnetic Iron Oxide Nanoparticles: Synthesis, Stabilization, Vectorization, Physicochemical Characterizations, and Biological Applications // Chem. Rev. 108 (2008) 2064–2110.

**NANO-SCALE AGGREGATES OF A β (1-16) FRAGMENT
PEPTIDES IN THE PRESENCE OF HEAVY METALS**

A. A. Mitel^{1,2}, M. Mihai², M. Murariu²

¹ "Gh. Asachi" Technical University, Faculty of Chemical Engineering and Environmental Protection, 71 Mangeron Bd., Iasi 700050, Romania

alexandra.mitel@yahoo.com

² "Petru Poni" Institute of Macromolecular Chemistry, 41A Grigore Ghica Voda Alley, Iasi 700487, Romania

manuelam@icmpp.ro

Amyloid-beta (known also as A β or A-beta or beta-amyloid) is a peptide of 36–43 amino acids that appears to be the main constituent of amyloid plaques in the brains of Alzheimer's disease (AD) patients (Fig. 1).

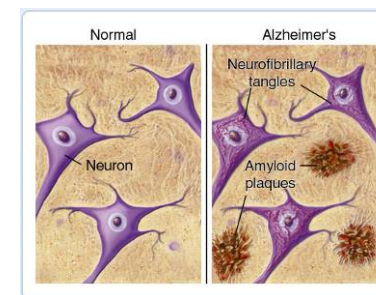


Fig. 1. Schematic representation of Amyloid- β (A β) aggregates associated with Alzheimer's disease.

The transformation process from α -helix to β -sheet structures appears to be one of the major factors in the genesis and evolution of a variety of neurodegenerative diseases such as AD, Parkinson's disease (PD), and several prion diseases [1,2]. Metal-based reactions of some polypeptides and proteins are considered as a common denominator for neurodegenerative diseases (Figure 2) [3,4]. Amyloid- β (A β) aggregates are associated with Alzheimer's disease (AD), and may be promoted by the trace amounts of metal ions like aluminium, iron, zinc or copper [5-11]. For example, copper ions cause the peptide aggregation to a great extent and highly increase the neurotoxicity exhibited by A β 1-40 in cell culture [11].

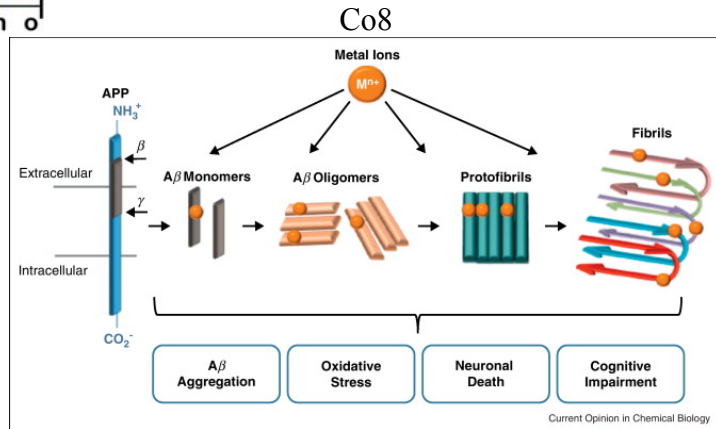


Fig. 2. Metal-associated amyloid- β species in Alzheimer's disease [11].

In this context, one normal (M0) and two mutant A β 1-16 peptides, in which histidine residues were replaced by alanine (M1) and by serine (M2) ones, were investigated using copper, aluminum, iron, silver and nickel ions as trace amounts of metal ions. Synthesis of β -amyloid fragment peptides was carried out by SPPS according to Fmoc strategy. Electrospray ionization mass spectrometry (ESI-MS) was used to characterize peptides and their complexes with metal ions, as well as their conformational changes; the spectra were acquired in the 50-2000 m/z range. SEM (Scanning Electron Microscope type Ultra plus-Carl Zeiss NTS), CD (MFP-3D device from Asylum Research, USA), and AFM (SPM Solver PRO-M AFM, Moscow, Russia) studies were done at various pH and peptide:metal ratios.

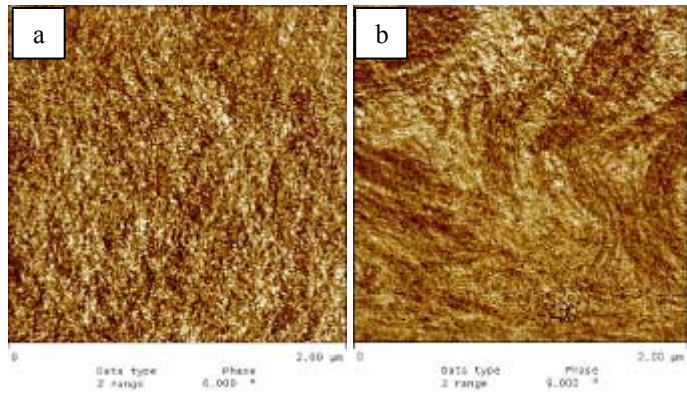


Fig. 3. AFM phase images of normal A β 1-16 peptide (M0) adsorbed on a glass surface from H₂O-based solutions (a) and Al₂SO₄ aqueous solutions (b).

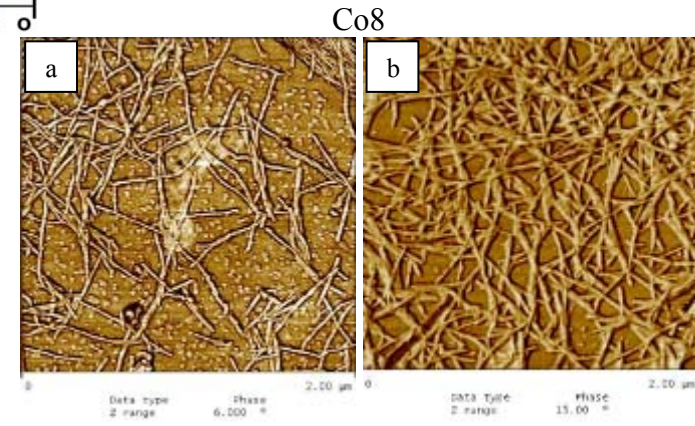


Fig. 4. AFM phase images of alanine modified A β 1-16 peptide (M1) adsorbed on a glass surface from H₂O-based solutions (a) and Al₂SO₄ aqueous solutions (b).

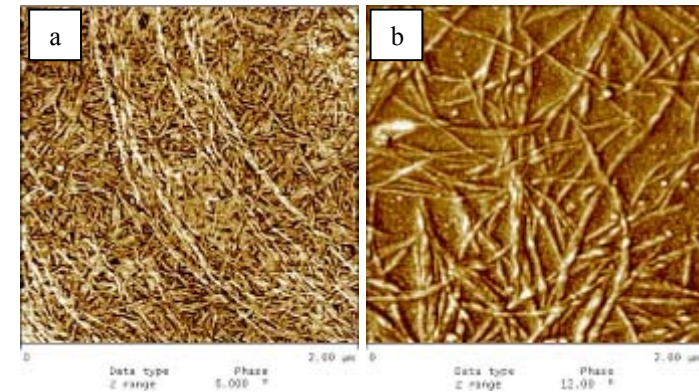


Fig. 5. AFM phase images of serine modified A β 1-16 peptide (M2) adsorbed on a glass surface from H₂O-based solutions (a) and Al₂SO₄ aqueous solutions (b).

There was demonstrated a close relationship between pH, metal concentration and the proportion of conformers of A β (1-16) fragments. Metal induced peptide aggregation was evidenced by AFM (Figures 3-5) and SEM. Such findings suggest that N-terminal sequence of A β peptides has the capability to be involved in metal binding associated with AD. However, it is not clear why some people do form such aggregates and others not. Consequently, further research is needed to explain metal induced aggregates associated with AD and ROS formation.

Acknowledgment: The author gratefully acknowledges the financial support from Romanian Government (Contract CNCSIS IDEI 313/2011).

1. Dobson C. M. Getting out of shape-protein misfolding diseases // Nature 418 (2002) 729–730.
2. Pagel K., Vagt T., Kohajda T., Koksche B. From α -helix to β -sheet – a reversible metal ion induced peptide secondary structure switch // Org. Biomol. Chem. 3 (2005) 2500-2502.
3. Bush A. I. Metals and neuroscience // Curr. Opin. Chem. Biol. 4 (2000) 184–191.
4. Selkoe D. J., Schenk D. Alzheimer's disease: molecular understanding predicts amyloid-based Therapeutics // Annu. Rev. Pharmacol. Toxicol. 43 (2003) 545-584.
5. Tougu V., Karafin, A., Palumaa, P. Binding of zinc(II) and copper(II) to the full-length Alzheimer's amyloid-beta peptide // J. Neurochem. 104 (2008) 1249-1259.
6. Murariu M., Dragan E. S., Drochioiu G. ESI-MS approach of conformationally-induced metal binding to oligopeptides // Eur J Mass Spectrom, 16 (2010) 511-521.
7. Murariu M., Dragan E. S., Drochioiu G. Model peptide-based system used for the investigation of metal ions binding to histidine-containing polypeptides // Biopolymers, 93 (2010) 497-508.
8. Drochioiu G., Manea M., Drăgușanu M., Murariu M., Drăgan E. S., Petre B. A., Mezo G., Przybylski M. Interaction of β -amyloid(1-40) peptide with pairs of metal ions: an ESI-MS model study // Biophys. Chem. 144 (2009) 9-20.
9. Murariu M., Dragan E. S., Drochioiu G. Synthesis and mass spectrometric characterization of a metal-affinity decapeptide: copper-induced conformational alterations // Biomacromolecules 8 (2007) 3836-3841.
10. Ma Q. F., Hu J., Wu W. H., Liu H. D., Du J. T., Fu Y., Wu Y. W., Lei P., Zhao Y. F., Li Y. M. Characterization of copper binding to the peptide amyloid-beta(1-16) associated with Alzheimer's disease // Biopolymers 83 (2006) 20-31.
11. Pithadia A. S., Lim M. H. Metal-associated amyloid- β species in Alzheimer's disease // Current Opinion in Chemical Biology 16 (2012) 67–73.

POLYELECTROLYTE MULTILAYERS OF CHITOSAN AND POLY(ACRYLIC ACID) CONSTRUCTED ONTO PLANAR SURFACES AND THEIR INTERACTION WITH A MODEL CATIONIC DYE

C.-A. Ghiorghita, F. Bucatariu, E.S. Dragan

“Petru Poni” Institute of Macromolecular Chemistry, Grigore Ghica Voda Alley
41A, Iasi 700487, Romania
claudiu.ghiorghita@icmpp.ro

Layer-by-layer (LbL) assembly is one of the most important techniques in fabricating nanoscale coatings with controlled properties [1,2]. The deposition conditions such as polymer concentration, pH, ionic strength or temperature, as well as the nature of building blocks employed (synthetic or natural polyelectrolytes, inorganic nanoparticles, dyes) have an important role on the driving forces which lead to the formation of the multilayers [3-5]. Furthermore, the subsequent properties of the multilayers can be controlled by changes in the external environment [6,7].

In this study, multilayer thin films of chitosan (CS) and poly(acrylic acid) (PAA) were constructed by LbL assembly onto silicon wafers and glass slides using deposition solutions in which the polymer concentration was 10^{-3} mol/L or 10^{-2} mol/L, and NaCl concentration was 10^{-2} mol/L or 10^{-1} mol/L. After construction, the CS/PAA multilayers were subjected to various post-treatment strategies in order to change their properties: (T₁) immersion in water with pH = 2.4 for 1 min, followed by 15 s immersion in pure water and drying 60 min at 80 °C; (T₂) immersion in pure water for 30 min, followed by drying 60 min at 120 °C and (T₃) immersion in water with pH = 2.4 for 5 min, followed by immersion in pure water for 1 min and drying 60 min at 120 °C. The influence of the post-treatments on the morphology and thickness was monitored by atomic force microscopy (AFM) and spectroscopic ellipsometry.

It was found that the post-treatment T₃ applied on the films constructed using deposition solutions in which $C_{\text{polymer}} = 10^{-2}$ mol/L and $C_{\text{NaCl}} = 10^{-1}$ mol/L gave the most significant changes of the film morphology (Fig. 1).

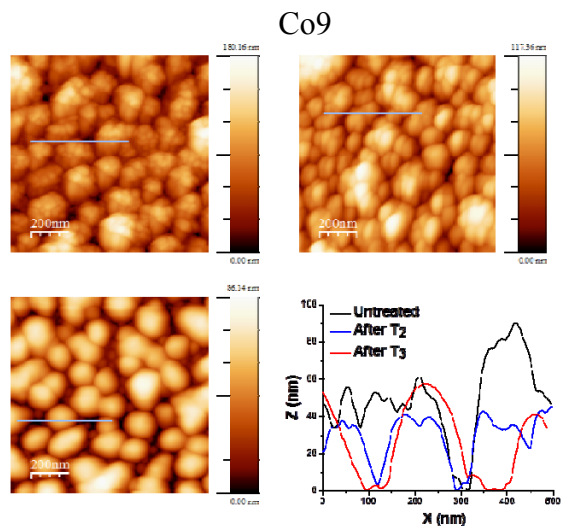


Fig. 1. AFM images ($1 \times 1 \mu\text{m}^2$) of (CS/PAA)_{5.5} multilayers deposited onto silicon wafers from solutions of $C_{\text{polymer}} = 10^{-2}$ mol/L and $C_{\text{NaCl}} = 10^{-1}$ mol/L, before (A) and after post-treatment (T₂) (B) and (T₃) (C). Image D shows the cross-section profiles which were drawn in images A, B and C.

Also, by ellipsometry it was determined that after the post-treatments the thickness of the multilayers decreased (Fig. 2).

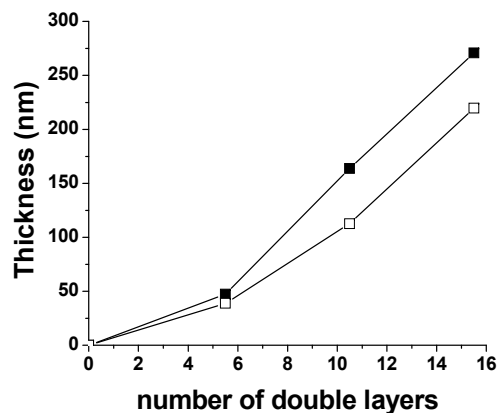


Fig. 2. Thickness of (CS/PAA)_n multilayers deposited from solutions of $C_{\text{polymer}} = 10^{-3}$ mol/L and $C_{\text{NaCl}} = 10^{-2}$ mol/L, before (■) and after (□) post-treatment T₁.

Co9

The thickness decrease could be explained by the diffusion of the Na⁺ and Cl⁻ ions from inside the multilayers, which led to the reorganization of the polymer layers and the regeneration of electrostatic interactions between the ionic groups of CS and PAA.

The sorption experiments were performed on the CS/PAA multilayers post-treated with T₃ using Toluidine Blue O (TBO) as a model cationic dye. The capacity of the CS/PAA multilayers to retain TBO was investigated as a function of double layer number deposited (Fig. 3).

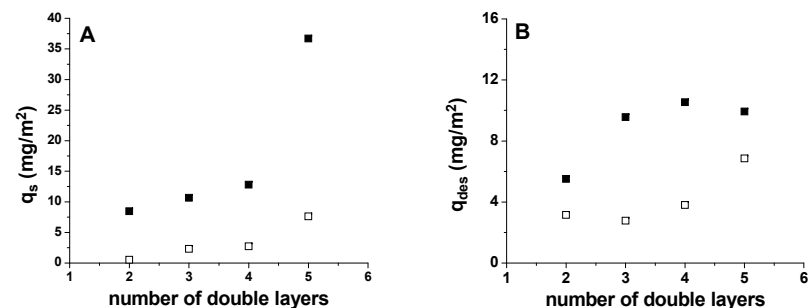


Fig. 3. Dependence of the amount of TBO sorbed (A) and desorbed (B) by the CS/PAA multilayers constructed onto glass slides, before (■) and after (□) post-treatment T₃, as a function of the number of double layers deposited.

The investigation of the reusability of CS/PAA multilayers in the sorption process of TBO showed that only the treated multilayers were able to sorb again dye molecules. This indicated that the post-treated multilayers were more stable on the solid surface than the pristine multilayers in the sorption/desorption experiments.

1. P. Bertrand, A. Jonas, A. Laschewsky, R. Legras, Ultrathin polymer coatings by complexation of polyelectrolytes at interfaces: suitable materials, structure and properties // *Macromol. Rapid Commun.* 21 (2000) 319-348.

2. S. A. Marcott, S. Ada, P. Gibson, T. A. Camesano, R. Nagarajan, Novel application of polyelectrolyte multilayers as nanoscopic closures with hermetic sealing // *ACS Appl. Mater. Interfaces* 4 (2012) 1620-1628.

3. I. Tokarev, S. Minko, Stimuli-responsive porous hydrogels at interfaces for molecular filtration, separation, controlled release, and gating in capsules and membranes // *Adv. Mater.* 22(2010) 3446-3462.

4. E. S. Dragan, S. Schwarz, K.-J. Eichhorn, Specific effects of the

counterion type and concentration on the construction and morphology of polycation/azo dye multilayers // *Colloids Surf. A* 372 (2010) 210-216.

5. F. Bucatariu, C.-A. Ghiorghita, F. Simon, C. Bellmann, E. S. Dragan, Poly(ethyleneimine) cross-linked multilayers deposited onto solid surfaces and enzyme immobilization as a function of the film properties // *Appl. Surf. Sci.* 280 (2013) 812-819.

6. S. S. Shiratori, M. F. Rubner, pH-dependent thickness behavior of sequentially adsorbed layers of weak polyelectrolytes // *Macromolecules* 22 (2000) 4213-4219.

7. J. Irigoyen, L. Han, I. Llarena, Z. Mao, C. Gao, S. E. Moya, Responsive polyelectrolytes multilayers assembled at high ionic strength with an unusual collapse at low ionic strength // *Macromol. Rapid Commun.* 33 (2012) 1964-1969.

COMPOSITIONAL MATERIALS BASED ON MODIFIED POLYPROPYLENE REINFORCED BY INORGANIC AND ORGANIC FIBERS

D. Chervakov, O. Chervakov

*SHEI "Ukrainian State University of Chemical Engineering", Gagarina ave. 8,
Dnepropetrovsk 49005, Ukraine*
dchervakov@e-mail.ua

Nowadays in the world are a lot of special application thermoplastic polymers with a different complex of physical-mechanical properties, but on the market of West Europe these polymers are absent.

We are propose the effective method of polypropylene (PP) modification [1] by polysiloxanepolyols (PSP) with different content of hydroxyl groups (modifiers PSP1, PSP2, PSP3 which content according to 7,3%, 1,8% and 0,6% hydroxyl groups).

The PP modification was carried out by its surface treatment with using benzoyl peroxide and polysiloxanepolyol solution in dimethyl ketone. The material was extruded by screw disc extruder with the temperature in normal stress area 210°C. The preference of this method is a possibility to carry out modification process in the ordinary plastic processing equipment.

Such technology provide to significant improvement of thermo-physical and mechanical properties of PP.

For example, by using a PSP1 the melt fluidity index growth from 2,29 to 6,13 g/10 min. and tensile strength growth from 29,6 to 49 MPa. By using of a PSP2 and PSP3 modifiers the tensile strength growth from 29,6 to 58 MPa and impact strength by Sharpay from 70 to 136 kJ/m². Increasing of physical-mechanical properties can be explained by nature of modifiers agents which take part in the forming of cross-links in polypropylene structure.

Analyzing the obtained data developed material can be used as polymer matrix for compositional materials which reinforced by mineral or synthetic fibers.

Developed material can be used as polymer matrix for compositional materials reinforced by mineral or synthetic fibers.

Difference of tensile strength between a initial and modified polypropylene matrix which are reinforced by 30w% of glass fibers is a 15% .

Difference of tensile strength between initial and modified polypropylene polymer matrixes (for polypropylene modified by PSP2 and benzoyl peroxide) reinforced by 30w% of basalt fibers modified by ethylsilicate-40 is a 110 %.

Difference of tensile strength between initial and modified polypropylene

Co10

polymer matrixes reinforced by 30w% of Kevlar fibers is a 65 %.

The use of PSP as a polypropylene modifier can purposefully change the physical and mechanical properties. The obtained materials have a number of advantages over the initial polypropylene, and they can be used as a polymer matrix for polymer compositional materials and as materials for construction purposes.

1. *Chervakov D. [et al.]* Constructional materials based on cross-linked polypropylene reinforced by modified basalt fibers//Chemistry & Chemical Technology 5/1 (2011) 101-105.

POSTERS

**POROUS ALGINATE/SDS BEADS FOR ADSORPTION OF
2-NITROPHENOL**

S. Peretz¹, D.F. Anghel¹, M. Florea-Spiroiu², D. Bala², R. Iordanescu³

¹ Romanian Academy, "Ilie Murgulescu" Institute of Physical Chemistry, Department of Colloids, 202 Spl. Independentei, 060021, Bucharest, Romania sanduperetz@gmail.com

² University of Bucharest, Faculty of Chemistry, Department of Physical Chemistry, 4-12 Regina Elisabeta Blvd., 030018, Bucharest, Romania

³ National Institute of R & D for Optoelectronics INOE 2000, Optospintronics Department, 409 Atomistilor St., 077125, Magurele, Romania iorda85@yahoo.com

Adsorption of organic pollutants from water by using biopolymers, is one of used method for decontamination, extensively studied in recent years [1, 2]. Nitrophenols are organic water pollutants which have adverse health effects on humans because they are toxic even at low concentrations [3].

Alginate is a biopolymer used currently to adsorb anionic and cationic pollutants from aqueous solutions [4]. Sodium alginate (Na-Alg) is a hydrophilic, biocompatible and inexpensive biopolymer that forms interconnected open pore networks by cross-linking with calcium ions [5]. The divalent calcium cation has the ability to fit into the guluronate structures like eggs in an egg box [6].

In order to increase their adsorption surface, porous calcium alginate/sodium dodecyl sulfate (SDS) beads have been prepared from sodium alginate using SDS as foaming agent, sodium chloride as porogen agent, and calcium chloride as cross-linker. These beads have been successfully used for adsorption of 2-nitrophenol (2-NP) from aqueous solutions.

The cross-linking process of alginate beads was studied at different CaCl₂ concentrations. The lyophilized samples of porous calcium alginate (Ca-Alg)/SDS were structurally investigated by Fourier Transform Infrared (FTIR) Spectroscopy. FTIR spectra showed sensitive shifts of hydroxyl and carboxyl peaks after the cross-linking of alginate with CaCl₂ in the presence of anionic surfactant.

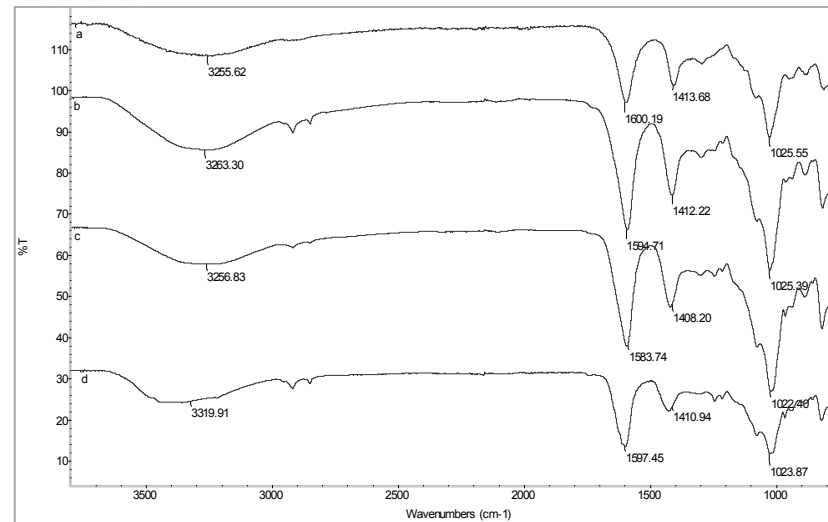


Fig. 1. FTIR spectra: (a) Na-Alg, (b) Alg-1, (c) Alg-2 and (d) Alg-3.

The pore dimensions and the morphology of calcium alginate beads were determined by Scanning Electron Microscopy (SEM).

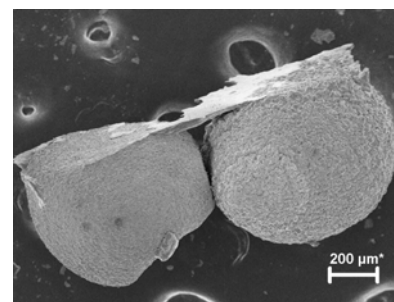


Fig. 2. SEM images of porous calcium alginate/SDS beads (Alg-2)

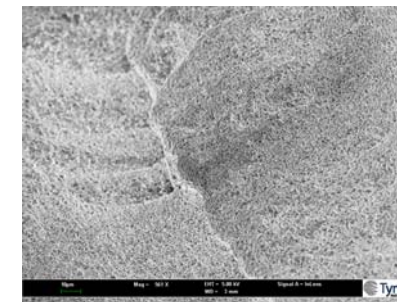


Fig. 3. Ca-Alg/SDS beads surface (Alg-2)

SEM revealed that the size of pores varies from 5-10 μm in the cross-linked matrices with 1 wt % CaCl₂ (Alg-1), 2-5 μm for Alg-2, while at 10 wt % CaCl₂ the lamellar micelles of SDS bind together the alginate chains by electrostatic bonds with calcium ions.

The porous Ca-Alg/SDS beads of 700 to 800 μm were employed to remove the 2-NP from water, and the adsorption reaches a maximum for pH = 7.

P1

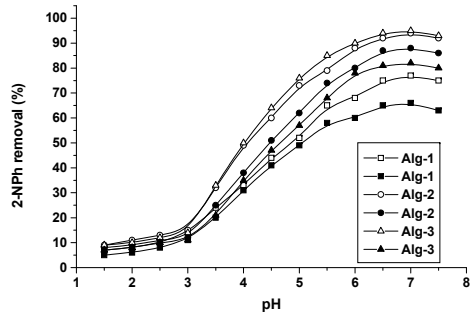


Fig. 4. Effect of pH on 2-NPh adsorption for different compositions of porous Ca-Alg beads, at two pollutant initial concentrations: $2 \times 10^{-5} \text{M}$ (empty symbols) and $4 \times 10^{-5} \text{M}$ (black symbols).

The adsorption and kinetic experiments indicated that the removal efficiency increases with the amount of porous calcium alginate/SDS beads, and decreases with raising the initial pollutant concentration.

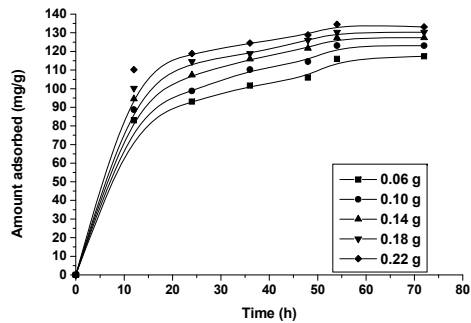


Fig. 5. Kinetics of 2-NP adsorption onto different amount of porous Ca-Alg beads (Alg-2).

The kinetics of 2-nitrophenol removal has three stages. The first is rapid and removes from 55 to 75% of the pollutant. The second and the third are slow, and remove 94-95 % of the initial amount of 2-nitrophenol from aqueous solutions.

Acknowledgement

This research was supported by Romanian Academy, the "Ilie Murgulescu" Institute of Physical Chemistry. The support of EU (ERDF) and Romanian Government (POS-CCE

P1

O2.2.1 project INFRANANOCHEM, No. 19/2009.03.01) and of (UEFISCDI) (Project PN-II-ID-PCE-2011-3-0916, Contract No. 177/2011) is gratefully acknowledged.

1. Erdem M., Yüksel E., Tay T., Çimen Y., Türk H. J. Coll. Interf. Sci. 333 (2009) 40-48.
2. Ngah W.S., Fatinathan S. Colloids and Surfaces A: Physicochem Eng Aspect 277 (2006) 214-222.
3. Busca G., Berardinelli S., Resini C., Arrighi L. J. Hazard Mater. 160 (2008) 265-288.
4. Aravindhan R., Fathima N.N., Rao J.R., Nair B.U., Colloids and Surfaces A: Physicochem. Eng. Aspect. 299 (2007) 232-238.
5. Klock G., Pfeffrman A., Ryser C., Grohn P., Kuttler B., Hahn H.J., Zimmermann U., Biomaterials 18 (1997) 707-713.
6. Schettinia E., Santagata G., Malinconico M., Immirzi B., Mugnozza G.S., Vox G. Resources, Conservation and Recycling 70 (2013) 9-19.

EVALUATION OF DNA BINDING TO HYPERBRANCHED POLYETHYLENEIMINE (PEI) OF SILOXANE CORE

C. M. Uritu, L. Ursu, A. Coroaba, M. Pinteala

“Petru Poni” Institute of Macromolecular Chemistry, Grigore Ghica Voda Alley
41A, Iasi 700487, Romania
uritu.cristina@icmpp.ro

The main goal of this work was to obtain a non-viral gene delivery system based on hyperbranched polyethylenimine and cyclic siloxane. The structure of cyclic siloxane – PEI conjugate (D4-PEI) was confirmed by ¹H NMR, FT-IR and XPS [1]. Agarose gel electrophoresis was performed to test DNA retention in D4-PEI complex, for various N/P ratios [2]. DLS studies at different pH values of DNA with different N/P ratios showed significant changes in particle size and zeta potential values [2, 3]. As a conclusion, D4-PEI presents a good ability to pack DNA and could have applicability in gene transfection which will be subject for further specific tests.

1. Jäger M., Schubert S., Ochrimenko S., Fischer D., Schubert U. S., Branched and linear poly(ethylene imine)-based conjugates: synthetic modification, characterization, and application, *Chem. Soc. Rev.*, 41 (2012), 4755-4767

2. Kim T., Seo H. J., Choi J. S., Yoon J. K., Baek J., Kim K., Park J.-S., Synthesis of Biodegradable Cross-Linked Poly(β-amino ester) for Gene Delivery and Its Modification, Inducing Enhanced Transfection Efficiency and Stepwise Degradation, *Bioconjugate Chem.*, 16, 5 (2005), 1140–1148

3. Choosakoonkriang S., Lobo B. A., Koe G. S., Koe J. G., Middaugh C. R., Biophysical characterization of PEI/DNA complexes, *J. Pharm. Sci.*, 92, 8 (2003) 1710-1722.

Acknowledgement:

This work was financially supported by project PN-II-ID-PCCE-2011-0028, contract: 4/30.05.2012.

FULLERENE C60 BASED NANOPARTICLES COATED WITH HYPERBRANCHED POLYETHYLENEIMINE (PEI) FOR GENE DELIVERY

C. M. Uritu, L. Ursu, C. D. Varganici, F. Doroftei, M. Pinteala

“Petru Poni” Institute of Macromolecular Chemistry, Grigore Ghica Voda Alley
41A, Iasi 700487, Romania
uritu.cristina@icmpp.ro

Polyethylenimine (PEI) was extensively investigated as a non-viral vector system due to its high content in amino groups. These provide a great ability to complex and condense negatively charged DNA or RNA. Fullerene (C60), which also showed a good potential in drug delivery, was derivatized onto the surface with hyperbranched PEI. The interaction between fullerene and PEI was conveniently followed by UV-Vis spectroscopy: the characteristic peak of C60, at $\lambda=330$ nm, decrease during the reaction until disappearance [1]. FT-IR, TGA/DSC and XPS data confirmed the structure of water soluble C60-PEI [2]. TEM exhibited a compact and spherical morphology of the C60-PEI conjugate. Depending on the C60 : PEI ratio, nanoparticles with diameters between 3 ÷ 80 nm were obtained, as DLS and TEM results indicated. Agarose gel electrophoresis assay, performed for several N/P ratios, showed that C60-PEI has a good DNA binding ability [3].

1. Manolova N., Rashkov I., Beguin F., van Damme H., Amphiphilic derivatives of Fullerenes Formed by Polymer Modification, *J. Chem., Soc., Chem. Commun.* (1993), 1725 – 1727.

2. Shi J., Zhang H., Wang L., Li L., Wang H., Wang Z., Li Z., Chen C., Hou L., Zhang C., Zhang Z., Pei-derivatized fullerene drug delivery using folate as a homing device targeting to tumor, *Biomaterials*, 34 (2013), 251–261.

3. Lu B., Xu X.-D., Zhang X.-Z., Cheng S.-X., Low Molecular Weight Polyethylenimine Grafted *N*-Maleated Chitosan for Gene Delivery: Properties and In Vitro Transfection Studies, *Biomacromolecules*, 9 (2008), 2594–2600.

Acknowledgement:

This work was financially supported by project PN-II-ID-PCCE-2011-0028, contract: 4/30.05.2012.

PROPERTIES OF ELASTOMER COMPOSITES WITH CARBON NANOMATERIALS

K. V. Vishnevskii, Zh. S. Shashok

*Belarusian State Technological University, 13a, Sverdlova str., Minsk 220006,
Belarus*

vik@belstu.by; shashok@belstu.by

At present, it is an important task to develop composite materials containing nanostructures. This is due to their unique physical and chemical properties, which differ from the properties of macro- and microparticles [1]. However, to achieve positive results from using nanoadditives in the rubber industry, a number of questions need to be addressed. One of these is the correct choice of the type of nanomaterial (in terms of structure and composition, particle size and shape, the presence of active centres, and reinforcing capacity) to achieve a positive effect on a specific elastomer matrix.

The aim of the present work was to determine the effect of carbon nanomaterial (CNM) on the plastoelastic properties and vulcanisation kinetics of rubber mixes based on general-purpose and special-purpose rubbers, and also on the physicomechanical properties of vulcanisates based on them. The initial carbon nanomaterial was obtained in a high-voltage discharge plasma and then, after complex acid treatment and annealing, was divided into fractions by ultrasound [1].

The investigation was conducted on rubber mixes based on crystallising isoprene rubber SKI-3 and non-crystallising oil-extended butadiene-styrene rubber SKMS-30 ARKM-15, which are general-purpose rubbers, and on rubber mixes based on special-purpose rubbers, namely butadiene-acrylonitrile rubbers of grades BNKS-18AN and BNKS-40M. The rubber mixes contained CNM in doses ranging from 0.05 to 0.2 phr. Specimens without nanoadditive were used for comparison.

The study revealed that application of carbon nanomaterials is most expedient in elastomeric compositions based on polar raw rubber with low and middle contents of polar groups, containing inactive fillers. Introduction of CNM fraction – «suspension» in dosages from 0.1 to 0.2 phr into the composition based on BNKS-18 with a sulphuric curing system and carbon black of inactive grade results in improvement of the mix processability, reduction of the time to achieve the vulcanization optimum, increase of heat ageing stability in the air, resistance to aggressive medium attack, abrasion as well as improvement of rubber endurance.

Thus, since the elastomer base was invariant, an inference can be drawn on the influence of introduced nanoadditives on the structure of the spatial network

formed in the process of vulcanization.

In the given case, the most probable is the surface interaction of nanoadditives with the polar components of the vulcanizing system (in particular, with N,N'-diphenylguanidine (DFG)). It may quite be that here deactivation of the polar agent of the vulcanizing group by the particles of nanomaterials takes place, and its tendency to agglomeration or condensation decreases, thus favoring better dispersion of DFG within the mixture [8]. Since in our case it is used as a secondary accelerator for the basic one (thiazole di-(2-benzothiazolyl disulfide), this favors a more intense, joint action of accelerators and of the vulcanizing system as a whole.

Improvement in the set of service properties of rubbers based on the BNKS-18A polar caoutchouc with carbon nanomaterials introduced into them can be explained by the formation of a more perfect spatial network due to the interaction of the active centers of carbon nanomaterials with both polar groups of ingredients (in particular, the vulcanizing system) and the nitrile groups of caoutchouc.

1. *Zhdanok S.A., Krauklis A.V. [et al.] Influence of process parameters upon the properties of carbon nanomaterials synthesized in the electric discharge // International workshop "Nonequilibrium processes in combustion and plasma based technologies." - Minsk, August 21-26, (2004) 205-209*
2. *Priss Z.V., Fel'dshman M.S. Effect of technical carbon on the kinetics of vulcanization of rubbers in the kinetic presence of various accelerators // Kauchuk i Rezina 12, (1977) 21-23.*

COAGULATION-FLOCCULATION PROCESSES IN WATER AND WASTEWATER TREATMENT. (II) FINE PARTICLES AND ITS REMOVAL USING POLYMERS**C. Zaharia**

Gheorghe Asachi Technical University of Iasi, Faculty of Chemical Engineering and Environmental Protection, Department of Environmental Engineering and Management, 73 Prof.Dr.docent D.Mangeron Blvd, Iasi 700050, Romania
czah@ch.tuiasi.ro or czaharia2003@yahoo.com

The fine turbidity particles are usual components in natural surface water resources, and different final effluents (*i.e.* industrial, domestic or other types of wastewaters), causing often taste, odor and color problems, among others. Also, few concerns are connected with abrasiveness (in the sewage pipe system, or sediments), and degradation or fermentation processes. Therefore, its separation from aqueous environments is among the principal objectives of a water and wastewater treatment. This research study proposes a presentation of different types of fine particles in natural state from different water resources [1,2] or wastewaters produced during some technological productive processes or domestic activities [3-7], and also a comparative discussion of some current treatment methods applied for removal of these fine particles, especially by coagulation and/or flocculation processes using mainly polymers as flocculants or coagulation adjuvants [3-9].

The fine particles (both hydrophilic and hydrophobic ones) possess electrokinetic property causing double layer formation, and consequently surface charges. *Hydrophilic fine particles* are often of biological origin (such as proteins) and usually consist of water-soluble functional groups like $-\text{NH}_2$, $-\text{COOH}$, $-\text{OH}$, $-\text{SO}_3\text{H}$, and $-\text{OPO}_3\text{H}_2$ (*e.g.*, a protein particle: $\text{HOOC} - \text{R} - \text{NH}_3^+$ form at low pH level, or $^-\text{OOC} - \text{R} - \text{NH}_2$ form at high pH level). The *hydrophobic fine particles* are especially of inorganic or mineral origin (such as clay, silt, and silica), and are charged at face boundaries of particle surfaces as result of different ionic exchanges or isomorphous replacements within the lattice (lattice imperfections). Most metal oxides and hydroxides are amphoteric, but can adsorb H^+ and HO^- ions or other complexes, and are changing their surface charges passing through zero, fact expressed mainly by pH_{ZPC} (pH of zero point of charge) [1,2].

The fine particles have an 'apparent' surface charge, and its magnitude and sign is dependent of pH value [1-9]. Repulsive and attractive forces analogous to gravitational forces exist between particles, and regulate the distance between them. Increasing ionic strength is produced by adding electrolytes (coagulants) or polyelectrolytes (coagulation adjuvants), termed as *compression of double layer*,

especially when the fine turbidity particles are moving from fresh water rivers into estuaries, or are aggregated in wastewater treatment processes.

In addition, the fine particles can be separated by chemical-mechanical interactions, in principal by coagulation and flocculation processes in natural self-purification systems of fresh surface water or induced *in situ* treatments of fresh waters or different types of wastewaters (*e.g.* industrial, municipal, or urban wastewater) that are normally carried out prior to sedimentation and filtration.

In general, *coagulation* is the process by which the fine turbidity solids are destabilized, and allowed to aggregate or flocculate to higher sizes that settle with satisfactory velocities, or are easily separated by filtration.

Flocculation usually refers to the postdestabilization process in which aggregations and large flocs are formed, as result of particle or small floc collision due to a rapid stirring either by Brownian motion or by velocity gradients [1-7]. Both rapid stirring and slow stirring are needed for a good and complete flocculation [3,4,7]. The separation of dense formed agglomerates or flocs from aqueous environment is achieved by sedimentation (usually referring to settling of the formed flocs without stirring for quiescence sedimentation) or filtration (usually referring to separation of the formed flocs by free, vacuum or under pressure passing through a granular solid layer of varying porosity and density). In natural aquatic environment, the separation of fine particles is in majority of cases achieved by sedimentation with or without coagulation-flocculation process [1].

Organic polymers (*e.g.* polyelectrolytes) provide a process of adsorption and bridging between fine particles as a more explicit example of flocculation process [3]. Cationic, anionic, and nonionic polyelectrolytes are available for use as flocculants, and all these types are extensively used in water treatment.

Choice of the most suitable polyelectrolyte for a given situation depends on both the type of particle being removed, and the wastewater characteristics. In some cases may result in a surprising situation where an anionic polyelectrolyte becomes the most suitable flocculant for a negatively charged fine particles [4,6,7]. Determination of the type, demand, or amount of flocculant to be used is based on laboratory or if possible pilot plant studies. Data on residual turbidity of the settled or filtrated flocculated waters or wastewaters in natural water or treated wastewater is influenced by the polymer dosage, pH, mixing rate and regime, temperature, and others. These data predict the fine particles removal efficiency, or natural water and/or effluent quality after the treatment with polymeric flocculants.

This research study discuss the action of some synthetic polyelectrolytes (neionic, anionic and/or cationic ones) applied to a natural watercourse sample and also to different types of effluents loaded with fine turbidity particles and organic matter, among others. The influence of some operating factors such as pH, temperature, stirring regime and rate, and also of some water or effluent characteristics expressed by some quality indicators such as total solids content (or suspended solids), organic matter content expressed by chemical oxygen demand

(COD) or biochemical oxygen demand (BOD₅) together with the tested polyelectrolyte type (neionic, anionic or cationic) and characteristics (mainly polyelectrolyte type and dosage) is clearly synthesized. The performed results permitted the appreciation of separation performance using polyelectrolytes in terms of turbidity, COD and color removals, and also modeling and optimization of these aggregation and separation processes of the fine turbidity particles from natural water resources or final treated effluents.

1. Zaharia C., Suteu D. Comparative overview of chemical processes in water of Bahlui River. (I) Coagulation-flocculation processes // Proceeding of International Conference of Applied Sciences, Chemistry and Chemical Engineering, 7th Edition, May 15-18, 2013, Bacau - Romania (2013) in press.

2. Zaharia C., Teodosiu C., Macoveanu M., Chițanu G. Applications of some polyelectrolytes for the treatment of surface waters, Anal Șt Univ "A.I.Cuza", s. Chemistry, VII(2) (1999) 387-394.

3. Zaharia C., Suteu D., Muresan A. Options and solutions for textile effluent decolorization using some specific physico-chemical treatment steps, Environ Eng Manag J (Proceedings ICEEM/06, September 1-4, 2011, Balatonalmadi, Hungary), 11(2) (2012) 493-509.

4. Zaharia C., Surpățeanu M. Study of flocculation with Prodefloc CRC 301 polyelectrolyte applied into a chemical wastewater treatment, Ovidius University Annals of Chemistry, 17 (1) (2006) 50-53.

5. Zaharia C., Surpățeanu M., Macoveanu M. The mathematical optimization of the advanced treatment of some wastewaters based on active carbon adsorption in the presence of polyelectrolyte (II), Bul Inst Polit Iași, s.: Chemistry and Chemical Engineering, XLVIII (LII), f.3-4 (2002) 101-114.

6. Zaharia C., Diaconescu R., Surpățeanu M. Optimization study of a wastewater chemical treatment with Ponilit GT-2 anionic polyelectrolyte // Environ Eng Manag J, 5(6) (2006) 1273-1290.

7. Zaharia C., Diaconescu R., Surpățeanu M. Study of flocculation with Ponilit GT-2 anionic polyelectrolyte applied into a chemical wastewater treatment // Central European Journal of Chemistry, 5(1) (2007) 239-256.

8. Zaharia C. Performances of natural polyelectrolytes based on starch in aggregation and stabilization of aqueous coal-containing systems, Bul.Inst.Polit. Iasi, series: Chemistry and Chemical Engineering, LVIII(LXII), f.1 (2012) 29-39.

9. Zaharia C., Diaconescu R. Optimization study of an wastewater treatment using electrocoagulation-electroflotation in the presence of polyelectrolyte // Proceedings of International Conference UNITECH'07, Gabrovo, Bulgaria, November 23-24, 2007, vol.II (2007) 265-266.

THERMOPHYSICAL PROPERTIES OF EPOXY-POLYSILOXANE COMPOSITES OF CATIONIC POLYMERIZATION

N. G. Leonova¹, V. M. Mikhal'chuk¹, Ye. P. Mamunya², V. V. Davydenko², M. V. Iurzhenko²

¹Donetsk National University, ul. Universitetskaya 24, Donetsk, 83001 Ukraine
natalka_leonova@mail.ru

²Institute of Macromolecular Chemistry, National Academy of Sciences of Ukraine, Khar'kovskoe sh. 48, Kyiv, 02160 Ukraine

Epoxy polymers feature high mechanical, electrical and adhesion properties, hardness and brittleness. The introduction of fillers obtained by the sol-gel method affords a decrease in the brittleness and increase in the operational characteristics. The formation and ripening of a sol can proceed both in the presence and in the absence of an organic component: the morphologies and properties of such composites differ.

The goal of present work was to study the effect of composition and production conditions of epoxy-polysiloxane composites of cationic polymerization on their thermophysical properties.

Epoxy-polysiloxane composites of cationic polymerization were synthesized based on epoxy resin EPONEX 1510 and tetraethoxysilane by two methods. The first one consisted in the formation of a sol in the presence of Eponex 1510: tetraethoxysilane (TEOS), 0.1 N aqueous solution of nitric acid, acetone, and epoxy resin were mixed simultaneously. In the synthesis of composites by the second method, a sol of polysiloxane particles (PSP) was formed in the absence of the resin: TEOS, 0.1 N aqueous solution of nitric acid, and acetone were mixed simultaneously and epoxy oligomer was added to the composition prior to the system evacuation and introduction of the polymerization catalyst. The thermophysical properties of the resulting polymers were studied.

The effect of the filler on thermophysical properties of the epoxy-polysiloxane systems of cationic polymerization was studied by means of differential scanning calorimetry. During the first scanning, the DSC curves of the physically aged polymers (the time of annealing at room temperature from the moment of film sample preparation until the experiment came to 200 days) revealed a discontinuity in the thermal capacity corresponding to the glass transition caused by the conformational changes, increase in the free volume, and change in the vibration motion parameters.

The analysis of DSC curves was performed upon repeated heating of the samples. The resulting DSC curves was characterized by the absence of endothermic peaks since, after the first run, the thermal and technological prehistories are leveled and the samples have a more homogeneous structure.

An increase the concentration of polysiloxane particles from 0.5 to 3.0 wt % leads to the low-temperature shift in the value of T_g , as well as an increase ΔC_p and the width of the glass-transition range compared to the unmodified polymer. Width of the glass-transition range ΔT changes nonmonotonically as the silica content grows (this effect is especially strong for the samples where the PSP sol was formed in the presence of the resin), which can be connected with the structure inhomogeneity of the samples under study.

To confirm the inhomogeneity of the structures of polymers under study, they were studied by thermomechanical (TMA) and differential thermomechanical (DTMA) analyses. The registration of curves in a differential form allows for the assignment of structural transitions which are not manifested on the TMA curves. According to the DTMA data, all the composites are characterized by the presence of several peaks, namely, the low-temperature peak T_{g1} at about 40°C and two more peaks (T_{g2} and T_{g3}), the positions of which depend on the composite composition and are situated within the range of 50-85°C. For the unmodified epoxy polymer, they are observed at $T_{g1} = 46^\circ\text{C}$ and $T_{g3} = 85^\circ\text{C}$, while peak T_{g2} is not manifested. These maxima relate to the transition from a glassy state into high elastic one for several structural regions with variable segment mobility. As is known, highly crosslinked epoxy polymers have a structure with microglobular regions. Microglobular structure of obtained polymers and composites were confirmed by transmission electron microscopy.

Hence, investigation of thermophysical characteristics of the epoxy-polysiloxane systems of cationic polymerization showed that introduction of the filler leads to a decrease in the density of crosslinking and glass transition point owing to the changes in the topological structure of composites. The resulting polymers have a heterogeneous structure that contains regions with increased molecular mobility showing their own values of the glass-transition point. The studied epoxy-polysiloxane polymers of cationic polymerization can be used as adhesives and protecting coatings. Previously, we established that the explored epoxy-polysiloxane composites of cationic polymerization provide for the high adhesion of coatings to aluminum substrate already at low concentration of PSP in the system. The lattice-cut method was used to estimate the adhesion of the unmodified polymer and hybrid materials to D-16 aluminum alloy surface. It was shown that effect of small additions (0.5-1.5 mas.%) in composites leads to decreasing of maximal rates of thermal degradation and high-temperature oxidation.

NEW PHENOL-FORMALDEHYDE RESINS FOR ANTIFRICTION AND CONSTRUCTION APPLICATION REINFORCED BY INORGANIC AND ORGANIC FIBERS

O. O. Lipko, V. S. Boiko, K. O. Herasymenko

*SHEI "Ukrainian State University of Chemical Engineering", Gagarina ave. 8,
Dnepropetrovsk 49005, Ukraine*
kodpua@gmail.com

Composite materials (PCM) of construction and antifriction application are widely used in aircraft, automobile, shipbuilding and engineering industries as well as in the aerospace production.

Nowadays, increasingly stringent requirements are imposed on polymeric composites as to their performance characteristics. They are to possess high physical and mechanical parameters, resistance to aggressive chemicals, high temperatures, and to damaging effects of the environment. Typically, a set of the required properties of new PCM is achieved by producing a matrix with enhanced physical and mechanical properties, and it depending on the individual properties of reinforcing fillers.

We have proposed a method of creating polymer composites intended for construction and antifriction applications, which are based on new polyamide modified phenol- formaldehyde resole resin (MPFR) reinforced by a blend of mineral and synthetic fillers (cut length fibers -12 mm). The method allows a combination of high-cost aramid (AF), carbon (CF) and polyoxadiazole (PODF) fibers with more affordable basalt (BF) or synthetic polyamide fibers (PAF), which results in obtaining more cost-competitive composites. The properties of some the PCM are shown in Table 1.

In the authors mind the special attention can be focused on the PCM, in which the polyamide fiber is used as part of the filler. Due to the high performance of these PCM and affordability of all the components, they can be widely used for the manufacture of mass-produced parts for both construction and antifriction purposes.

A separate promising area of application of PCM that contain aramid fibers may be creating materials similar to Kevlar® K129 (DuPont, USA).

Table 1.

The composition of the polymer matrix+filler	Impact strength, kJ/m ²	Ultimate strength, MPa		Martens thermal stability, °C	Water absorption, %	Friction coefficient*	Mass wear, mg/cm ² km
		static bending strength	compression strength				
No modified resin +BF	120	203	154	>300	0,44	0,32	4,07
MPFR +BF	146	383	165	> 300	0,25	0,25	1,53
MPFR +(BF + PAF)	150	404	160	290	0,14	0,13	0,76
MPFR +(BF + PODF)	153	428	170	266	0,27	0,18	0,81
MPFR + (BF + AF)	250	453	178	300	0,28	0,19	0,96
MPFR + (BF + CF)	150	468	160	290	0,26	0,12	0,85

*Sliding speed of 0.3 m/s and a specific load pressure of 2.5 MPa (heavy-friction conditions of operation).

EPOXY-SILICA COATINGS FOR ANTICORROSIVE PROTECTION OF ALUMINUM ALLOYS

R. I. Lyga, D. V. Gurtovoj, V. M. Mikhal'chuk

Donetsk National University, Universitetskaya str. 24, Donetsk 83001, Ukraine
lygarita@mail.ru

Recently special attention has been focused on research of nanocomposites on the basis of epoxy compounds and metals alkoxides obtained by the sol-gel method with high chemical resistance, resistance to stretching, flexibility, good strength and adhesive characteristics [1]. Such hybrid systems possess high barrier properties therefore they are often used as protective coatings for surfaces of different nature from the influence of aggressive environment [2].

The goal of the present work was studying the influence of *in situ* formed silica filler at water, mineral acids and alkali solutions resistance and anticorrosive properties of amine-cured epoxy-silica coatings for aluminum alloy D-16 by electrochemical method. Polymeric component of the composites was received on the basis of epoxy oligomer – diglycidyl ether of dicyclohexylolpropane (Eponex 1510). Silica component was formed by hydrolytic polycondensation of tetraethoxysilane.

It was shown that mineral acids and water resistance of epoxy-silica composites with silica filler content in the range of 0.5 – 6.0 wt.% remains at the level of unmodified polymer. In the alkaline solutions the composites with filler concentration up to 1.5 wt.% are characterized by quite high chemical resistance.

Anticorrosive properties of organic-inorganic coatings on aluminum alloy D-16 were estimated according to potentiodynamic measurements in 5% NaCl water solution using the three-electrode cell. Coatings were applied on the alloy surface degreased by acetone and activated by alkali. The formation of coatings was carried out both at room temperature and after their curing during 1 hour at 120 °C. Working surface area of the alloy plate was 1 cm². Potentiodynamic measurements were carried out at room temperature.

It was shown that the studied film composite coatings cured at room temperature increase values of corrosion potential and pitting corrosion potential of the substrate a little (potentials of corrosion and pitting corrosion accept more positive values). Use of epoxy-silica coatings increases anticorrosive resistance of the working electrode from 0.25 kOm·cm² to 1.25 – 2.08 kOm·cm². As a result the density of corrosion current decreases from $I_{\text{corr}}^{\circ} = 1.00 \cdot 10^{-4} \text{ A} \cdot \text{cm}^{-2}$ to $1,20 \cdot 10^{-5} - 1,99 \cdot 10^{-5} \text{ A} \cdot \text{cm}^{-2}$. Calculated corrosion protection efficiency of room cured

composite coatings with silica particles content from 0.5 to 3.0 wt.% on D-16 alloy is 82 – 88 %. However at filler concentration 4.5 wt.% and more the tendency to decrease of corrosion protection efficiency of aluminum alloy was observed. It may be related to the fact that formation of epoxy and siloxane networks does not occur independently and extent of organic cross-linking has a direct effect on the extent of the inorganic network formation, and vice-versa [3].

To receive maximum degree of polymerization and increase epoxy matrix network density post-curing of coatings at 120 °C was carried out. After such heat treatment the parameters characterizing protective anticorrosive properties of coatings have changed considerably. It was shown that anticorrosive resistance of the substrate reaches 3.15 – 9.95 kΩ·cm² and corrosion current density decreases to 2.51·10⁻⁶ – 7.94·10⁻⁶ A·cm⁻² as the silica content in composites increases from 0.5 to 6 wt.%. At certain SiO₂ concentrations post-cured coatings increase values of corrosion potential of the aluminum substrate by 57 – 151 mV. Big difference between the values of corrosion potential and pitting corrosion potential for the plates covered by composites indicates a small susceptibility of samples to corrosion.

Potentiodynamic curves corresponding to the covered plates showed the pronounced area of corrosion current density passivation of sufficiently big extension (to 1.5 V). This means that the presence of the studied coatings really creates a physical barrier to water and corrosion agents (chloride ions, oxygen), i.e. blocks electrochemical process.

The calculated corrosion protection efficiency for aluminum alloy D-16 by these composite coatings based on epoxy oligomer Eponex 1510 and tetraethoxysilane is 92.1 – 97.5%. Taking into account that applied epoxy-siloxane composites represent thin film coatings (10±2 microns) received by single treatment of the metal surface, the above electrochemical data give evidence of excellent anticorrosive properties of epoxy-silica coatings on the surface of aluminum alloy D-16.

1. *Metroke T. L., Kachurina O., Knobbe Ed. T.* Spectroscopic and corrosion resistance characterization of amine and super acid-cured hybrid organic-inorganic thin films on 2024-T3 aluminum alloy // *Progress in organic coatings*. 44 (2002) 185-199.

2. *Vreugdenhil A. J., Gelling V. J., Woods M. E.* The role of crosslinkers in epoxy-amine crosslinked silicon sol-gel barrier protection coatings // *Thin Solid Films*. 517 (2008) 538-543.

3. *Davis St. R., Brough A. R., Atkinson A.* Formation of silica/epoxy hybrid network polymers // *Journal of Non-Crystalline Solids*. 315 (2003) 197-205.

DIELECTRIC AND ELECTRICAL PROPERTIES OF NEW EPOXY-PHOSPHOTUNGSTIC POLYMERIC NANOMATERIALS

**O. K. Matkovska¹, Ye. P. Mamunya¹, G. Boiteux², A. Serghei²,
M. I. Shandruk¹, O. V. Zinchenko¹, E. V. Lebedev¹**

¹ *Institute of Macromolecular Chemistry of National Academy of Sciences of Ukraine, Kharkivske shosse 48, Kyiv 02160, Ukraine*
omatkovska@ukr.net

² *Université de Lyon, Université Lyon 1, Ingénierie des Matériaux Polymères, UMR CNRS 5223, 15 Boulevard Latarget, F-69622 Villeurbanne, France*

Epoxy composites are widely used for different applications in many technical areas due to their valuable properties, particularly as isolating adhesive materials with high mechanical properties. The original approach that allows receiving epoxy polymer nanomaterials with ionic conductivity is proposed in this work. The characteristics of epoxy composites depend on type of curing agents. Phosphotungstic heteropolyacid (PTA), which has a high catalytic activity and high proton conductivity, is a perspective hardener that in combination with epoxy resin creates epoxy-phosphotungstic polymer nanocomposites (EPTP) that can possess high ionic conductivity. Epoxy resins (ER) of different chemical nature (aromatic and aliphatic) have been used for synthesis of EPTP. EPTP polymers were synthesized due to cationic polymerization of the ER, which is caused by the catalytic effect of the PTA. This heteropolyacid was added to the reactive mixture as water solutions. The dielectric characteristics (permittivity, impedance, conductivity) in a wide range of frequencies (3·10⁻¹ - 1·10⁷ Hz) and temperatures (-40 - 200°C) have been studied. It is shown the influence of the structure on characteristics of the EPTP. The same content of the protons in every system (the protons source is 1% of the PTA in the reactive mixture) gives different level of conductivity depending on chemical nature of the ER and solvent (water) content in the reactive mixture. It is provided with the different activation energy of the protons moving within the epoxy matrix with different chain structure.

SOL-GEL SYNTHESIS OF EPOXY-TITANIA NANOCOMPOSITES

F. N. Pavlii, E. A. Volyanyuk, S. V. Zhil'tsova, V. M. Mikhal'chuk

Donetsk National University, Universitetskaya Str. 24, Donetsk 83001, Ukraine
svetlana_zhiltsova@rambler.ru

Sol-gel method is widely used for the obtaining of polymeric nanocomposites. Combination of inorganic and organic constituents' properties at the nanometer scale allows formation of high performance materials for different applications. Depending on the way of sol formation, chemical nature of components used and reaction conditions one can easily change the structure and properties of the resulting materials. The goal of the research was synthesis of optically transparent nanocomposites using epoxy resin and titania nanoparticles formed in situ via the sol-gel technique.

The components used for polymeric matrix formation were diepoxide EPONEX™ 1510 and amine curing agent JEFFAMINE® T-403. TiO₂ particles were received via the sol-gel method by mixing tetrabuthtoxytitanium, water, ethanol and acetic acid in a definite sequence. The samples were cured at room temperature for 3 days with a post-curing stage for 3 h at 120 °C. TiO₂ content in the received materials was 0.5–3 % (wt.) according to thermogravimetric analysis data. The received composites possess high transparency. The microscopic analysis data shows the formation of spherical TiO₂ particles with the size of ~100 nm and uniform distribution in epoxy matrix.

The results of thermomechanical analysis demonstrate the shift of glass transition temperature of composites to lower values compared to unmodified epoxy polymer. At the same time the interval of glassy-to-viscoelastic state transition becomes wider. This may be due to growth of chain molecular mobility inhomogeneity at the interphase "titania nanoparticle – epoxy matrix" and decrease of network density [1]. Such changes can be positive in terms of raise of impact strength of the received materials because neat epoxy polymers are often brittle.

Thus the synthesis scheme of transparent epoxy-titania nanocomposites has been developed using sol-gel method for TiO₂ nanoparticles formation. The presence of the in situ formed nanofiller results in increase of epoxy matrix molecular motion and decrease of composites' glass transition temperature.

1. N.G. Leonova, V.M. Mikhal'chuk, Y.P. Mamunya, V.V. Davydenko, M.V. Iurzhenko. Thermophysical properties of epoxy-polysiloxane composites of cationic polymerization // Polym Sci, Ser. D. 6(N3) (2013) 210-217.

WEAK BASE MICROPOROUS RESINS AS TEMPLATES FOR CaCO₃ MINERALIZATION

F. Doroftei,¹ M. Mihai,¹ I. Bunia,¹ E. Marlica,¹ B.C. Simionescu^{1,2}

¹*"Petru Poni" Institute of Macromolecular Chemistry, Grigore Ghica Voda Alley 41A, Iasi 700487, Romania*
marcelas@icmpp.ro

²*"Gh. Asachi" Technical University, Faculty of Chemical Engineering and Environmental Protection, Iasi, Romania*

Gels are an important subclass of soft matter composed of three dimensional polymer networks swollen in solvents. Ion exchange resins are covalently cross-linked, insoluble (co)polymers, supplied as beads. The beads have either a dense internal structure with no discrete pores (gel resins, also called microporous resins) or a porous, multichannelled structure (macroporous or macroreticular resins). Functionalized crosslinked polymers have gained importance in the preparation of a great number of ion exchangers, as carrier matrices in a variety of medical, hydrometallurgical, environmental and biomedical applications due to several possibilities of modification of their chemical and physical properties. Polymeric resins can provide selective removal of heavy metals and could be used for purification and for treatment of final wastewaters [1]. Acrylic copolymers represent interesting macromolecular supports for the ion exchangers due to their high physico-chemical stability and the hydrophilic structure [2,3]. The acrylic matrices could have a high potential application for the synthesis of the ion exchangers with the improved ion exchange properties. The modification of the acrylic matrices is a method of obtaining compounds with ionic or ionizable groups and high hydrophilicity of the structures.

In biological systems, biominerals are commonly formed in gel-like extracellular networks which use the supramolecular assemblies of organized biomolecules to control the biomineraliation process [4]. Previous studies showed that the protein macromolecules affect the crystallization of inorganic substance, such as CaCO₃ [5]. The functional groups (especially carboxylic groups) on the gel-like structures influence the formation of crystals from the aspects of electrostatics, spatial location, match of crystal lattices, stereochemistry, etc. [6-9].

In this study, gel-like crosslinked polymeric beads with weak base functional groups were used. The crosslinked acrylic copolymers were obtained as published before [10], using water suspension radical polymerization of divinylbenzene (DVB, 3 wt%), acrylonitrile (AN, 20 wt%) and ethylacrylate (EtA,

P11

77 wt%) in the presence of toluene as an inert component ($D = 0.4$), benzoyl peroxide as initiator (1 wt%) and poly(styrene-co-maleic anhydride) ammonium salt as 0.5 wt% aqueous solution as the continuous phase. The copolymers were then aminolysed with ethylenediamine (EDA), for 16 h using the copolymer/amine wt-ratio of 1/3 and temperatures of 110 °C, obtaining weak base beads, with primary amino groups as side groups (Fig. 1a). Usually, the copolymers synthesized in the presence of toluene have porosity in the swelling state (Fig. 1b), the network being flexible and can swell more at a low percent of DVB. Some characteristics of the crosslinked weak base beads are summarized in Table 1.

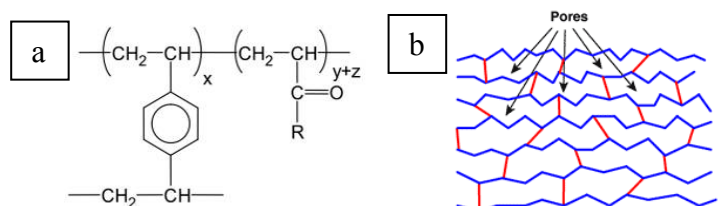


Fig. 1. (a) Chemical structure of weak base beads, $x = 3$, R: $-(CH_2)_2-NH_2$. (b) Schematic representation of the structure of gel type network.

Table 1. Characteristic data of weak base copolymers.

Characteristics	
Matrix	Cross-linked DVB:AE:AN
Active group	EDA
Chemical form	Free base
Physical form	Spherical beads
Mean particles size	0.3 – 0.8 mm
Total exchange capacity	0.53 meq mL ⁻¹ 7.217 meq g ⁻¹
pH range	1-14
Operational temperature	< 80 °C
Chemical stability	Good in acid and basic media

The crystallization of CaCO₃ on weak base gel-like beads was carried out in glass beakers, at ~25 °C, by colloidal crystallization from supersaturated (relative to CaCO₃) solution. The process was initiated by rapid mixing of equal volumes of CaCl₂ and Na₂CO₃ solutions, with equal concentrations. The morphology of composite spheres was evidenced by SEM, and the polymorphs content by X-ray diffraction.

Figure 2 shows the SEM micrographs and Fig. 3 the X-ray diffractograms of calcium carbonate microparticles formed on the gel beads, with different CaCO₃ content, comparative with bare spheres.

P11

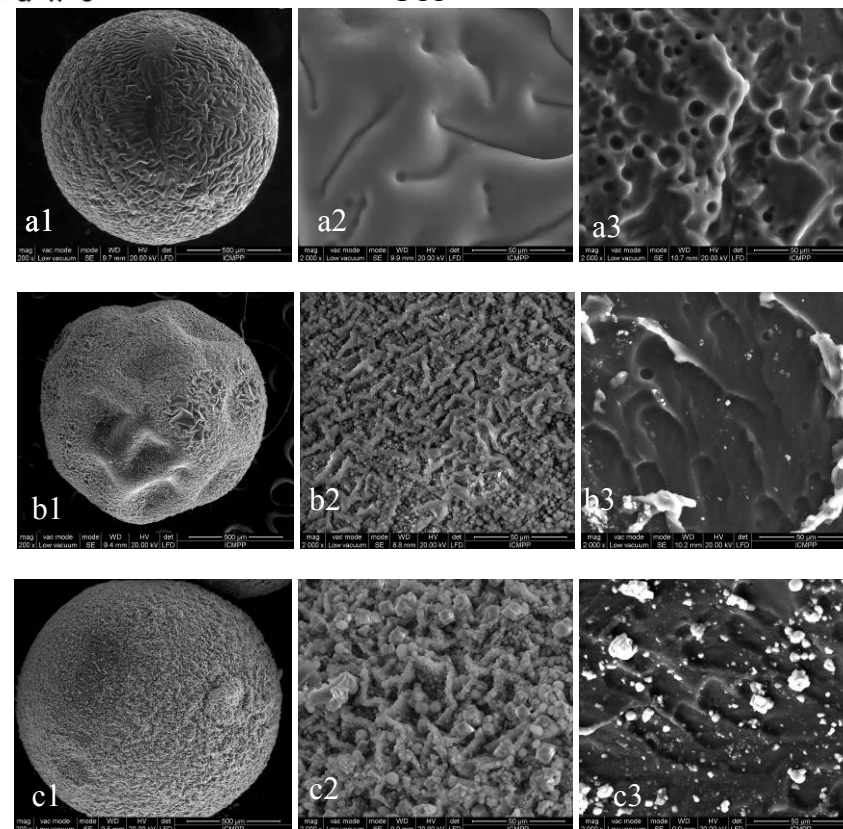


Fig. 2. SEM images of bare gel-like particles (a1) and composites with 0.1M (b1) and 0.3 M (c1) CaCO₃ content in starting mixtures; (a2, b2, c2) detail on the spheres surface and (a3, b3, c3) on spheres section.

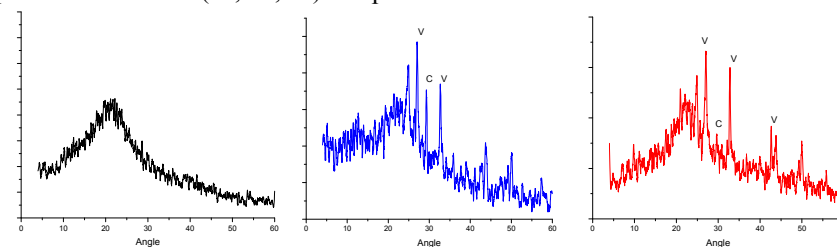


Fig. 3. X-ray diffractograms of bare gel-like particles (a) and composites with 0.1M (b) and 0.3 M (c) CaCO₃ content in starting mixtures.

A very good coverage of particles surface took place, irrespective of initial inorganic mixture concentration, a higher amount of CaCO₃ crystals into the particles being observed at higher inorganic concentration. X-ray diffractograms evidenced the vaterite (v) and calcite (c) polymorphs formation in the composite with lower inorganic content, whereas almost only vaterite has been obtain when inorganic content increased. The investigations on the growth of CaCO₃ crystals using gel-like beads as template could help to deeper understanding the biomineralization mechanism in living organisms.

The financial support of Project ID_313/2011 is gratefully acknowledged.

1. *Buhaceanu R., Sarghie I., Barsanescu A., Dulman V., Bunia I.* Silver sorption on acrylic copolymers functionalized with amines. Equilibrium and kinetic studies // Cent. Eur. J. Chem. 7 (2009) 827-835.

2. *Dragan S., Grigoriu G.* Ion exchange resins. I. Anion exchangers with tertiary amine groups on poly(acrylonitrile-codivinylbenzene) networks // Angew. Makromol. Chem. 200 (1992) 27-36.

3. *Neagu V., Bunia I.* Synthesis and morphological characterization of ethylacrylate : acrylonitrile : divinylbenzene copolymers // Rev. Roum. Chim. 54 (2009) 1041-1049.

4. *Antonietti M., Breulmann M., Goltner C.G., Colfen H., Wong K, Walsh D., Mann S.* Inorganic/organic mesostructures with complex Architectures: Precipitation of calcium phosphate in the presence of double-hydrophilic block copolymers // Chem-Eur J 4 (1998) 2493-2500

5. *Gower L.A, Tirrell D.A.* Calcium carbonate films and helices grown in solutions of poly(aspartate) // J. Cryst. Growth 191 (1998) 153-160.

6. *Grassmann O., Muller G., Lobmann P.* Organic-inorganic hybrid structure of calcite crystalline assemblies grown in a gelatin hydrogel matrix: relevance to biomineralization // Chem. Mater. 14 (2002) 4530-4535.

7. *Kato T., Suzuki T., Amaniya T., Irie T., Komiyama M., Yui H.* Effects of macromolecules on the crystallization of CaCO₃ the formation of organic/inorganic composites // Supramol. Sci. 5 (1998) 411-415.

8. *Butler M.F., Glaser N., Weaver A.C., Kirkland M., Heppenstall-Butler M.* Calcium carbonate crystallization in the presence of biopolymers // Cryst. Growth Des. 6 (2006) 781-794.

9. *Grassmann O., Lobmann P.* Biomimetic nucleation and growth of CaCO₃ in hydrogels incorporating carboxylate groups // Biomaterials 25 (2004) 277-282.

10. *Maxim S., Flondor A., Bunia I., Rabia I., Zerouk J., Farida I., Guettaf H.* Acrylic three-dimensional networks. II. Behavior of different acrylic ion exchangers in the retention and elution processes of some metal cations // J. Appl. Polym. Sci. 72 (1999) 1387-1394.

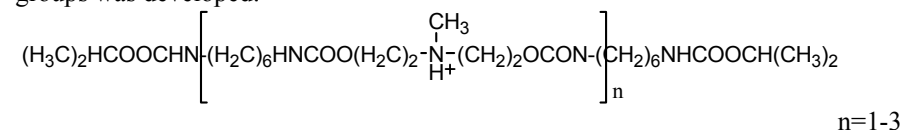
NEW MONTMORILLONITE MODIFICATION METHODS FOR MAKING NANOCOMPOSITES BASED ON POLAR GETEROCHAINED POLYMERS

A. N. Gonchar, Yu. V. Savelyev

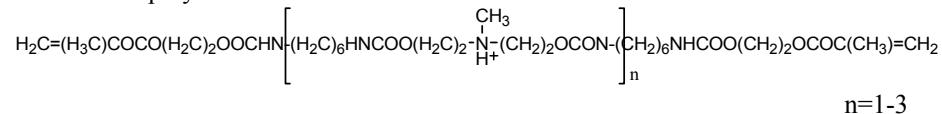
Institute of Macromolecular Chemistry NAS of Ukraine, Kharkovskoe shosse 48, 02160, Kiev

lexgon@ukr.net

The forming of nanocomposite which contain a complex of enhanced or new properties is a promising direction of modern polymere science. Natural inorganic structures such as montmorillonite (MMT) are commonly used for making polymer nanocomposites. Incompatibility of organic and inorganic components — the main problem, which should be solved while composing such materials. The compatiability problem of organic and inorganic components is solved by modification of MMT with an organic matter. To create nanocomposites based on different polyurethane types a synthesis method of a new modifier based on oligouretane ammonium chloride (OUACI) which contains urethane groups was developed:



The new modifier provides a full exfoliation of a nanofiller in a polyurethane matrix, which increases durability of polyurethane materials. By analogy with OUACI, olygourethane methacrilate ammony chloride (OUMAACI) was synthesised. Beside urethane groups, which provide a stable physical bond with a polyurethane matrix, there are reactive groups, which can form a chemical bond with a polymer matrix:



Unlike classical surfactants used in MMT modifications new modifiers provide a high affinity of modified MMT with polymere matrix due to the possibility of physical and chemical bonding.

Research of modified MMT swelling in organical solvents showed that MMT modified with urethane fragment containing modifiers forms a stable gel in a medium of dimetylformamide (DMFA) and dimethylsulphoxyde (DMSO).

The fact of gel forming suggests a high intercalation degree of a solvent into the MMT interlayer space and a physical network formation.

WAXS study of modified MMT and urethane based nanocomposites with modified MMT prove a new type of modifier intercalation into the interlayer space MMT and full exfoliation of modified silicate in the polymer matrix. WAXS study of polyurethane based nanocomposites with modified MMT prove whole and semantic exfoliation of the filler in the polymer matrix. The absence of absorption peak which is typical for modified MMT in all nanocomposite samples with contained MMT from 0,5 to 5 w.% proves it.

Thus by modifying MMT with our new modifiers the full exfoliation of nanofiller in the polymer matrix was reached and the strength of polymer materials was reached by 40% for linear polyurethanes and by 250% for crosslinked polyurethaneacrylates.

CdS/ZnS-doped silicate films prepared by sol-gel method

R. Iordanescu¹, I. Feraru^{1*}, S. Peretz², M. Elisa¹, I. C. Vasiliu¹, R. D. Trusca³,
E. Vasile⁴

¹*Optospintronics Department, National Institute of R & D for Optoelectronics INOE 2000, 409 Atomistilor Str., Magurele 077125, Romania
E-mail of the corresponding author (*): feraru_i@yahoo.com
iorda85@yahoo.com*

²*Institute of Physical Chemistry "I. Murgulescu", Romanian Academy, Department of Colloids, 202 Spl. Independentei, Bucharest, Romania*

³*METAV-CD, 31 C.A. Rossetti, Bucharest, Romania*

⁴*University Politehnica of Bucharest, 313 Spl. Independentei, Bucharest, Romania*

Semiconductor quantum dots (QDs) show optical properties that depend on their size and are of great interest for various applications in photovoltaic devices [1], optical amplifier for telecommunication networks [2], and for biolabeling [3].

The good photostability, high photoluminescence (PL) intensity and broad emission tunability make these QDs an excellent choice as novel chromophores. To assemble QDs into solid matrices is a critical stage required for their integration with solid-state devices.

Luminescence films play an important role in various devices including high resolution devices such as cathode ray tubes, thin film electroluminescent panels, and field emission displays. Cadmium sulfide (CdS) embedded in a film matrix as the protective shell have been reported to provide a high density of light emitting centers by varying the size and concentration of QDs in an ensemble [4].

Many researchers have incorporated CdS into transparent silica matrix [5] and explored their potential applications in QD lasers, wave-guides and high-speed optical switches [6].

Recently silica thin films with different CdS quantum dot concentrations are deposited on glass substrates by a sol-gel dip-coating process, followed by thermal treatment at different annealing temperatures. The effects of CdS concentration and annealing temperature on the structural and optical properties of the composite films are investigated [7].

The core shell nanoparticles (CdS/ZnS) were fabricated in a two-step route: initial synthesis of core nanoparticles (CdS), followed by a purification step, and the subsequent shell growth reaction using ZnS.

In the first step there have mixed under stirring (at 500 rpm) two aqueous solution of cadmium nitrate ($\text{Cd}(\text{NO}_3)_2$) with sodium sulfide solution (Na_2S), in

order to obtain the colloidal cadmium sulfide particles. The system was purged with N_2 gas for 30 minutes to prevent the photocorrosion and the formation of the colloidal sulphur. The solution containing nanoparticles were centrifuged (5000 rpm, 10 min) and washed several times with bidistilled water and ethanol, and after dried in air at $40^\circ C$ for 24 hours under controlled environment.

In the next step of shell growth reaction, the obtained CdS nanoparticles were introduced in a 1% (w/v) chitosan solution and mixed under intense stirring (7000 rpm) with an aqueous Na_2S solution over 30 min. Subsequently, to the above mixture was added a solution of zinc acetate ($Zn(CH_3COO)_2$), and the stirring continued for 30 minutes for reaction ripening, under atmosphere of nitrogen. The obtained solution was centrifuged, washed with bidistilled water and ethanol, and CdS/ZnS particles remain under preserving in an ethanol solution.

Silicate films doped with CdS/ZnS quantum dots (QDs) have been deposited by sol-gel method, spin coating technique. Initially, a precursor solution (PS) composed of tetraethoxysilane (TEOS) and ethanol (EtOH) has been prepared. Then, dimethylformamide (DMF) as surfactant and stabilizer reagent was added, followed by CdS/ZnS QD, under continuous stirring. Three compositions of CdS/ZnS QD-doped silica films have been prepared, as follows: (TCdS1) - PS/DMF/QD: 1/1/1 volume ratio and TEOS/EtOH = 0.02 molar ratio; (TCdS2) - PS/DMF/QD: 1/1/1.3 volume ratio and TEOS/EtOH = 0.04 molar ratio; (TCdS3) - 1/1/3 volume ratio and TEOS/EtOH = 0.04 molar ratio. The pH = 3 for the final solutions was found to be optimum for the deposition process and gelification and it was adjusted by adding few droplets of HCl 0.1 N. The films have been deposited on silicon substrates that were previously cleaned with HF, followed by water and EtOH. Multilayer films have been obtained consisting of 10 coatings, 2000 rpm rotation rate of the substrate, 20 s deposition duration, each layer was heat treated at $200^\circ C$, for 2 min.

Raman spectra were recorded by using a LabRAM HR 800 UV-VIS-NIR Horiba Jobin-Yvon system, at room temperature, the samples being excited with 514 nm line of an Ar^+ ion laser. Figure 1 show Raman spectra of CdS/ ZnS quantum dots in EtOH solution (dopant), TCdS3 thin film and silicon substrate collected in the range 130- 1200 cm^{-1} . As it can be seen in the fig. 1, Raman spectra of the deposited film reveal the same pattern as Raman spectrum of the silicon substrate. This can be explained by the small thickness of the deposited film, Raman signal from the silicon substrate being more pregnant. Thus, the resulted spectrum is dominated by the bonds related to silicon substrate. Also, the small size of quantum dots and the large relative volume of the silicate matrix, affect the properties of the localized phonons and their interaction with excitation radiation, being difficult to obtain specific vibration of CdS quantum dots. The specific Raman line of CdS is located at about $300\ cm^{-1}$ [8] and it is overlapped by Raman line of silicon substrate as it can be seen from Fig. 1.

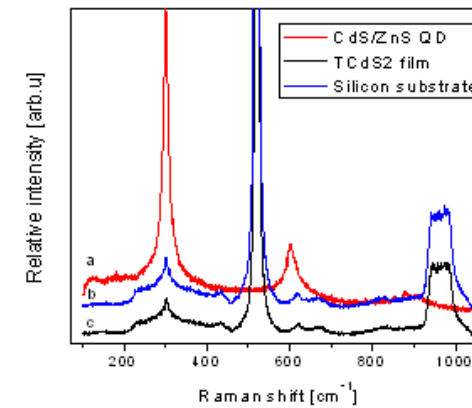


Fig. 1. Raman spectra of a) CdS/ZnS QD dopant; b) silicon substrate; c) TCdS2 film.

In the Fig. 2 FTIR, spectrum of TCdS2 film in the range 400-1200 cm^{-1} is presented.

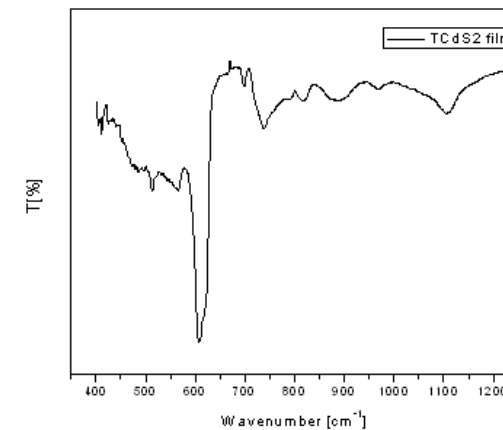


Fig. 2. FTIR spectrum of TCdS2 film.

The FT-IR spectral studies shows that the stretching frequencies for cadmium sulfide appeared at 609 and 736 cm^{-1} that match the reported values presented in the graph from the fig. 2 [9, 10].

In the Fig. 3, fluorescence spectrum of TCdS2 film is presented, provided by 400 nm light excitation.

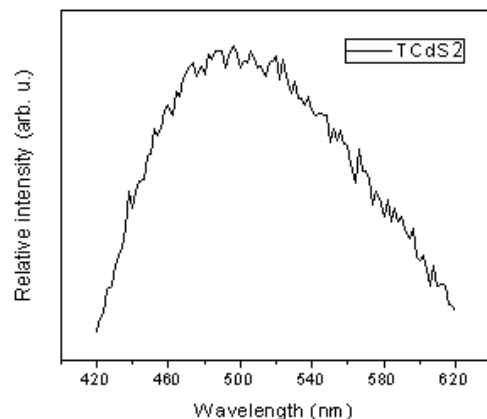


Fig. 3. Fluorescence spectrum of TCdS2 film provided by 400 nm excitation.

As it can be seen from the Fig. 3, an emission at about 500 nm is found characterized by a relative large luminescence band possible due to a large size range of the dopant from the silica network.

In the Fig. 4, TEM image of the TCdS2 sample is presented. Small CdS nanocrystallites embedded in the silica network, having 2-4 nm size, are revealed.

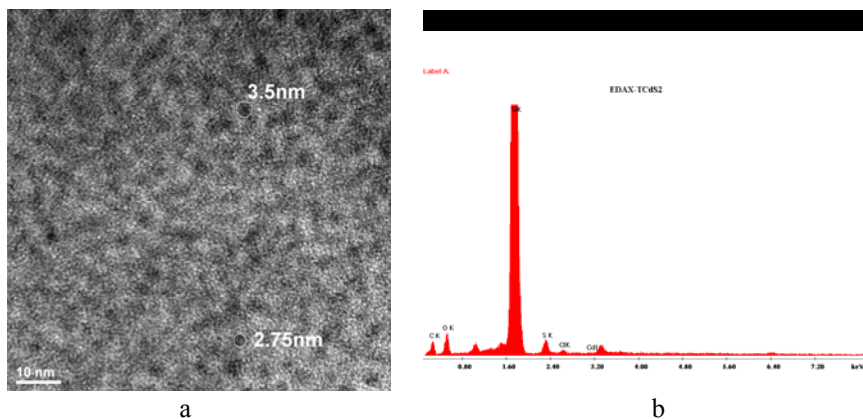


Fig. 4. a) TEM image of TCdS2 sample; b) EDAX spectrum of TCdS2 sample.

EDAX spectrum shows in evidence specific lines for the silica matrix (Si, O) and substrate as well as for the dopant, *i.e.* Cd and S.

Acknowledgments

The authors are grateful to UEFISCDI (Executive Unity for Financing of Higher Education, Research and Innovation) for the financial support in the frame of project IDEAS, contract No. 51/5.10.2011.

1. Rai R. Sharma S. Synthesis, characterization and optical properties of nanosized CdS hollow spheres. // *Adv. Mat. Lett.* 1(3) (2010) 269. DOI: 10.5185/amlett.2010.7140.

2. Harrison M. T. Kershaw S. V. Burt M. G. Rogach A. L. Kornowski A. Eychmuller A. Weller H. Colloidal nanocrystals for telecommunications: Complete coverage of the low loss fiber windows by mercury telluride quantum dots. // *Pure Appl. Chem.* 72 (2000) 295-307.

3. Han M. Gao X. Su J. Z. Nie S. Quantum-dot-tagged microbeads for multiplexed optical coding of biomolecules. // *Nat. Biotechnol.* 19 (2001) 631-635.

4. Cheng Z. Su F. Pan L. Cao M. and Sun Z. CdS quantum dot-embedded silica as luminescent down-shifting layer for crystalline Si solar cells *J. Alloys Comp.*, 494 2010 (1-2) L7-L10.

5. Hullavarad N. V. Hullavarad S. S. Synthesis and characterization of monodispersed CdS nanoparticles in SiO₂ fibers by sol-gel method. // *Photonic Nanostruct.* 5 (2007) 156-163.

6. Reda S. M. Synthesis and optical properties of CdS quantum dots embedded in silica matrix thin films and their applications as luminescent solar concentrators. // *Acta Materialia* 56 (2) (2008) 259-264.

7. Chen Z. Qin J. Zhang X. Zhang M. Shi W. Wang L. Synthesis and optical properties of CdS quantum dot-embedded silica film for luminescent down-shifting layer. // *Proc. SPIE 7995*, Seventh International Conference on Thin Film Physics and Applications, 79952M (2011) doi:10.1117/12.888425.

8. Prabhu R. R. Khadar M. A. Study of optical phonon modes of CdS nanoparticles using Raman spectroscopy. // *Bull. Mater. Sci.*, 31 (3) (2008) 511-515.

9. Sabah A. Siddiqi S. A. Salamat A., *World Academy of Science, Engineering and Technology* 45 (2010) 82-89.

10. Barman R. Borah J. P. Sarma K. C., *Opt. Adv. Mater. – Rap. Com.* 2 (12) (2008) 770 – 774.

HEAT-RESISTANT HYBRID POLYMER NANOCOMPOSITES CONTAINING FUSIBLE METALS

**M. Iurzenko^{1,2}, Ye. Mamunya^{1,2}, G. Boiteux³, E. Lebedev¹,
I. Parashchenko¹, E. Gladkiy¹**

¹*Institute of Macromolecular Chemistry of National Academy of Sciences of Ukraine, Kharkivske shosse 48, Kyiv 02160, Ukraine*
4ewip@ukr.net

²*Center for Thermophysical Investigations and Analysis of the NAS of Ukraine*

³*Université de Lyon, Université Lyon 1, Ingénierie des Matériaux Polymères, UMR CNRS 5223, IMP@LYON1, France*

The aim of the present work was understanding the impact of dispersed fusible metallic powders, namely tin and lead, separately as well as commonly with modifiers of inorganic component on thermal, thermomechanical and electrical properties of the hybrid polymer nanocomposites (HPN).

HPN were synthesized by joint polymerization process of organic and inorganic components. Organic component was a mixture of polyisocyanate (PIC) and macrodiisocyanate (MDI). Heat-resistant composites with 80%wt. of PIC and 20%wt. of MDI were taken as the basic for further processing and filling. Inorganic component was water solution of sodium silicate (SS). Aerosil A175 and powdered glass were used for SS modification. Tin powder with particle diameter $d \approx 2 \mu\text{m}$ and lead powder with $d \approx 20 \mu\text{m}$ were dispersed in the reactive mixtures of organic and inorganic components during HPN synthesis. The contents of the metallic powders in the synthesized HPN were varied from 0 to 40%vol. Polymerization of pure HPN, modified HPN and filled HPN passed at $T = 20 \pm 2 \text{ }^\circ\text{C}$ during 24 hours.

The structure of the modified HPN obtained was found in the form of membrane with regularly shaped interconnecting pores with $\sim 90 \mu\text{m}$ in diameter. The formation of such structure was due to the emission of carbon dioxide in the set of reactions, which run during OIS polymerization. Sodium silicate interacts with inorganic particles (such interaction is more intensive with nanodimensional particles of Aerosil A175). It decreases the ability of sodium silicate to absorb carbon dioxide. Due to that the porous structure in HPN bulk may appear. The introducing of inorganic particles into sodium silicate leads to the appearance of the specific hydroxyl groups on the surface. The presence of sodium ions Na^+ structures a water layer, the electrostatic field of ions deforms water grating. Inorganic particles can interact with each other forming aggregates as well as with

sodium silicate that impact on the properties of HPN.

The introduction of metallic fillers in the modified porous structure of HPN increases rates of transport, dissipation and uniform distribution of thermal energy in HPN bulk. That leads to higher values of thermal stability, precise structural transitions and broad operating temperature range of the filled HPN. However, the level of electrical conductivity of the filled HPN ($\sigma_{\text{DC}} \approx 10^{-12} \text{ S/cm}$) changed insufficient comparing to the pure HPN ($\sigma_{\text{DC}} \approx 10^{-14} \text{ S/cm}$).

Heating of the filled HPN to the temperatures higher than structural transitions temperatures of HPN and melting temperatures of metallic particles (separately for HPN filled with tin and lead particles) leads to electron conducting phase formation in the porous HPN bulk. Further cooling of the filled HPN to the temperature lower than structural transitions temperatures of HPN and crystallization temperatures of metallic particles leads to formation of continuous electron-conducting metal cluster in HPN volume with level of conductivity $\sigma_{\text{DC}} \approx 10^{-3} \text{ S/cm}$.

Acknowledgement

The results of the presented studies were obtained with use of equipment of the Center of Thermophysical Investigations and Analysis of the NAS of Ukraine (<http://www.ihvs.kiev.ua/CCUE/>) in the Institute of Macromolecular Chemistry of the NAS of Ukraine.

EQUAL-CHANNEL MULTIPLE ANGULAR EXTRUSION - AN EFFECTIVE METHOD OF A STRUCTURAL MODIFICATION OF CRYSTALLIZED POLYMERS

V. Beloshenko, A. Voznyak, Y. Voznyak

Donetsk Institute for Physics and Engineering named after A.A. Galkin, National Academy of Sciences of Ukraine, 72 R. Luxemburg st., 83114 Donetsk, Ukraine
voznyak@vnet.dn.ua (Y. Voznyak)

In the last 10-15 years, the specialists dealing with creation and investigation of metallic materials with new properties pay great attention to nanostructural materials. Now a number of the methods of nanostructure formation have been developed. The methods of severe plastic deformation (SPD) become a frequent practice, e.g. high pressure torsion, comprehensive forging, equal-channel angular extrusion (ECAE), twist extrusion [1].

In contrast to metals, application of SPD to polymers is not aimed at formation of a nanostructural state but at creation of orientation ordering without change of the shape of the initial billet. The method of ECAE becomes the most often used [2-9]. ECAE of semicrystalline polymers results in enhancement of rigidity and strength with the plasticity conserved at sufficiently high level. In the case of natural semicrystalline polymers, ECAE processing allows obtaining bulk monolith materials with the full density and mechanical properties, which are comparable with that of synthetic polymers [10,11]. At the same time, as distinct from the traditional solid-phase extrusion, ECAE provides realization of controlled molecular orientation at conserved billet size. The last fact is of special importance when orientation order is formed in large-sized samples. The features of the scheme of equal-channel multiple angular extrusion (ECMAE) [12] allows considering it as a more effective method of solid-phase processing of polymers beside ECAE, which gives certain opportunities: - to avoid undesired relaxation processes related to cooling and subsequent heating of the deformed samples up to the extrusion temperature T_e ; - to solve the problems with accumulation of the plastic deformation ε , that arise in the course of ECAE because of warping of the polymeric billet even after the first deformation cycle; - to change the position of the shear plane due to combination of different deformation routes and to realize the routes impossible at ECAE.

The present work tests ECMAE effect on the structure and the properties of semicrystalline polymers.

The subjects of research were high density polyethylene (HDPE) CESTILENE HD1000; polyamide-6 (PA-6) – ERTALON 6SA; polyoxymethylene

(POM) – TECAFORM AH. The billets of the required size for ECMAE (15 mm in diameter, 50 mm in length) were cut from cylindrical rods obtained by melt extrusion.

The structural state of the polymers was varied by the change of the degree of accumulated plastic deformation and ECMAE route (Fig.1). With account of designations used for ECAE, we introduced and used the following ECMAE routes in the present work: route C, when pair-connected oblique deforming channels are in the same plane; route E, when the deforming channels are rotated in turn through the angle of $\pm 90^\circ$ to the vertical axis; route F, when the rotation of pairs of oblique deforming channels is performed with the step of 90° ; routes B+C and D+C analogous to routes E and F with the pairs of oblique channels separated by vertical channels (Fig. 1). Changed location of the deforming channels provides creation of different positions of the simple shear planes and directions.

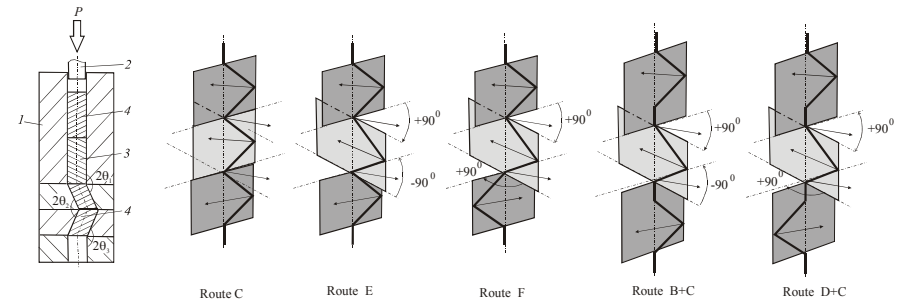


Fig. 1. Scheme of ECMAE process: 1- die, 2 – punch, 3 – polymeric billet, 4 – sacrificed billets.

The value of equivalent plastic deformation ε was calculated as

$$\varepsilon = 2 \sum_{i=1}^n \frac{\text{ctg} \theta_i}{\sqrt{3}}, \text{ where } \theta_i \text{ is a half of the angle of channel intersection, } n \text{ is the}$$

number of the angles of channel intersection [12]. The rate of extrusion was $0.6 \cdot 10^{-3}$ m/s, T_e was 383 K (HDPE), 408 K (POM), 423 K (PA-6), according to the optimum conditions of the process [13,14].

The effect of ε and deformation route on the mechanical properties of PA-6 is illustrated by Table 1. When ε increases, increase in the modulus of elasticity E , yield strength σ_y , tensile strength σ_T is observed. Anisotropy of

microhardness ΔH ($\Delta H = 1 - \frac{\bar{H}^\perp}{\bar{H}^\parallel}$, where $\bar{H}^\perp, \bar{H}^\parallel$ are the average values of

microhardness in longitudinal and transversal sections of extrudates) that characterizes the difference in strength properties in longitudinal and transversal

directions [15] is reduced. Among the realized ECMAE routes, the best set of mechanical properties was associated with route D+C that provided not only enhanced rigidity and strength but also the plasticity (strain at break ε_b) conserved at the level of the initial polymer (Table 1). As $H \sim \sigma_y$ [15], almost zero anisotropy of microhardness allowed us to make a conclusion that yield strength corresponding to the longitudinal and transversal directions in extrudates was about the same.

One can observe correlation between deformation and strength characteristics of polymers extruded with varied ε along different routes and thermal properties. Non-deformed materials have one wide endothermic melting peak in DSC curves.

Table 1. Effect of ECMAE route on the mechanical properties of PA-6

Route	ε	ΔH	E	σ_y	σ_T	ε_b
			[MPa]			[%]
Non-deformed	0	0.02	900	67	69	148
E	6.7	0.15	1450	130	132	125
	9.1	0.08	1480	140	144	128
F	6.7	0.15	1400	128	130	126
	9.1	0.08	1500	140	145	128
B+C	6.3	0.14	1470	132	135	130
	8.5	0.07	1600	142	142	134
D+C	6.3	0.10	1560	138	140	132
	8.5	0.05	1900	150	154	143

The extruded samples have two endothermic peaks in the same temperature range. The highest values of positions of the primary melting peak T_{1max} and the secondary one T_{2max} are characteristics of polymers processed along route D+C. The values of these parameters for the mentioned route are listed in Table 2 as well as the enthalpy of fusion ΔH_f and the degree of crystallinity χ_c at $\varepsilon=8,5$ in the case of HDPE. It is seen that ECMAE increases χ_c substantially. The obtained results are in good agreement with the data of X-ray analysis and density measurements where χ_c increases as ε grows and reaches the maximum value at the extrusion along route D+C [16].

In [16], it was demonstrated by the methods of electron microscopy and wide-angle x-ray scattering that ECMAE formed biaxially oriented structures differing in the degree of development of the net of interwoven fibrils. The last parameter is determined by the deformation route and ε magnitude. The doublet

Table 2. Effect of ECMAE on the degree of crystallinity and thermal properties of polymers

Treatment	T_{1max}	T_{2max}	ΔH_f	χ_c	ν_1	ν_2	l_{1c}	l_{2c}	α^\perp	α^\parallel
	[K]	[K]					[nm]	[nm]	$\cdot 10^6, [K^{-1}]$	$\cdot 10^6, [K^{-1}]$
HDPE										
Non-deformed	403	–	182	0.63	16	–	16	–	220	210
After ECMAE	410	412	238	0.83	34	145	30	39	–7	–6

appearing in DSC curves can be related to arising inhomogeneous fibril structure that consists of two types of microfibrils. The evaluation of the size of supermolecular formations (the parameter of intra-chain cooperativity of melting is $\nu_i = 2R(T_{i true})^2 / \Delta \dot{O}_{i true} \Delta \dot{I}_f$, where $\dot{O}_{i true}$ is the true value of the temperature of the melting peak and $\Delta \dot{O}_{i true}$ is the true value of the width of the melting interval) and the thickness of lamellae l_{ic} in the tested polymers (Table 2) allow suggestion that the crystals determining the appearance of the second melting peak include straightened sections of macromolecules that integrate the neighbor crystallites and the disordered layer. The crystals determining the first melting peak do not almost have straightened sections of macromolecules passing through the neighbor crystallites.

Formation of biaxially oriented structures in the course of ECMAE is also confirmed by the results of dilatometric tests. The most interesting result is that biaxial invar-effect can be observed in ECMAE-modified semicrystalline polymers at certain conditions. It is revealed at very low and weakly varied values of the elongation in the longitudinal and transversal directions at heating in a wide temperature range. The values of temperature coefficients of linear expansion α are many times smaller than that of non-deformed polymers and approach α , magnitudes characteristic of invar alloys (Table 2). This behavior of thermal expansion was detected for the samples cut of the extrudates along the corresponding directions of dominating orientation of fibrils. The structure of polymers formed in the course of ECMAE is characterized by high thermal stability that provides stable enhanced level of properties even at the annealing temperature \dot{O}_{an} , close to the melting temperature. The dependences of $\dot{I}(\dot{O}_{an})$ that allow separation of three characteristic areas are presented in Fig.3: I and III, where heating is not accompanied by the change of H , and II, where \dot{I} is reduced as \dot{O}_{an} increases.

P15

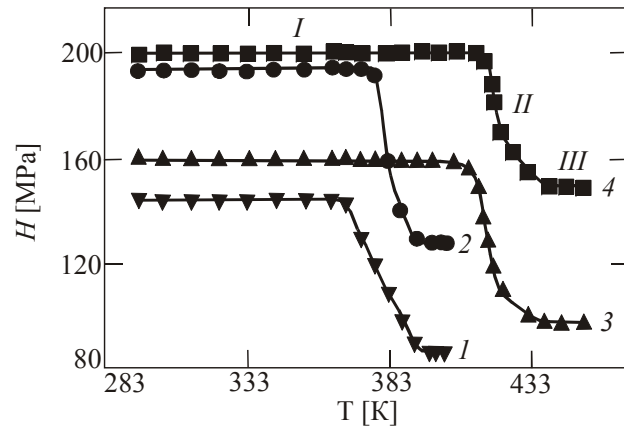


Fig. 3. Annealing temperature dependences of microhardness of HDPE (1,2) and PA-6 (3,4) extrudates (in the cross-section). 1,3 - $\varepsilon = 6.3$; 2,4 - $\varepsilon = 8.5$. Route D+C.

With increasing ε , the temperature of the microhardness drop \dot{O}_d is increased and the temperature interval $\Delta\dot{O}$ is reduced, where softening occurs. At fixed ε , higher values of \dot{O}_d and lower $\Delta\dot{O}$ are achieved in the succession: route C \rightarrow route F \rightarrow route D+C.

Enhanced thermal stability of extrudates can be related to creation of a dense net of physical nodes that contributes to enhanced stability of the deformed polymers to thermal effect, as is known, and to transition of a part of folded chain crystals into the partially extended chain crystals in extrudates.

ECMAE allows formation of a unique set of mechanical characteristics of rode articles made of semicrystalline polymers (combination of high plasticity and strength with low strength anisotropy). The polymers become endowed with new functional properties (biaxial invar effect), being at the same time provided with higher thermal stability, as compared to uniaxially oriented polymers.

1. C.P. Wang, F.G. Li, L. Wang, H.J. Qiao, Review on modified and novel techniques of severe plastic deformation, *Sci.China Tech. Sci.* 55 (2012) 2377-2390.

2. H.J. Sue, C.K.Y. Li, Control of orientation of lamellar structure in linear low density polyethylene via a novel equal channel angular extrusion process, *J. Mater. Sci. Lett.* 17 (1998) 853-856.

3. B. Campbell, G. Edwards, Equal channel angular extrusion of polyalkenes,

P15

Plast. Rubb. Comp. 28 (1999) 467-475.

4. Z.Y. Xia, H.J. Sue, T.P. Rieker, Morphological evolution of poly(ethylene terephthalate) during equal channel angular extrusion, *Macromolecules* 33 (2000) 8746-8755.

5. Z.G. Wang, Z.Y. Xia, Z.Q. Yu, E.Q. Chen, H.J. Sue, C.C. Han, B.S. Hsiao, Lamellar formation and relaxation in simple sheared poly(ethylene terephthalate) by small-angle X-ray scattering, *Macromolecules* 39, (2006) 2930-2939.

6. A. Phillips, P. Zhu, G. Edward, Simple shear deformation of polypropylene via the equal channel angular extrusion process. *Macromolecules* 39, (2006) 5796-5803.

7. F. Zaïri, B. Aour, J.M. Gloaguen, M. Naït-Abdelaziz, J.M. Lefebvre, Steady plastic flow of a polymer during equal channel angular extrusion process: Experiments and numerical modeling. *Polym. Engin. Sci.* 48, (2008) 1015-1021.

8. T. Wang, S. Tang, J.Chen, Effects of processing route on morphology and mechanical behavior of polypropylene in equal channel angular extrusion, *J. Appl. Polym. Sci.* 122, (2011) 2146-2158.

9. J. Qin, T. Murata, X. Wu, M. Kitagawa, M. Kudo, Plastic deformation mechanism of crystalline polymer materials in the equal channel angular extrusion process, *J. Mater. Proc. Tech.* 212, (2012) 1528-1536.

10. X. Zhang, X. Wu, D. Gao, K. Xia, Bulk cellulose plastic materials from processing cellulose powder using back pressure-equal channel angular pressing, *Carbohydrate Polym.* 87 (2012) 2470-2476.

11. X. Zhang, D. Gao, X. Wu, K. Xia, Bulk plastic materials obtained from processing raw powders of renewable natural polymers via back pressure equal channel angular consolidation, *Eur. Polym. J.* 44 (2008) 780-792.

12. V. Beloshenko, V. Spuskanyuk, ECAE methods of structure modification of materials, *Intern. J. Mater. Chem.* 2, (2012) 145-150.

13. V.A. Beloshenko, V.N. Varyukhin, A.V. Voznyak, Yu.V. Voznyak, Equal-channel multiangular extrusion of semicrystalline polymers. *Polym. Eng. Sci.* 50 (2010) 1000-1006.

14. V.A. Beloshenko, V.N. Varyukhin, A.V. Voznyak, Yu.V. Voznyak, Polyoxymethylene orientation by equal-channel multiple angular extrusion, *J. Appl. Polym. Sci.* 126 (2012) 837-844.

15. A. Flores, F. Ania, F.J. Balta-Calleja, From the glassy state to ordered polymer structure: A microhardness study. *Polymer*, 50, (2009) 729-746.

16. V.A. Beloshenko, V.N. Varyukhin, A.V. Voznyak, Yu.V. Voznyak, Control of the mechanical and thermal properties of semicrystalline polymers via a new processing route of the equal-channel multiple angular extrusion, *Polym. Eng. Sci.* (2013) DOI: 10.1002/pen.23583.

INVESTIGATION OF POLYSTYRENE SCINTILLATOR PROPERTIES PRODUCED BY INJECTION MOLDING METHOD

D.A. Blyznyuk¹, V.L. Avramenko²

¹Institute of Scintillation Materials, National Academy of Sciences of Ukraine,
Lenin Avenue 60, Kharkov, 61001, Ukraine

mittay2006@ukr.net

²National Technical University "Kharkiv Polytechnic Institute", str. Frunze, 21,
61002 Kharkov, Ukraine

avramenko@kpi.kharkov.ua

Scintillation method confidently holds the leading position in the field of registration of a variety high-energy radiation at the present stage of science and technology development.

The appearance of plastic scintillators (PSC) has become a new landmark in the development of scintillation method, due to their unique properties.

Depending on the type of detected radiation is used PSC with different composition and size.

A number of technological methods is used for manufacture of PSC: bulk polymerization (block), extrusion, compression, injection molding and others [1].

One of the most suitable ways to mass-production process one-type scintillator's detector method is injection molding method, but molding tiles typically have 15-20% less light output compared with plates received by machining from polymerization's blocks. Therefore, it was reasonable to explore the influence of the modes of making PSC with injection molding method on the properties of the produced tiles.

Traditional technology of manufacturing of PSC with this method has the step of mixing the polymer with luminescent additives and with specificity of molding of optically transparent products, relate to mold filling process melt, product's cooling process in mold, and the requirements for the construction of molds for such products. [2]

During the operation were tried out general purpose polystyrene pellets of various brands: BASF 143E, TOTAL 1540, Edistir N2560 and Nizhnekamsk 525.

Injection molding was done on the injection molding machine HAITIAN SA2000 with four socket die mold. Dimensions of tile 60*60*4 mm. The pills were mixed with scintillating additives before casting.

It was studied 36 modes of casting for each material. Such parameters were varied: the mold temperature (T_m) = 20°C, 40°C, 60°C, the material cylinder

temperature (T_c) = 195-200°C; 210-215°C; 225-230°C, injection pressure (P_{inj}) = 50 mPa; 100 mPa and injection speed (V_{inj}) = 60 g/sec, and 100 g/sec.

Physico-mechanical properties, superficial properties and measured relative measure of light attenuation (RMLA) of obtained samples were studied.

1. *Grinjov B.V.* Plastic scintillators / B.V. Grinjov, V.G. Senchishin. - KH.: Acta, 2003. - 324 p.

2. *Barashkov N.N.* Optically transparent polymers and materials on their basis / N.N. Barashkov, T.V. Sahno. - M.: Chemistry, 1992. - 77 p.

**NANOSTRUCTURED SYSTEMS BASED ON
MEO/POLYMER AS NEW MATERIALS WITH POSSIBLE
APPLICATION IN MEDICAL DENTISTRY****G. Calin¹, L. Olaru², N. Olaru², L. Dartu¹, V. Burlui¹***¹ "Apollonia" University, Iasi, Romania**² "Petru Poni" Institute of Macromolecular Chemistry, Grigore Ghica Voda Alley
41A, Iasi 700487, Romania*

Nanostructured systems based on MeO/polymer have attracted a lot of attention in the last years because of their applications in multiple areas. Nanofibres based on polymers are used in many domains such as nanocatalysis, controlled release of medicines, environmental protection and so on. In this work, we report the synthesis of the nanostructured compounds type MeO/polymer nanofibres (Me=Zn, Ni) with possible application in medical dentistry. In order to analyze the structural and textural features, the obtained materials were characterized using advanced physical-chemical techniques such as X-ray diffraction (XRD), Atomic Force Microscopy (AFM), Scanning Electron Microscopy (SEM) and Transmission Electron Microscopy (TEM). The XRD patterns show the characteristic reflections of ZnO with a hexagonal type wurtzite structure and the broad peaks of the polymer. The SEM images reveal the presence of ZnO nanoparticles on top of the polymer nanofibres. It is well known that composite materials based on ZnO present application in medical dentistry and taking into account the results obtained we propose in the future to test the obtained materials as dental composite for temporary restorations and dental implant.

**HIGHLY EFFICIENT REMOVAL OF ORGANIC DYES
USING NANOSTRUCTURED MATERIALS TYPE LDHS****L. Dartu¹, G. Carja², C. Zaharia²***¹ "Apollonia" University Iasi, Romania**² "Gh. Asachi" Technical University, Faculty of Chemical Engineering and
Environmental Protection, Department of Chemical Engineering, 71 Bd.
Mangeron, 700050 Iasi, Romania*

This study presents an introduction of new materials based on layered double hydroxides (LDHs), and their application as adsorbents for the removal of methyl orange dye from aqueous environments using separative non-destructive treatments.

In this context, the new LDH type materials containing in their structure different specific elements were characterized using advanced physical-chemical analysis techniques. Thus, the structural features were analyzed using X-ray diffraction (XRD) and thermal analysis (TG-DTG) while the textural properties were determined by scanning electron microscopy (SEM). In this context, the XRD pattern revealed the structure of LDHs, by the appearance of the characteristic reflections. The TG-DTG analysis was used to determine the thermal stability of LDHs, the thermal degradation of the samples taking place in four steps. The SEM images indicated similar textural patterns, confirmed by well-shaped nanoparticles with diameters extending over the nanometer scale. The influence of some operating factors such as type of LDH, concentration of polluting organic species, and operational/contact time are considered, and the highest treatment performance at its optimal operating value found. In order to fit the experimental data, a sorption kinetics model was predicted for each type of LDH studied.

ELASTIC, INELASTIC CHARACTERISTICS AND DEFECT NANOSTRUCTURE OF POLYPROPYLENE, TEFLON WITH CARBON NANOTUBES AND AUTOMATED SYSTEM OF ANISOTROPY ANALYSIS

A. P. Onanko, G. T. Prodayvoda, Y. A. Onanko

*Kyiv National University, Volodymyrs'ka str., 64, 01601, Kyiv, Ukraine
onanko@univ.kiev.ua*

The mechanical characteristics of composite based on polypropylene, teflon and multiwall carbon nanotubes (MWCNT) and automated system of ultrasound anisotropy measuring data analysis were researched. In this paper the absolute value of the elastic module E , elasticity limit σ_E , inelasticity limit $\sigma_{0,2}$, ultimate stress limit σ_S of the nanocomposites based on polypropylene + MWCNT 5%, polypropylene + MWCNT 0,5%, polypropylene + MWCNT 0,1% were determined. The influence of ultrasonic deformation ε was researched on mechanical properties of nanocomposite based on polypropylene, teflon and MWCNT.

The nanocomposite based on MWCNT and polypropylene total deformation consists of elastic and inelastic constituents $\varepsilon_{\Sigma} = \varepsilon_E + \varepsilon_{IE}$. Elastic deformation ε_E takes a place "instantly". Inelastic deformation ε_{IE} is conditioned motion of dislocations [1-3]. An important value is in a position of formation in the polymeric matrix of molecular structures, as MWCNT serve as the centers of crystalline phase origin.

For measuring the diagram tension – deformation $\sigma - \varepsilon$ the device IMASH-20-75 was used. For measuring elastic module E and internal friction (IF) the impulse method on frequency $f \approx 1,67; 5$ MHz and the method of complete piezoelectric oscillator on frequency $f \approx 118$ kHz was used at deformation $e \approx 10^{-6}$ in vacuum $P \approx 10^{-3}$ Pa. A measuring error relative change of the elastic module $\Delta E/E_0 \approx 0,5\%$ [4]. With the purpose of determination of temperature position of relaxation of the elastic module $\Delta E/E_0$ simultaneously with the IF measuring temperature dependence of E was measured. Annealing of structure defects bends out of shape the type of IF temperature spectrum. At annealing admixtures, vacancies go out. The oscillogram of impulses with transversal polarization, which are reflected in nanocomposite based on teflon-4 and MWCNT is represented on Fig. 1.

A. s. u.

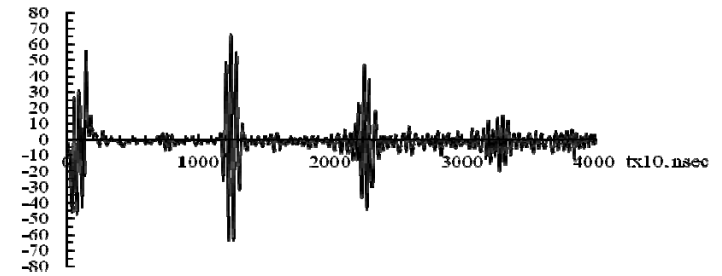


Fig. 1. Oscilloscopegram of impulses with transversal polarization, which are reflected in nanocomposite based on teflon-4 and multiwall carbon nanotubes.

For MWCNT 5% + polypropylene the elastic module $E \approx 1,623$ GPa, elasticity limit $\sigma_E \approx 20,83$ MPa, inelasticity limit $\sigma_{0,2} \approx 30,72$ MPa, ultimate stress limit $\sigma_S \approx 40,09$ MPa were determined.

The absolute value of longitudinal velocity V_{\parallel} and shear velocity $V_{\perp} = 617 \pm 10$ m/sec of nanocomposites based on MWCNT and teflon-4 were determined. After an irradiation, there is diminishing of the velocity value of longitudinal ultrasound elastic waves V_{\parallel} , of the velocity value of transversal ultrasound elastic waves V_{\perp} , elastic module E and shear module G of specimen. The absolute value of longitudinal velocity V_{\parallel} and shear velocity $V_{\perp} = 893 \pm 10$ m/sec of nanocomposites based on MWCNT and modify teflon-3M were determined. Correlation of crystalline and amorphous component of polymers macromolecules, which co-operate with hard MWCNT, will influence on inelastic and elastic characteristics of nanocomposites. The concentration dependence of elastic module E of nanocomposite based on MWCNT and modify teflon-3M is represented on Fig. 2.

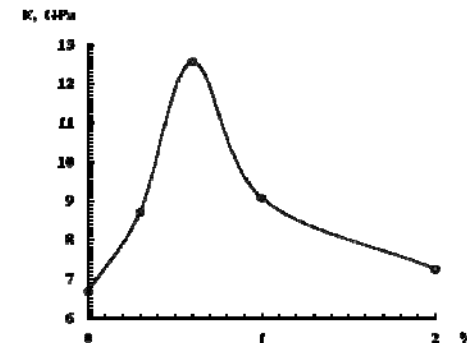


Fig. 2. Concentration dependence of elastic module E of nanocomposite based on MWCNT and modify teflon-3M.

For MWCNT 0,5% + polypropylene the elastic module $E \approx 1,262$ GPa, elasticity limit $\sigma_E \approx 21,15$ MPa, inelasticity limit $\sigma_{0,2} \approx 28,37$ MPa were. For MWCNT 0,1% + polypropylene the elastic module $E \approx 0,8942$ GPa, elasticity limit $\sigma_E \approx 18,78$ MPa, inelasticity limit $\sigma_{0,2} \approx 21,19$ MPa were determined. The value of Δ is determined the amount of microrelaxations of different type and them individual contribution to inelastic deformation at temperature T. The holdings of different microrelaxations are summered. At temperatures, when growth the defect of elastic module $\Delta E/E$ grows sharply, there are relaxation maximums IF Q_M^{-1} on temperature dependences. A considerable width on the temperature of the elastic module relaxation $\Delta E/E$ specifies distributing of activating parameters H of the proper relaxation processes on wide. The concentration dependence of elastic module E of nanocomposite based on MWCNT and polypropylene is represented on Fig. 3.

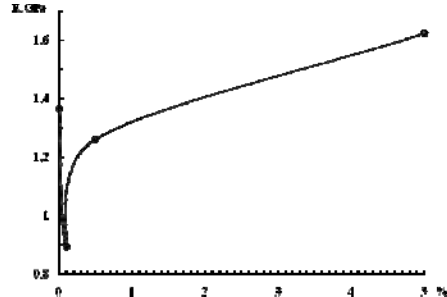


Fig. 3. Concentration dependence of elastic module E of nanocomposite based on MWCNT and polypropylene

It is important in modification of composite polymeric materials the adhesion degree on verge of division, which is determined co-operating of macromolecules with MWCNT. As aromatic groups, which are in different families of free monomers, are the effective traps of radicals, it allows to carry out their co-operating with MWCNT. Such co-operation due to covalently forces of connection results to fixing of polymeric chains nanotubes and also migrations of radicals on traps.

The free vibrations are under acts of internal forces. The conditions of free vibrations are: 1) one force on specimen are function of coordinates; 2) must be equilibrium position, at withdrawal from which the nonzero resultant of all forces must be direct to equilibrium position; 3) friction forces must be enough small. The Poisson coefficient μ is equal to ratio of relative transversal compression to relative longitudinal lengthening and i equal [1]:

$$\mu = - \frac{\varepsilon_{\rightarrow}}{\varepsilon_{\downarrow}} = - \frac{\frac{\Delta X}{X}}{\frac{\Delta l}{l}} = - \frac{\Delta X}{\Delta l} \times \frac{l}{X}, \quad (1)$$

$$\mu = \frac{\frac{1}{2} V_{\parallel}^2 - V_{\perp}^2}{V_{\parallel}^2 - V_{\perp}^2}. \quad (2)$$

Table 1. The Poisson coefficient μ materials

Material	$V_{\parallel}, \text{m/cek}$	$V_{\perp}, \text{m/cek}$	μ
teflon-4	1365	617	0,3716
teflon-3M	1815	893	0,3403
Ti(BT1-0)	6210	3201	0,3191
Д16(2)	6471	3064	0,3555
Al	6260	3080	0,3403
Fe45	5899	3275	0,2772
Fe	6070	3230	0,3025
Cu	4730	2298	0,3455
Pb	2160	700	0,4413

Debye model sets the conditions existence stand waves in solid state. The quantum nature of elementary oscillators takes into consideration. The thermal capacity – parameter of the thermodynamic system equilbril state in Debye model. Therefore waves, that elementary oscillators excite, can't carry the energy. There are stand waves. One oscillator produce 3 waves: 1 longitudinal and 2 transversal. Debye temperature θ_D was determined after the formula [1]:

$$\theta_D = \frac{h}{k_B} \cdot \left(\frac{9N_A \rho}{4 \pi A} \right)^{1/3} \cdot \left(\frac{1}{V_{\parallel}^3} + \frac{2}{V_{\perp}^3} \right)^{1/3}. \quad (3)$$

Thus, the increase of nanocomposite crystalline degree at growth of MWCNT concentration, filling with the nanotubes of matrix results in the decline of content of well-organized phase.

1. *Aleksandrov L.N., Zotov M.I.* Internal friction and defects in semiconductors. - Novosibirsk: Nauka, 1979. - 159 p.
2. *Onanko A.P., Kulish M.P., Melnikova N.O.* Influence of electron irradiation on inelastic-elastic characteristics of Al and Ti alloys // Questions of atomic science and technology. – 1998. – № 5(71) – P. 24 - 26.

3. *Onanko A.P.* Influence of hydrogen on directional surface of inelastic-elastic body Ti0.5Al0.5 alloy // Metalphysics and new technology. – 2011. – V. 33, № 2. – P. 253 - 261.

4. *Zabolotniy M.A., Onanko A.P., Kulish M.P. et al.* The determination method of absorb dose of metal radioactive irradiation / Ukrain Patent on invention № a 2011 05118. – 21.04.2011. - 7 p.

ION-CONDUCTIVE POLYMER SYSTEMS ON THE BASE OF AN ALIPHATIC EPOXY OLIGOMER AND LiClO₄

L. K. Matkovska¹, M. V. Iurzhenko¹, O. K. Matkovska¹, Ye. P. Mamunya¹, E. V. Lebedev¹, G. Boiteux², A. Serghei²

¹*Institute of Macromolecular Chemistry of National Academy of Sciences of Ukraine, Kharkivske shosse 48, Kyiv 02160, Ukraine*

4ewip@ukr.net

²*Université de Lyon, Université Lyon 1, Ingénierie des Matériaux Polymères, UMR CNRS 5223, IMP@LYON1, France*

Nowadays an urgent need in developing and creation of ion-conductive solid electroactive polymers for modern instrument engineering exists [1]. For example, it is known that the use of such compounds as oligooxyethylene offers possible existence of ionic conductivity in dry conditions, which extends the range of operating conditions and, accordingly, the scope of their practical use [2]. The presence of oxygen atoms with significant electro-donor energy in polyethylene oxide chains promotes the formation of bonds with cations [3]. At the same time, an aliphatic epoxy oligomer (DEG) contains ether oxygen, i.e. its chemical structure is similar to the structure of polyethylene oxide (PEO) (Table 1). That enables to take it as a basic product for creation of ion-conductive (Li⁺ by using LiClO₄) polymer materials [4]. In such materials cation transport from one “oxygen-area” to another under the impact of the external electrical field depends on segmental mobility of polymer chains, which is in turn a function of the glass transition temperature of the polymer matrix [5]. Such features of chemical structure and charge transport mechanisms in the proposed materials allow obtaining the high temperature ion-conductive materials.

Table 1. Chemical structures of PEO and DEG

Name	Chemical formula
Polyethylene oxide (PEO)	$\text{OH}-\text{CH}_2-\left[\text{CH}_2-\text{O}-\text{CH}_2\right]_n-\text{CH}_2-\text{OH}$
Aliphatic epoxy oligomer, (DEG)	$\text{CH}_2-\underset{\text{O}}{\text{C}}-\text{CH}-\text{CH}_2-\text{O}-\left[\text{CH}_2-\text{CH}_2-\text{O}\right]_n-\text{CH}_2-\underset{\text{O}}{\text{C}}-\text{CH}_2$

Epoxy oligomer DEG and lithium perchlorate salt LiClO₄ were used for synthesis of ion-conductive epoxy polymer material. LiClO₄ content was varied from 0 to 20 phr, DEG content cases was 90 phr for all. Polyethylene polyamine

hardener (PEPA) was used as a curing agent. The content of PEPA was 10 phr for all cases.

Thermal characteristics studied by differential scanning calorimetry in the temperature range from -70 to +150°C with a heating rate of 10°C/min are shown of Fig. 1a.

Glass transition temperature (T_g) of the composites obtained depending on the content of lithium perchlorate in the reactive mixture was determined from the DSC curves at the second heating (Fig. 1b). As one see that increasing the content of LiClO_4 from 0 to 20 phr leads to increase of glass transition temperature of the obtained polymers from -10 to 25 °C.

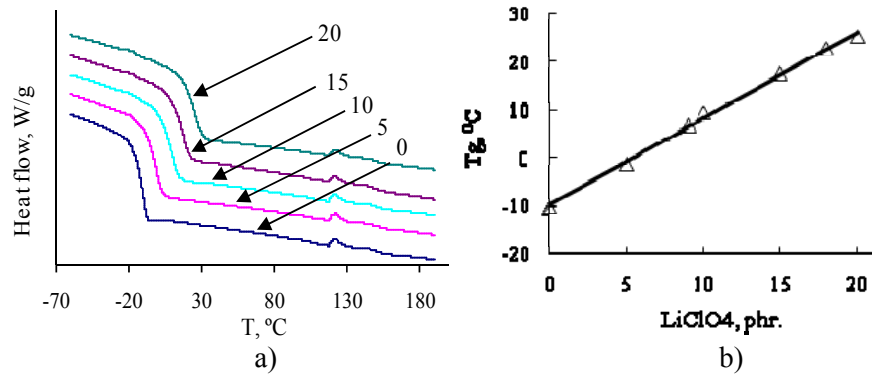


Fig. 1. DSC curves and content dependence of the glass transition temperature of the composites obtained.

Dielectric studies of the synthesized composites were carried out using broadband dielectric spectroscopy in the frequency range 10^{-1} - 10^7 Hz and the temperature range from -60 to +200 °C.

The impact of the LiClO_4 content on electrical and dielectric properties of the epoxy polymer systems obtained can be analyzed from the Fig. 2. Fig 2 shows the isothermal spectra of the real part of complex conductivity (σ') and permittivity (ϵ') for different concentrations of LiClO_4 in the reaction mixture in the temperature range from -60 to 200 °C. Obviously, values and character of the curves of σ' and ϵ' depend on two factors: LiClO_4 content and temperature at which the measurements were performed. In particular, the increase of temperature leads to an increase in the level of conductivity and permittivity, while the equilibrium plateaus of their values shift to higher region. At the same time conductivity multiplies more than two orders of magnitude with increasing the content of LiClO_4 and reaches maximum value $\sigma' = 1,1 \cdot 10^{-3}$ at $T = 200$ °C. The values of permittivity ϵ' tend to 10^6 (Table 2).

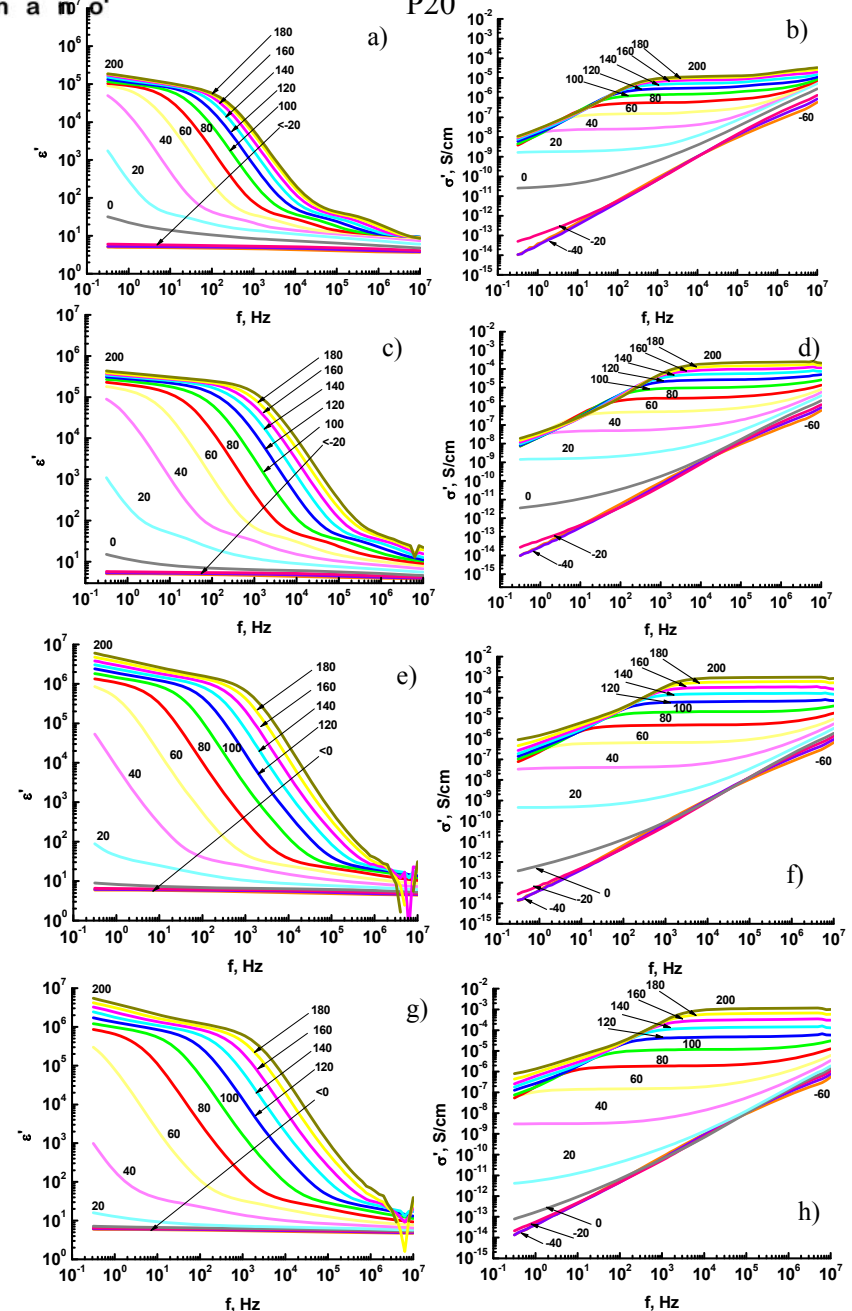


Fig. 2. Spectra of permittivity (a, c, e, g) and real part of complex conductivity (b, d, f, h) of the composites obtained with contents of LiClO_4 : a, b) 0; c, d) 5; e, f) 10; g, h) 20 phr.

Table 2. Electrical and dielectric characteristics of epoxy polymers with different content of LiClO₄

Content LiClO ₄ , phr	ϵ' (10^3 Hz) / σ' (S/cm)			
	60 °C	100 °C	160 °C	200 °C
0	36 / $1,7 \cdot 10^{-7}$	254 / $1,4 \cdot 10^{-6}$	3220 / $8,1 \cdot 10^{-6}$	6040 / $1,3 \cdot 10^{-5}$
5	68 / $4,7 \cdot 10^{-7}$	3140 / $1,0 \cdot 10^{-5}$	60800 / $9,6 \cdot 10^{-5}$	128000 / $2,3 \cdot 10^{-4}$
10	48 / $6,96 \cdot 10^{-7}$	2720 / $1,97 \cdot 10^{-5}$	208000 / $3,2 \cdot 10^{-4}$	680000 / $9,97 \cdot 10^{-4}$
20	33 / $1,5 \cdot 10^{-7}$	1650 / $1,2 \cdot 10^{-5}$	212000 / $3,2 \cdot 10^{-4}$	626000 / $1,1 \cdot 10^{-3}$

Thus, the synthesis of epoxy polymer in the presence of lithium perchlorate yielded ion-conductive polymer materials with high ionic conductivity and permittivity. It is shown that the increase of lithium perchlorate content, on the one hand, leads to an increase in σ' and ϵ' since LiClO₄ is a source of cations Li⁺ and, on the other hand, it affects the hardening process of epoxy matrix (DEG) as evidenced from a significant increase in the glass transition temperature with increasing of LiClO₄ concentration in the reaction mixture.

1. Mamunya Ye., Iurzhenko M., Lebedev E., Levchenko V., Chervakov O., Matkovska O., Sverdlikovska O. *Electroactive Polymer Materials // Alpha-Reklama* (2013) 402.

2. Shevchenko V., Klimenko N., Stryutskyy O., Lisenkov E., Vortman M., Rudakov V. // *Ukr. Chem. J.* 77 (2011) 66-70.

3. Klepko V., Zhyhir O. // *Polym. J.* 3 (2008) 246-250.

4. Matkovska O., Mamunya Ye., Shandruk M., Zinchenko O., Lebedev E., Boiteux G., Serghei A. // *Polym. J.* 1 (2013) 54-59.

5. Gray F.M. *Polymer Electrolytes // Royle Society of Chemistry* (1997) 176.

POLYMERIC MATERIALS WITH GIANT PERMITTIVITY

V. Levchenko¹, M. Samet^{1,2}, A. Khalel², E. Beyou¹, G. Boiteux¹, G. Seytre¹,
A. Serghei^{1*}

¹Université Lyon 1, CNRS UMR 5223, Ingénierie des Matériaux Polymères, 69622 Villeurbanne, France

²Faculté des Sciences de Sfax, Laboratoire des Matériaux Composites Céramiques et Polymères, 3018 Sfax, Tunisie

anatoli.serghei@univ-lyon1.fr

ENHANCING ELECTRICAL PERFORMANCE BY SURFACE STRUCTURING

A. Serghei^{1*}, V. Levchenko¹, G. Boiteux¹, G. Seytre¹, F. Kremer², T.P. Russell³

¹*Université Lyon 1, CNRS UMR 5223, Ingénierie des Matériaux Polymères, F-69622 Villeurbanne, France*

²*University of Leipzig, Institute for Experimental Physics I, 04103 Leipzig, Germany*

³*Department of Polymer Science and Engineering, University of Massachusetts Amherst, Amherst MA 01003, USA*

anatoli.serghei@univ-lyon1.fr

ELECTRICAL AND DIELECTRIC PROPERTIES OF IONIC LIQUIDS

A. Serghei^{1*}, M. Tress², J. Sangoro³, F. Kremer²

¹*Université Lyon 1, CNRS UMR 5223, Ingénierie des Matériaux Polymères, 69622 Villeurbanne, France*

²*University of Leipzig, Institute for Experimental Physics I, 04103 Leipzig, Germany*

³*Chemical Sciences Division, Oak Ridge National Laboratory, Oak Ridge, TN, USA*

anatoli.serghei@univ-lyon1.fr

**FROM BULK TO ATTOGRAMS OF MATTER: Applications
of Broadband Dielectric Spectroscopy in polymer nanoscience**

A. Serghei¹, F. Kremer², T.P. Russell³

¹*Université Lyon 1, CNRS UMR 5223, Ingénierie des Matériaux Polymères, F-69622 Villeurbanne, France*

²*University of Leipzig, Institute for Experimental Physics I, 04103 Leipzig, Germany*

³*Department of Polymer Science and Engineering, University of Massachusetts Amherst, Amherst MA 01003, USA*

anatoli.serghei@univ-lyon1.fr

Author's index

Anghel D.F. 51
Asandulesa M. 35
Avramenko V.L. 89

Bala D. 51
Barboiu M. 35
Beloshenko V. 83
Bercea M. 32
Beyou E. 102
Bibire L. E. 32
Blyznyuk D.A. 89
Boiko V. S. 64
Boiteux G. 4, 11, 22, 68, 81, 98, 102, 103
Botko M. 39
Bucatariu F. 16, 44
Bunia I. 70
Burlui V. 91
Buruiana E. C. 25
Buruiana T. 25

Calin G. 91
Carja G. 32, 92
Cazacu M. 39
Chervakov D. 48
Chervakov O. V. 4, 48
Chibac A. L. 25
Cocarta A.I. 27
Coroaba A. 55
Cozan V. 39

Damian V. 36
Dartu L. 91, 92
David G. 8
Davydenko V.V. 62
Doroftei F. 56, 70

Dragan E. S. 16, 27, 44

Elisa M. 76
Epure L. 36
Espuche E. 22

Fainleib O. M. 20, 22
Feher A. 39
Feraru I. 76
Florea-Spiroiu M. 51

Gerard J. F. 11
Ghiorghita C.-A. 16, 44
Gierszewska-Druzynska M. 27
Gladkiy E. 81
Gonchar A. N. 74
Gouanve F. 22
Grande D. 22
Grigoryeva O. P. 20, 22
Gurtovoj D. V. 66
Gusakova K. G. 20, 22

Harabagiu V. 35
Herasymenko K. O. 64
Houachtia A. 11
Hurduc N. 36

Iacob M. 39
Ignat M. 39
Iordanescu R. 51, 76
Iurzhenko M.V. 4, 20, 62, 81, 98

Kajňaková M. 39
Khalel A. 102

Kremer F. 103, 104, 105

Lavrenyuk N. S. 20
Lebedev E. V. 4, 68, 81, 98
Leonova N.G. 62
Levchenko V. 102, 103
Lipko O. O. 64
Lyga R. I. 66

Mamunya Ye. P. 4, 62, 68, 81, 98
Marlica E. 70
Matkovska L. K. 98
Matkovska O. K. 68, 98
Melinte V. 25
Mihai M. 12, 40, 70
Mikhal'chuk V.M. 62, 66, 69
Mitel A.A. 40
Morariu S. 32
Murariu M. 40

Olaru L. 91
Olaru N. 91
Onanko A. P. 93
Onanko Y. A. 93

Parashchenko I. 81
Pavlii F. N. 69
Peretz S. 51, 76
Pinteala M. 55, 56
Popescu I. 33
Prodayvoda G. T. 93

Racles C. 39
Russell T.P. 103, 105
Rusu G. B. 35

Sacarescu L. 39
Saiter J.-M. 22

Samet M. 102
Sangoro J. 104
Sava I. 36
Savelyev Yu.V. 74
Serghei A. 4, 11, 22, 68, 98, 102, 103, 104, 105
Seytre G. 102, 103
Shandruk M. I. 68
Shashok Zh.S. 57
Simionescu B.C. 8, 70
Starostenko O.N. 22
Stoica I. 36
Stompel V.I. 4
Sverdlikovs'ka O.S. 4

Timpu D. 33, 39
Totolin M. I. 35
Tress M. 104
Trusca R. D. 76
Turta C. 39

Uritu C.M. 55, 56
Ursu L. 55, 56

Varganici C. D. 56
Vasile E. 76
Vasilii I. C. 76
Vishnevskii K. V. 57
Volyanyuk E. A. 69
Voznyak A. 83
Voznyak Y. 83

Youssef B. 22

Zaharia C. 59, 92
Zhil'tsova S. V. 69
Zinchenko O. V. 68